Advancement of Nitrifying Wastewater Treatment

Design and Operation

This thesis is submitted in partial fulfillment of the requirements for the degree of Doctor of Philosophy in Environmental Engineering

Alexander Gerald Schopf

Ottawa-Carleton Institute for Environmental Engineering

Department of Civil Engineering

Faculty of Engineering

University of Ottawa

ABSTRACT

There is an urgent need to develop ammonia removal treatment systems for municipal and industrial wastewater treatment due to the increasingly stringent ammonia effluent discharge regulations implemented by Canada, the United States, and the European Union. The objective of this dissertation is to develop new understanding and advance the current design and operation of total ammonia nitrogen (TAN) removal via the moving bed biofilm reactor technology (MBBR) for municipal and industrial wastewaters. The first specific objective is to develop a passive, low operationally intensive, efficient and robust design strategy for municipal wastewater treatment to achieve partial nitritation (PN) as a pre-treatment to anammox treatment without using control strategies such as operating at low dissolved oxygen, or the use of inhibitors. This first objective includes developing new knowledge of the biofilm, biomass and microbiome of attached growth PN systems. The second specific objective is to investigate the impact of defining a maximum biofilm thickness, via bio-carrier design, to enhance the effects of free nitrous acid inhibition for PN of municipal wastewaters. The third objective is to investigate the effect of influent copper concentration on nitrifying MBBR systems over long-term operations, to demonstrate the feasibility of the nitrifying MBBR as a solution for TAN removal from gold mining wastewaters.

The results pertaining to the first objective, achieved via a study investigating the operation of a nitrifying moving bed biofilm reactor at elevated TAN surface area loading rates (SALRs) of 3, 4, 5, and 6.5 g TAN/m^2·d with the aim of achieving passive PN, demonstrates that operating at a TAN SALR value of 6.5 g TAN/m^2·d can achieve PN without restricting dissolved oxygen or using inhibitors. Operating at a TAN SALR value of 6.5 g TAN/m^2·d achieves a TAN surface area removal rate (SARR) of 3.5 g TAN/m^2·d, and a nitrite accumulation of 99.8% of the oxidized TAN, demonstrating the suppression of nitrite oxidizing bacteria (NOB) activity, while achieving

elevated TAN SARR values. At the molecular-scale, there is a statistically significant change in the ammonia oxidizing bacteria (AOB) to NOB ratio from 1:2.6 to 8.7:1 as the TAN SALR increases from 3 to 6.5 g TAN/m^2·d; however, even at a TAN SALR value of 6.5 g TAN/m^2·d there is an NOB abundance of approximately 2%; thus demonstrating that NOB remain present in the biofilm, while their activity is suppressed by operation at elevated TAN SALR values. Furthermore, this system was shown to achieve stable PN consistently for over a period of 10 months of operation, demonstrating a robust, passive, low operational strategy for attached growth PN.

The second objective of this dissertation is addressed through a study that compared the carrier design of defined maximal biofilm thickness (z-prototype carrier) to undefined maximal biofilm thickness (chip-prototype carrier) for PN via free nitrous acid inhibition of tertiary, low carbon, municipal wastewaters. The study demonstrates that defined maximal biofilm thickness is a preferred design choice to achieve attached growth PN. The chip-prototype carrier shows biofilm thicknesses and biofilm mass values that are ten-fold higher than the z-prototype carrier, which is shown to contribute to the impact of free nitrous acid on AOB and NOB activities. The z-prototype carrier shows PN is achieved after 3 hours of exposure to free nitrous acid while the chip-prototype carrier does not achieve PN within this same time of exposure. Therefore, the defined maximal biofilm thickness carrier is identified in this research as the preferred design option to achieve attached growth PN for municipal, low carbon, tertiary wastewater treatment.

The results of the third objective, achieved via a study investigating the effects of influent copper concentrations on nitrifying MBBR during long term operations to gold mining wastewaters, demonstrates that there is no AOB inhibition in attached growth systems exposed to 0.1, 0.3, 0.45, and 0.6 mg Cu/L for long exposure times. A trend of increasing nitrite accumulation

with increasing influent copper concentrations is shown, indicating that NOB inhibition occurs at influent copper concentrations of 0.3 mg Cu/L and greater, with the greatest NOB inhibition observed with an influent copper concentration of 0.6 mg/L. There is no statistically significant difference in biofilm characteristics at the copper concentrations tested; however, there is a trend of increasing biofilm thickness and biofilm roughness with increasing copper concentrations. This study demonstrates the resilience of the nitrifying biofilm to copper inhibition and demonstrates that the nitrifying MBBR is a promising system for removing TAN in mining wastewater in the presence of copper.

PREFACE

This dissertation is an original work performed by Alexander Schopf under the supervision of Dr. Robert Delatolla and Dr. Kathlyn Kirkwood. This dissertation is comprised of four manuscripts that are published or have been submitted for publication in peer reviewed journals. The published manuscripts, or the submitted versions in the case of submitted manuscripts, are presented in Chapters 3-6 of this dissertation. For each manuscript, the title, reference, authorship, and author contributions are provided below.

Chapter 3:

A version of the manuscript presented in this chapter has been published: Schopf, A., Delatolla, R., Kirkwood, KM. (2019) "*Partial nitritation at elevated loading rates: Design curves and biofilm characteristics*". *Bioprocess and Biosystems Engineering* 42(11): 1809-1818.

Alexander Schopf contributed to the research question and experimental design, performed experimental testing, performed data collection and analysis, interpreted the results, and wrote the manuscript.

Robert Delatolla (supervisor) conceptualized the research question, experimental design, interpretation of the results, and revised the manuscript.

Kathlyn Kirkwood (co-supervisor) contributed to the interpretation of the results and revised the manuscript.

Chapter 4:

A version of the manuscript presented in this chapter will be submitted in early 2021: Schopf, A., Delatolla, R., Tsitouras, A., Kirkwood, K.M. "*Microbial community analysis of partial nitritation achieved using elevated loading rates*".

Alexander Schopf contributed to the research question and experimental planning, performed experimental operations, performed data collection and analysis, interpretation of results, and wrote the manuscript.

Robert Delatolla (supervisor) conceptualized the research question, experimental design, interpretation of the results, and revised the manuscript.

Alexandra Tsitouras performed the microbial processing and assisted in microbial data analysis.

Kathlyn Kirkwood (co-supervisor) contributed to the interpretation of the results and revised the manuscript.

Chapter 5:

A version of the manuscript presented in this chapter will be submitted in early 2021: Schopf, A., Christensson, M., Piculell, M., Tian, X., Delatolla, R. "*Maximal defined biofilm growth to achieve partial nitritation using free nitrous acid*."

Alexander Schopf contributed to the experimental design, performed experimental operations, performed data collection and analysis, interpretation of results, and wrote the manuscript.

Magnus Christensson contributed to the research question, experimental design, interpretation of the results, and revision of the manuscript.

Maria Piculell contributed to the research question, experimental design, and interpretation of the results.

Xin Tian contributed to the experimental design, performed experimental operations, and performed data collection and analysis.

Robert Delatolla (supervisor) contributed to the research direction and revised the manuscript.

Chapter 6:

A version of the manuscript presented in this chapter was published in the journal of *Bioprocess and Biosystems Engineering* in 2019: Schopf, A., Delatolla, R., Matthew, R., Tsitouras, A., Kirkwood, K.M. (2018) "*Investigation of copper inhibition of nitrifying moving bed biofilm reactors (MBBR) during long term operations*". *Bioprocess and Biosystems Engineering* 41(10): 1485-1495.

Alexander Schopf contributed to the experimental design, performed experimental operations, performed data collection and analysis, interpretation of results, and wrote the manuscript.

Robert Delatolla (supervisor) conceptualized the research question, experimental design, interpretation of the results, and revised the manuscript.

Rochelle Matthew contributed to the start-up of the experiment.

Alexandra Tsitouras contributed to the data collection and revision of the manuscript.

Kathlyn Kirkwood (co-supervisor) contributed to the interpretation of the results and revised the manuscript.

I declare that I am aware of the academic regulations set by the University of Ottawa, and I certify that I have obtained written permission from each of the co-authors to include the above materials in my thesis. I certify that the above work was completed during my time at the University of Ottawa as a full-time graduate student.

ACKNOWLEDGEMENTS

Firstly, I would like to acknowledge and thank Dr. Robert Delatolla, who has been my supervisor and mentor throughout my Masters and PhD. He has taught me so much about research, interpreting results and disseminating results. My writing would not be where it is now without his hard work, patience, and guidance. I would also like to thank Dr. Kathlyn Kirkwood for her support, for allowing me to be her student in the TECHNOMISE program, and for being so sympathetic when I was going through difficulties. She will be greatly missed. I would like to thank the NSERC CREATE TECHNOMISE program and all of the professors, support staff, and guest speakers who dedicated their time and effort to the program which imparted not only scientific knowledge but also professional development skills and opportunities that contributed significantly to my professional development. I would like to acknowledge and thank Anox Kaldnes, specifically Dr. Magnus Christensson, Dr. Maria Piculell, and Dr. Fernando Morgan-Sagastume, for allowing me to join them in Lund, Sweden for an internship opportunity in their research group. I would also like to thank and acknowledge my colleagues; Patrick D'aoust, Alexandra Tsitouras, Dr. Warsama Ahmed, Dr. Xin Tian, Neda Arabgol and Dr. Bradley Young who were excellent sources of expertise, knowledge and support over the years. Lastly, I would like to thank my family and friends for all of their support throughout this long journey, especially my partner Catherine who kept me together through the writing of this thesis throughout Covid-19.

TABLE OF CONTENTS

LIST OF FIGURES

LIST OF TABLES

LIST OF ABBREVIATIONS AND ACRONYMS

Anammox	Anaerobic Ammonia Oxidation
AOB	Ammonia Oxidizing Bacteria
BAF	Biologically Active Filter
BOD	Biochemical Oxygen Demand
cBOD	carbonaceous Biochemical Oxygen Demand
CLSM	Confocal Laser Scanning Electron Microscope
COD	Chemical Oxygen Demand
CSTR	Continuously Stirred Tank Reactor
DNA	Deoxyribonucleic Acid
DO	Dissolved Oxygen
EPS	Extracellular Polymeric Substance
FA	Free Ammonia
FNA	Free Nitrous Acid
HRT	Hydraulic Retention Time
IFAS	Integrated Fixed film Activated Sludge
LC_{50}	Lethal Concentration for 50% Mortality
MBBR	Moving Bed Biofilm Reactor
NOB	Nitrite Oxidizing Bacteria
OTU	Operational Taxonomical Unit
PCR	Polymerase Chain Reaction
PFR	Plug Flow Reactor
PI	Propidium Iodide
PN	Partial Nitritation
PN/A	Partial Nitritation with Anammox
QIIME	Quantitative Insights into Microbial Ecology
RNA	Ribonucleic Acid
SAGR	Submerged Attached Growth Reactor
SALR	Surface Area Loading Rate
SARR	Surface Area Removal Rate
sCOD	Soluble Chemical Oxygen Demand
SG	Specific Gravity
SRT	Solids Retention Time
TAN	Total Ammonia Nitrogen
TSS	Total Suspended Solids
VPSEM	Variable Pressure Scanning Electron Microscope
VSS	Volatile Suspended Solids
WRRF	Wastewater Resource Recovery Facility

WSER Wastewater Systems Effluent Regulations

CHAPTER 1 - INTRODUCTION

1.1 Background

The discharge of deleterious substances from municipal and industrial wastewater into natural receiving waters has negative impacts on the environment, such as deoxygenation of the receiving water along with acute and chronic toxicity to aquatic wildlife. In response to the growing awareness of the environmental impacts of wastewater release on natural surface waters, governments such as in Canada, the European Union and the United States have implemented discharge guidelines, with the intent of limiting the discharge of pollution from this source to receiving waters (US EPA, 1972; EU ECC 1991; Canada Gazette. 2012).

Deleterious substance regulations, as set by the Canadian Fisheries Act Wastewater Systems Effluent Regulations (WSER), are set to a discharge limit of an average of 25 mg/L of total suspended solids (TSS), 25 mg/L of carbonaceous biochemical oxygen demand (cBOD), 0.02 mg Cl/L of residual chlorine, and a maximum of 1.25 mg NH_3-N/L (at 15°C) of unionized ammonia (NH_3). Wastewater effluent from industrial sources, such as that of mining wastewater, can have total ammonia nitrogen (TAN) concentrations greater than 100 mg TAN/L (Acheampong *et al*., 2013), and is likely to exceed the unionized ammonia limit of 1.25 mg NH_3-N/L (at 15°C) at pH values typical of industrial effluent wastewaters (pH 7-8). Conversely, wastewater effluent from municipal sources have typical TAN concentrations of 20-30 mg TAN/L and are unlikely to exceed the maximum unionized ammonia limit at pH values typical to municipal effluent wastewaters. However, in the WSER effluent discharge regulations, discharged wastewater must also pass a static, 96-hour acute lethality test (LC_{50}) where less than 50% mortality of rainbow trout must be recorded after 96 hours in 100% raw discharged wastewater at 15°C (Environment

Canada, 2007). Typical municipal and industrial wastewater effluents often fail the 96-h LC_{50} test, as concentrations of 15-20 mg TAN/L have been shown to fail (Di Giulio and Hilton, 2008) even if the maximum unionized ammonia limit is not exceeded. Although an acute toxicity test failure due to TAN toxicity can be waived in the current federal regulations (WSER), treatment of municipal and industrial wastewater discharges is necessary to remove TAN to protect the receiving waters.

TAN is conventionally removed from both municipal and industrial wastewaters using nitrification; which is the two-step autotrophic aerobic oxidation of ammonia/ammonium to nitrite (nitritation) and the subsequent oxidation of nitrite to nitrate (nitratation). To completely remove nitrogen from the system, conventionally nitrate is reduced to nitrogen gas via heterotrophic, anoxic denitrification. Conventional wastewater treatment technologies in Canada, some countries of the EU and in the US include suspended growth systems such as activated sludge (AS) and lagoons; however, suspended growth technologies have a number of challenges such as sensitivity to toxicity, large footprints, and total loss of activity at low temperatures (Ødegaard, 1999). Therefore, to ensure adequate and consistent treatment, attached growth technologies have been developed and implemented worldwide. Attached growth technologies have demonstrated resiliency to toxicity and adverse conditions, and they maintain a high bacterial density that results in a smaller footprint (Ødegaard, 1999; White and Gadd, 2000; Delatolla *et al.*, 2009; Hoang *et al.*, 2014; Young *et al*., 2015).

The moving bed biofilm reactor (MBBR) is an attached growth technology that is a continuously stirred tank reactor (CSTR) filled with high density plastic carriers on which bacteria grow. The carriers, with the attached biofilm, are kept in constant motion in the reactors via agitation induced by aerators or mixers. As such, the removal capacity of the MBBR technology

is based on the quantity of available surface area in the reactor, supplied by the carriers, onto which the bacterial cells attach, grow and are maintained. The MBBR is a low operational intensity, attached growth technology that does not require backwashing and can often easily be upgraded for increased loading by the addition of carriers in the unit. The MBBR technology has been implemented for nitrification in municipal and industrial wastewater resource recovery facilities (WRRF) (Hem *et al.*, 1994; Rusten *et al.*, 1995; Andreottola *et al.*, 2003; Chen *et al.*, 2007; Kermani *et al.*, 2008; Lei *et al.*, 2010; Abzazou *et al.*, 2016); however, due to ever increasing cost of operation and maintenance, dwindling space for infrastructure and construction, and stringent discharge regulations, there is increasing need to optimise the design and operation of current applications.

Nitrification and denitrification are the conventional means to remove nitrogen from municipal and many industrial wastewaters; however, this pair of technologies lacks synergy. The biological process of nitrification is inhibited by the presence of organic carbon (Ødegaard, 1999), as heterotrophs outcompete autotrophs for oxygen when organic carbon is available; thus, nitrification requires low carbon wastewater. Denitrification, on the other hand. is a heterotrophic biological process that requires a substantial quantity of organic carbon. This means that either a carbon source needs to be added to perform the post-nitrification, denitrification step, which is an additional resource cost for WRRFs, or raw wastewater is required to be bypassed to the nitrification unit as a carbon source, which results in the release of untreated ammonia (Metcalf and Eddy, 2014).

Recently, alternative ammonia-nitrogen removal technologies are being developed and optimized, primarily the anaerobic ammonia oxidation (anammox) process in which TAN and nitrite are oxidized to nitrogen gas directly (Strous *et al.*, 1998; Lackner *et al.*, 2014). To obtain an

ideal 1:1.3 TAN to nitrite ratio needed for the anammox process, a partial nitritation (PN) upstream treatment step is required prior to anammox treatment. PN is the intentional incomplete nitritation process with the objective of oxidizing a portion of the TAN to nitrite, while limiting any nitrate production, thereby engaging the ammonia oxidizing bacteria (AOB) and completely supressing the nitrite oxidizing bacteria (NOB) activity. The partial nitritation and anammox processes (PN/A) are both autotrophic processes that overall require 60% less total oxygen, 89-100% less added carbon (depending on post-process denitrification required), and 78% less biomass production than the combined nitrification and denitrification process (Strous *et* al., 1998; Metcalf and Eddy, 2014). Therefore, the PN/A treatment strategy has the potential for significant economic benefit compared to conventional nitrogen removal.

Achieving PN using the MBBR technology has been studied under many configurations over the past two decades (Fux *et al.*, 2004; Rosenwinkel and Cornelius, 2005; Christensson *et al.*, 2013; Gilbert *et al.*, 2014; Piculell *et al.*, 2016; Klaus *et al.*, 2017). In particular, the MBBR technology has been studied as a single tank MBBR PN/A and also, but to a lesser degree, as a two tank PN MBBR system used as a pre-treatment unit prior to anammox treatment. Primarily the MBBR technology has been studied as a single tank MBBR PN/A sidestream treatment system fed with sludge digester centrate (800-1000 mg TAN/L, 30°C). This application has been well studied and applied at full-scale due to the high temperature and resulting high anammox bacterial activity that is achieved in sidestream treatment systems compared to the lower temperatures more typical to mainstream treatment (10-20°C).

In recent years, there have been renewed interest and hence more studies exploring PN/A at conditions more typical to mainstream municipal treatment. To achieve PN many control strategies have been used, such as: low dissolved oxygen (DO) concentrations (0.1-1.5 mg O_2/L);

exposure to free ammonia (FA); exposure to free nitrous acid (FNA); limiting alkalinity; pH regulated DO control; biofilm thickness; intermittent inhibition; and DO/TAN ratio (Hao *et al.*, 2002; Fux *et al*., 2004; Wett, 2007; Lackner *et al*., 2014; Metcalf and Eddy, 2014; Gilbert *et al.*, 2015; Piculell *et al.*, 2016; Laureni *et al.*, 2016; Duan *et al.*, 2019). Despite various control strategies, there has been difficulty in attaining long-term, stable PN due to the long solids retention time inherent to biofilm systems which allow NOB to select for, and adapt to the adverse conditions (Fux *et al*., 2004).

The success of the single tank MBBR PN/A to sidestream treatment trains is based on an operational strategy of maintaining the bulk DO concentration low (0.1-0.5 mg O_2/L) which is preferentially used by the AOB community, thereby largely starving the NOB community of oxygen and suppressing their activity in the one tank system (Gilbert *et al.*, 2014). However, a disadvantage of single tank PN/A is that it is very difficult to increase the rate of PN, identified as a potentially rate limiting step in this single reactor, as the PN can become oxygen rate limited with the anammox process that requires low DO (<1.5 mg O_2/L) occurring in the same tank (Kouba *et al.*, 2016). A two tank PN/A system has been achieved using intermittent and alternating FA and FNA exposure (Duan *et al*., 2019), intermittent aeration (Yang *et al*., 2015; Malovanny *et al.*, 2015), or intermittent exposure to reject water (Piculell *et al.*, 2016); however, these control strategies are operationally intensive and do not provide robust operation and stable effluent quality. Therefore, there is a need for stable, robust, and low operationally intensive design strategy systems to achieve PN.

Many of the studies investigating PN focus on TAN oxidation kinetics and investigate the microbiome using digester centrate (Gilbert *et al.*, 2014; Abzazou *et al.*, 2016; Kouba *et al*., 2016; Xu *et al.*, 2018; Duan *et al.*, 2019). However, there is a lack of research on the influence of the

meso-scale, biofilm characteristics of attached growth systems NOB activity suppression, which can enhance current understanding of these systems and impact the optimization of PN systems. In particular, there is a gap of knowledge on the influence of the meso-scale, biofilm characteristics such as morphology, thickness, and mass, along with carrier geometry on PN kinetics and the microbiome to achieve PN using FNA for municipal treatment.

MBBR systems have the potential to be used as economical, low operational intensity and small footprint systems for the treatment of TAN in industrial wastewaters, such as gold mining wastewater, that contain toxic compounds such as copper, nickel, arsenic, and cobalt (White and Gadd, 2000; Teitzel and Parsek, 2003; Harrion *et al.*, 2004; Flemming *et al.*, 2007). Biofilms provide a structural barrier that limits exposure of bacteria to toxic compounds (including metals), thus protecting the embedded bacteria from inhibitory effects. There have been numerous studies to determine the inhibitory concentrations of copper on nitrifying bacteria which revealed a large range of values from 0.08 – 40 mg Cu/L (Skinner *et al*., 1961; Cenci and Morozzi, 1979; Sato *et al*., 1988; Gerardi, 2002; Juliastuti *et al*., 2003; Çeçen *et al*., 2010; Ochoa-Herrera *et al*., 2011). The inhibitory copper concentrations in current literature; however, were derived from batch tests or short-term studies performed primarily on suspended growth systems or pure cultures. Therefore, this current literature does not accurately address the effects of metal toxicity on attached growth systems. Additionally, due to the time limitation of the studies performed in the literature, there is a lack of understanding as to the fate of copper absorbed and adsorbed onto the biofilm of attached growth systems that have undergone long term operation. Thus, there is a need for a long term study of the fate of copper and the effects of copper on nitrifying kinetics, biofilm characteristics, and the microbiome of nitrifying MBBR systems designed to treat mining wastewaters.

1.2 Research Objectives

The main objective of this research is to investigate design and operational strategies to optimize nitrifying and PN MBBR systems for novel and important applications in the treatment of low carbon wastewaters. This research endeavours to provide a new understanding of nitrifying biofilms and their associated systems and develop new knowledge at the macro-, meso-, micro-, and molecular scale. The specific objectives of this research are as follows:

1. Design a stable, robust, and low operationally intensive design strategy to achieve PN using MBBR technology;
2. Optimize the operation of a stable, robust, and low operationally intensive design strategy to achieve partial MBBR nitritation through the relation between measured biofilm characteristics, biomass viability, and shifts in the microbiome at various operational conditions. In addition, develop new knowledge of biofilm, biomass and microbiome of attached growth PN MBBRs;
3. Determine the effects of carrier design, specifically defined maximal biofilm thickness versus undefined biofilm thickness, and the associated biofilm characteristics and microbiome on the suppression of the NOB activity to achieve PN at municipal wastewater conditions via FNA exposure and inhibition;
4. Determine the effects of bulk copper concentrations on nitrifying MBBR kinetics, and biofilm characteristics and determine the fate of copper in terms of adsorption and absorption to the nitrifying biofilm of MBBR systems treating mining wastewaters to improve the understanding of copper interactions with biofilms during long-term operations;

1.3 Thesis Organization

This dissertation is written in the form of a manuscript-based thesis as specified by the school of Graduate and Postdoctoral Studies at the University of Ottawa. The organization of the thesis is as follows:

Chapter 2 is a literature review presenting the fundamental knowledge related to TAN removal via conventional nitrification and PN using the MBBR attached growth/biofilm technology.

Chapter 3 is a published research article entitled "*Partial nitritation at elevated loading rates: Design curves and biofilm characteristics*". This article has been published in *Bioprocess and Biosystems Engineering* in 2019. In this study, nitrification kinetics and biofilm characteristics were quantified at elevated TAN loading rates to develop a novel, low operational intensity design strategy to achieve PN. A single MBBR was operated at TAN SALRs of 3, 4, 5, and 6.5 g TAN/m^2·d for a total of 3 years, and operated at a TAN SALR of 6.5 g TAN/m^2·d for more than 10 months to ensure steady operations.

Chapter 4 is a research article entitled "*Microbial community analysis of partial nitritation achieved using elevated loading rates".* This article is in preparation for submission for publication. In this study, a single MBBR was operated at elevated TAN loading rates to quantify cell viability and the microbiome. The microbiome and cell viability data are combined with nitrification kinetics and biofilm characteristics to propose the method of NOB suppression used to achieve PN at elevated TAN loading rates.

Chapter 5 is a research article entitled "*Defined maximal biofilm thickness to achieve partial nitritation using free nitrous acid".* This article is in preparation for submission for

publication. This research investigates the effect of defining the maximal biofilm thickness as a carrier design choice on achieving PN using free nitrous acid. In this study, two differently designed carriers, one with a defined maximal biofilm thickness and one with an undefined maximal biofilm thickness, were exposed to FNA and batch tests were used to quantify the impact of FNA on nitrification kinetics.

Chapter 6 is a published research article entitled "*Investigation of copper inhibition of nitrifying moving bed biofilm (MBBR) reactors during long term operations".* This article was published in *Bioprocess and Biosystems Engineering* in 2018. In this study, four identical, parallel, nitrifying MBBRs were loaded with various copper concentrations for 11 months for long term operation. This research investigates the effects of various copper concentrations on nitrification kinetics and biofilm characteristics, including biofilm thickness, mass, and morphology.

Chapter 7 summarizes and discusses the main conclusions of the research as well as discusses the novelty, contributions, and practical applications.

Chapter 8 presents suggestion for future work to expand on the research presented in this thesis.

1.4 References

Abzazou T, Araujo RM, Auset M, Salvado H (2016) Tracking and quantification of nitrifying bacteria in biofilm and mixed liquor of a partial nitrification MBBR pilot plant using fluorescence in situ hybridization. *Science of the Total Environment* 541: 1115-1123

Andreottola G., Foladori P., Gatti G., Nardelli P., Pettena M., Ragazzi M. (2003) Upgrading of a small overloaded activated sludge plant using a MBBR system. *Journal of Environmental Science and Health*, Part A, 38(10): 2317-2328

Almstrand R., Lydmark P., Lindgren PE., Sörensson F., Hermansson M. (2012) Dynamics of specific ammonia-oxidizing bacterial populations and nitrification in response to controlled shifts of ammonium concentrations in wastewater. *Applied Microbiology and Biotechnology* 97:2183-2191

Canada Gazette. (2012). *Wastewater Systems Effluent Regulations, Part II* (Vol. 145).

Chen S., Sun D., Chung JS. (2007) Simultaneous removal of COD and ammonium from landfill leachate using an anaerobic-aerobic moving-bed biofilm reactor system. *Waste Management* 28: 339-346

Christensson M., Ekström S., Andersson Chen A., Le Vaillant E., Lemaire R. (2013) Experience from start-ups of the first ANITA Mox plants. *Water Science & Technology*. 67(12): 2677-2684

Ciesielski S., Kulikowska D., Kaczowka E., Kowal P. (2010) Characterization of bacterial structures in a two-stage moving-bed biofilm reactor (MBBR) during nitrification of the landfill leachate. *Journal of Microbiology and Biotechnology* 20(7): 1140-1151

Council Directive 91/271/EEC of 27 May 1991 Concerning urban waste water treatment. https://www.ecolex.org/details/legislation/council-directive-91271eec-concerning-urban-waste-water-treatment-lex-faoc013224. Accessed Dec 2020

Delatolla R, Berk D, Tufenkji N (2008) Rapid and reliable quantification of biofilm weight and nitrogen content of biofilm attached to polystyrene beads. *Water Research* 42(12): 3082-3088

Delatolla R, Tufenkji N, Comeau Y, Gadbois A, Lamarre D, Berk D (2009) Kinetic analysis of attached growth nitrification in cold climates. *Water Science and Technology* 60:1173-1184

Di Giulio, R.T., Hinton, D.E., 2008. The toxicology of fishes, in: The Toxicology of Fishes, pp. 1–1080.

Duan, H., Ye, L., Lu, X., Yuan, Z. (2019) Overcoming Nitrite Oxidizing Bacteria Adaptation through Alternating Sludge Treatment with Free Nitrous Acid and Free Ammonia. *Environmental Science and Technology* DOI:10.1021/acs.est.8b06148

Fux C, Huang D, Monti A, Siegrist H. (2004) Difficulties in maintaining long-term partial nitritation of ammonium-rich sludge digester liquids in a moving bed biofilm reactor (MBBR). *Water Science and Technology* 49(11-12): 53-60

Gilbert EM, Agrawal S, Karst SM, Horn H, Nielson PH, Lackner S. (2014) Low temperature partial nitritation/anammox in a moving bed biofilm reactor treating low strength wastewater. *Environmental Science and Technology*. 48(15): 8784-8792

Gilbert, EM., Agrawal, S., Schwartz, T., Horn, H., Lackner, S. (2015) Comparing different reactor configurations for partial nitritation/anammox at low temperatures. *Water Research* 81: 92-100

Hao, X., Heijnen, JJ., van Loosedrecht, MCM. (2002) Sensitivity analysis of a biofilm model describing a one-stage completely autotrophic nitrogen removal (Canon) process. *Biotechnology and Bioengineering* 77: 266-277

Hem LJ, Rusten B, Ødegaard H. (1994) Nitrification in a moving bed biofilm reactor. *Water Research* 28(6): 1425-1433

Hoang V, Delatolla R, Laflamme E, Gadbois A (2014) An investigation of moving bed biofilm reactor nitrification during long-term exposure to cold temperatures. *Water Environment Research* 86:36-42

Houda N, Abdelwaheb C, Asma BR, Ines M, Ahmed L, Abdennaceur H. (2015) Tertiary nitrification using moving-bed biofilm reactor: a case study in Tunisa. *Current Microbiology* 70: 602-609

Kermani M, Bina B, Movahedian H, Amin MM, Nikaein M. (2008) Application of moving bed biofilm process for biological organics and nutrients removal from municipal wastewater. *American Journal of Environmental Sciences* 4(6): 682-689

Klaus S, Baumler R, Rutherford B, Thesing G, Zhao H, Bott C. (2017) Startup of a partial nitritation-anammox MBBR and the implementation of pH-based aeration control. *Water Environment Research* 89(6): 500-508

Kouba V, Widiayuningrum P, Chovancova L, Jenicek P, Bartacek J (2016) Applicability of one-stage partial nitritation and anammox in MBBR for anaerobically pre-treated municipal wastewater. *Journal of Industrial Microbiology & Biotechnology* 43: 965-975

Lackner, S., Gilbert, EM., Vlaeminck, SE., Joss, A., Horn, H., van Loosdrecht, MCM. (2014) Full-scale partial nitritation/anammox experiences–an application survey. *Water Research* 55: 292–303

Laureni, M., Falâs, P., Robin, O., Wick, A., Weissbrodt, DG., Nielsen, JL., Ternes, TA., Morgenroth E, Joss A. (2016) Mainstream partial nitritation and anammox: long-term process stability and effluent quality at low temperatures. *Water Research* 101: 628-639

Lei G, Ren H, Ding L, Wang F, Zhang X. (2010) A full-scale biological treatment system application in treated wastewater of pharmaceutical industrial park. *Bioresource Technology* 101:5852-5861

Malovanyy A, Yang J, Trela J, Plaza E (2015) Combination of upflow anaerobic sludge blanket (UASB) reactor and partial nitritation/ anammox moving bed biofilm reactor (MBBR) for municipal treatment. *Bioresource Technology* 180: 144-153

Morgenroth, E., Joss, A. (2016) Mainstream partial nitritation and anammox: long-term process stability and effluent quality at low temperatures. *Water Research* 101: 628-639

Metcalf and Eddy, Wastewater Engineering: Treatment and Resource Recovery. McGraw-Hill, New York, USA, 5th edition., 2014.

Ødegaard H (1999) The moving bed biofilm reactor. *Water Environmental Engineering and Reuse of Water,* Hokkaido Press:250-305

Piculell, M., Christensson, M., Jönsson, K., Welander, T. (2016) Partial nitrification in MBBRs for mainstream deammonification with thin biofilms and alternating feed supply. *Water Science and Technology* 73: 1253-1260

Rosenwinkel KH, Cornelius A. (2005) Deammonification in the moving bed-bed process for the treatment of wastewater with high ammonia content. *Chemical Engineering Technology* 28(1): 49-52

Rusten B. Hem LJ, Ødegaard H. (1995) Nitrification of municipal wastewater in moving-bed biofilm reactors. *Water Environment Research* 67(1): 75-86

Strous, M., Heijnen, JJ., Kuenen, JG., Jetten, MSM. (1998) The sequencing batch reactor as a powerful toll to study very slowly growing micro-organisms. *Applied Microbiology and Biotechnology* 50: 589-596

U.S. Clean Water Act, 33 U.S.C. § 1251 et seq. 1972. U.S Environmental Protections Agency, Washington. https://www.epa.gov/laws-regulations/summary-clean-water-act. Accessed Dec 2020

Wett, B. (2007) Development and implementation of a robust deammonification process. *Water Science and Technology* 56: 81-88

White C, Gadd GM (2000) Copper accumulation by sulfate reducing bacterial biofilms. *FEMS Microbiology Letter*. 183:313-318

Young, B., Delatolla, R., Ren, B., Kennedy, K., Laflamme. E., Stintzi, A. (2016) Pilot-scale tertiary MBBR nitrification at 1° C: characterization of ammonia removal rate, solids settleability and biofilm characteristics. *Environmental Technology*. 37: 2124-2132

CHAPTER 2 - LITERATURE REVIEW

2.1 Wastewater treatment

Wastewater treatment (Fig 2.1) conventionally consists of mainstream treatment (operations 1-9), which consists of pre-treatment (1 and 2), primary treatment (3), secondary treatment (4 and 5), tertiary treatment (6-8) and disinfection (9), and sidestream (operations 10-13) treatment, which consists of sludge thickening (10), anaerobic digestion (11), nutrient removal (12), and dewatering (13) (Metcalf and Eddy, 2014). Mainstream treatment consists of the following operations:

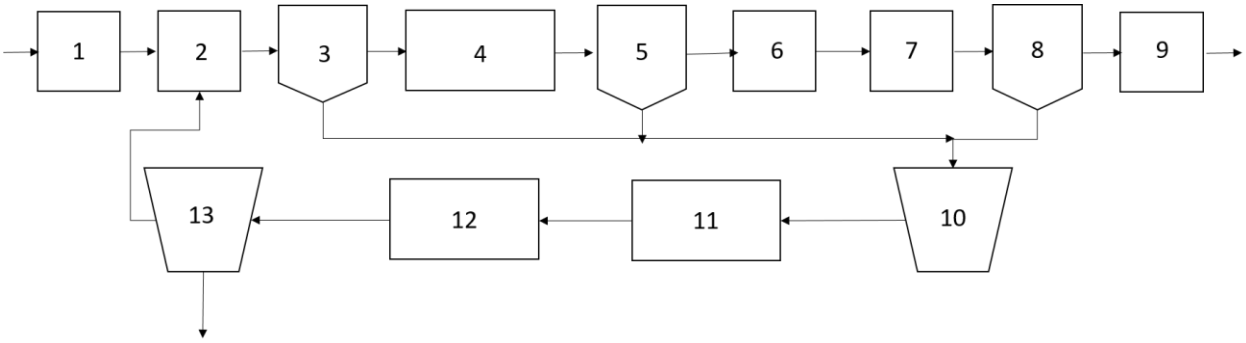

Figure 2.1 Wastewater treatment block flow diagram

1. Wastewater passes through large and small screens to remove large objects that may interfere with subsequent processes.
2. The wastewater passes through a grit chamber where sand and grit are removed by gravity.
3. Primary treatment is conventionally a large settling tank or clarifier where gravity is used to remove solids. Primary clarification can be chemically enhanced using coagulants to remove phosphorus. The settled solids are sent to sidestream treatment. Primary treatment typically removed 60% of total suspended solids (TSS) and 35% of biochemical oxygen demand (BOD_5).

4. Secondary treatment consists of an aerobic biological treatment where bacteria consume organic carbon and oxygen and produce biosolids. Secondary treatment removes the remainder of the BOD_5 required to meet the BOD_5 effluent discharge regulations.
5. Secondary clarification follows secondary treatment to remove the biosolids produced by secondary treatment through gravity settling. The settled biosolids are sent to sidestream treatment. Secondary clarification removes the remainder of the TSS required to meet the TSS effluent discharge regulations.
6. Tertiary treatment consists of biological or chemical nutrient removal and polishes the treated wastewater. Conventionally biological nitrification is used to oxidize total ammonia nitrogen (TAN) to nitrate.
7. Denitrification conventionally follows nitrification and is used to biologically convert nitrate to nitrogen gas to remove nitrogen from the wastewater.
8. Tertiary clarification follows nitrification and denitrification to remove the biosolids produced. The biosolids are sent to sidestream treatment.
9. Disinfection is used to deactivate bacteria that remained in the treated wastewater. The water is then discharged into the environment.

Sidestream treatment consists of the following operations:

10. Biosolids from primary, secondary, and tertiary treatment are collected and thickened by removing water to reduce the sludge volume. Reducing the sludge volume increases the solids concentration and decreases the size required for subsequent processes.
11. The thickened sludge undergoes anaerobic digestion which degrades the biosolids and organic carbon to produce biogas and TAN. Due to the temperature of anaerobic digestion the sludge stream leaves the digester at approximately 30°C.

12. The digested sludge can undergo TAN removal. In some operations the digested sludge goes straight to dewatering.
13. The sludge goes through a dewatering process, such as centrifuging, to produce a sludge cake and liquid centrate which is returned to mainstream wastewater treatment.

2.2 Ammonia in Wastewater

The release of TAN to natural receiving waters is a significant environmental concern due to eutrophication and acute toxicity to wildlife. TAN is the collective term for the sum of the inorganic nitrogen contained in the toxic compound ammonia (NH_3), also referred to as unionized ammonia, and the lesser toxic conjugate acid ammonium (NH_4^+), also referred to as ionized ammonia, as defined by eqn 2.1. TAN speciation is both temperature and pH dependent as seen in eqns 2.2 and 2.3, respectively, where T is the temperature (°C) and pK_a is the acid dissociation constant (Emerson *et al.*, 1975; Erickson, 1985; Clement and Merlin, 1995).

$$NH_3 + H^+ \leftrightarrow NH_4^+ \quad 2.1$$

$$pK_a = 0.09 + \frac{2730}{273 + T} \quad 2.2$$

$$\%NH_3 = \frac{1}{1 + 10^{pK_a - pH}} \times 100\% \quad 2.3$$

Wastewater discharges containing TAN can come from municipal or industrial sources. Sources of TAN in mainstream municipal wastewater include waste from residential areas, pretreated industrial wastewater, rain runoff, and nutrient drainage, with typical mainstream municipal TAN concentrations of 12-50 mg TAN/L (Henze *et al.*, 2002). Conversely, industrial sources of wastewater containing TAN include ammonia production facilities which producing fertilizers, explosives, household cleaners, and ammonium salts, and have typical TAN concentrations of 20-300 mg TAN/L (Metcalf and Eddy, 2014). Mining wastewater, specifically

gold mining, is a significant industrial source of TAN in wastewater with TAN concentrations of greater than 100 mg TAN/L (Acheampong *et al.,* 2013) due to the oxidation of cyanide (eqn 2.4) by cyanide dioxygenase (Ebbs, 2004), used in gold extraction, to TAN as well as TAN residue from nitrogen based explosives (Environment Canada, 2009). Mining wastewater also contains other contaminants such as heavy metals including copper, cadmium, nickel, arsenic, and zinc which are toxic to the environment, wildlife, and bacteria (Environment Canada, 2009).

$$HCN + O_2 + 2H^+ + NAD(P)H \rightarrow NH_3 + CO_2 + NAD(P)^+ \qquad 2.4$$

Due to the toxicity of TAN present in municipal and industrial wastewaters, federal governments worldwide have set wastewater discharge limits. Specifically, Canada has regulated the discharge of unionized ammonia to 1.25 mg NH_3-N/L at 15°C in the wastewater systems effluent regulations (WSER) under the Canadian Fisheries Act (2012). Due to the typical conditions of municipal wastewater (pH = 7-8, TAN =12-50 mg TAN/L), it is unlikely that municipal discharge would exceed the unionized-ammonia WSER; whereas industrial wastewaters may exceed the unionized-ammonia WSER due to the typical industrial TAN range of 20-300 mg TAN/L, especially if the pH approaches or exceeds 8. This is because as the pH increases, the extra H^+ on the ammonium is released and the ammonium is converted to unionized-ammonia, and high TAN concentrations (100 - 300 mg TAN/L) can result in hazardous unionized ammonia concentrations even at low conversion rates. The WSER contains an additional regulation that states that all wastewater discharge must pass an acute lethality test referred to as the LC_{50}. The LC_{50} is defined as 50% mortality of rainbow trout in undiluted wastewater effluent after 96 hours (Canada Gazette, 2012). The LC_{50} obliges municipal WRRF to treat TAN prior to discharge as it has been reported that a TAN range of 15-20 mg TAN/L fails the mortality test,

whereas municipal wastewater TAN concentrations are generally at or above this TAN concentration range (Di Giulio and Hinton, 2008).

2.3 Nitrification

Nitrification is the two-step aerobic, autotrophic biological oxidation of TAN to nitrate. This oxidation is split into the following steps (Metcalf and Eddy, 2014):

$$NH_4^+ + 1\frac{1}{2}O_2 \rightarrow NO_2^- + 2H^+ + H_2O \quad (2.5)$$

$$NO_2^- + \frac{1}{2}O_2 \rightarrow NO_3^- \quad (2.6)$$

$$Overall\ Reaction: NH_4^+ + 2O_2 \rightarrow NO_3^- + 2H^+ + H_2O \quad (2.7)$$

Nitritation is the first step of nitrification (eqn 2.5), where ammonium is oxidized by aerobic ammonia oxidizing bacteria (AOB) to form nitrite, water and hydrogen ions. Nitritation requires 3.43 g O_2/g NH_4^+-N and produces 1 g NO_2^--N/g NH_4^+-N (Metcalf and Eddy, 2014) and has a free energy of –274.74 kJ/mol NH_4^+. In the second step of nitrification (eqn 2.6), nitratation, nitrite is oxidized to nitrate by aerobic NOB and has a free energy of –74.14 kJ/mol NO_2^-. Nitratation requires 1.14 g O_2/g NO_2^--N. Overall, to oxidize 1 g NH_4^+-N to 1 g NO_3^--N requires 4.57 g O_2. Nitritation is the rate limiting step in nitrification (Stephanopoulos *et al.,* 1998). Equation 2.7 represents the overall equation for nitrification as a combination of nitritation and nitratation. Alkalinity is required to perform the nitrification reaction as an inorganic carbon source, as well as to act as a buffer to mitigate the decrease of pH associated with the release of H^+ atoms, thus keeping the system in a suitable pH range, limiting the production of FNA at low pH (pK_a = 3.4 at 20°C), and free ammonia (pK_a = 9.3 at 20°C). The alkalinity requirement is 7.14

g $CaCO_3$/g NH_4^+-N consumed (Metcalf and Eddy, 2014). The full biological nitrification equation, including cell production is defined in eqn 2.8 (Rittman and McCarty, 2014). For eqn 2.8, each gram of NH_4^+-N consumes 4.25 g O_2, 7.07 g $CaCO_3$ of alkalinity (to mitigate the proton production and the resulting change in pH) and 0.08 g inorganic C (totalling approximately 7.14 g $CaCO_3$/g NH_4^+-N) and produces 0.16 g of new cells (where $C_5H_7O_2N$ represents new cells) resulting in a yield of 0.16 g cells/g NH_4^+-N.

$$NH_4^+ + 1.863O_2 + 0.098CO_2 \rightarrow 0.0196C_5H_7O_2N + 0.98NO_3^- + 0.941H_2O + 1.98H^+ \quad 2.8$$

2.4 Nitrifying Bacterial Communities

Nitrification is facilitated by two groups of bacteria; with the first step of nitritation being facilitated by AOB which oxidize ammonia to nitrite, and the second step of nitratation being facilitated by NOB which oxidize nitrite to nitrate. The nitrifying groups of bacteria, AOB and NOB, are aerobic chemolithoautotrophs, meaning that they use inorganic carbon (i.e., carbonate, carbon dioxide) as their carbon source and an inorganic electron donor (ammonia or nitrite) (Rittman and McCarty, 2014). As autotrophic catabolic pathways have a low free energy (ΔG^0 = -43.61 kJ/e^-eq); therefore, many catabolic reactions are required per anabolic reaction resulting in a low biomass yield (e.g., 0.16 g cells/g N), whereas heterotrophic catabolic pathways produce much more energy (ΔG^0 = –110 kJ/e^-eq) resulting in a higher biomass yield (e.g., 0.44 g cells/g $C_6H_{12}O_6$). This difference in yields/ cell production causes autotrophs to be easily outcompeted by chemoorganoheterotrophs. Therefore, nitrification is difficult to achieve when there is a significant concentration of BOD relative to the TAN concentration as the BOD will be preferentially consumed by heterotrophs and nitrifiying bacteria will be outcompeted by the heterotrophs for the

available oxygen. The bacterial communities are dependent on the substrate concentrations at the treatment site (Qin *et al.,* 2018).

The dominant nitrifying bacterial communities are dependent on the environmental conditions of the reactor including; substrate profile, substrate concentration, presence of inhibitors, DO concentration, pH, and temperature. Substrate concentration in the bulk liquid phase can have a significant influence on the dominant AOB and NOB, as in the case of r-strategists and k-strategists. R-strategists are bacteria that thrive in the presence of high concentrations of substrate (such as in a PN reactor), whereas k-strategists thrive in the presence of low concentrations of substrate (such as in a full nitrification system) (Pianka *et al.,* 1970). Additionally, while r-strategists reproduce fast granting r-strategist AOB and NOB the advantage in low stress conditions, k-strategist AOB and NOB may have the advantage in high stress conditions such as the presence of inhibitors. Thus, the species of AOB and NOB that thrive depend on the environmental conditions in which they develop.

2.4.1 Ammonia Oxidizing Bacteria

AOB are bacteria that possess the gene for producing ammonia oxidizing enzymes and their genus have the prefix *Nitroso-*. Common AOB found in nitrification systems include *Nitrosomonas* and *Nitrosospira* (Gerardi *et al.,* 2002) and have a reported doubling time of 7-8 h (Bock *et al*., 1986). The *Nitrosomonas* genera, such as *Nitrosomonas europaea* and *Nitrosomonas eutropha,* are the most commonly found AOB in wastewater treatment as they are r-strategists and therefore function well at TAN concentrations typical to wastewater (Schramm *et al.,* 1999). *Nitrosospira* and species of *Nitrosomonas,* specifically *Nitrosomonas oligotropha*, are k-strategists and dominate at lower ammonia concentrations such as those found in natural waters

(Schramm *et al.,* 1999). Other AOB include *Nitrosococcus, Nitrosolobus* and *Nitrosorobrio* (Gerardi *et al.,* 2002).

2.4.2 Nitrite Oxidizing Bacteria

NOB are bacteria that contain the gene for the nitrite oxidizing enzyme hydroxylamine oxidoreductase (HAO) and the genus has the prefix *Nitro-*. NOB have been reported to have a doubling time of 10-13 hours (Bock *et al*., 1986). *Nitrobactor* has, in the past, been thought of as the dominant bacteria responsible for the oxidation of nitrite due to culturing methods; however, recent genetic identifying techniques have suggested that the most prominent NOB in wastewater treatment is most likely *Nitrospira (*Gerardi *et al.,* 2002*)*. *Nitrospira* is a k-strategist and *Nitrobactor* is an r-strategist (Schramm *et al.,* 1999), which indicates that at low nitrite concentrations (<1 mg NO_2^-–N/L), as is typical in municipal wastewater, *Nitrospira* will outcompete *Nitrobactor*. This is due to the fact that nitritation is the rate limiting step in nitrification which means that nitrite is conventionally oxidized at a faster rate than ammonia is oxidized; therefore, there is often very little nitrite accumulation in conventional nitrification systems. However, in industrial settings and specialized systems, where elevated nitrite concentrations could be present, *Nitrospira* may not be the dominant NOB. Other NOB include *Nitrococcus, Nitrospina,* and *Nitroeystis* (Gerardi *et al.,* 2002).

2.4.3 Toxicity to AOB and NOB

Nitrification is a sensitive process due to the sensitive nature of nitrifying bacteria, and the effectiveness of nitrification is influenced by environmental factors such as pH, presence of metals, temperatures, and other inhibitors. Nitrifying bacteria can be inhibited by un-ionized versions of substrates used during the nitrification process: un-ionized ammonia also referred to as free ammonia (FA), and un-ionized nitrous acid (HNO_2) also known as free nitrous acid (FNA)

(Anthonisen *et al*., 1976). The extent of inhibition varies depending on the concentrations of FA and FNA which are, in turn, dependent on total nitrogen species concentrations, temperature and pH. NOB have been shown to experience inhibition from FA and FNA at concentrations of 0.1-10 mg NH_3-N/L (Anthonisen *et al.,* 1976) and 0.02 mg HNO_2-N/L (Vadivelu *et al.,* 2006), respectively, while AOB have been shown to experience inhibition from FA and FNA at concentrations of 10-150 mg NH_3-N/L and 0.2-2.8 mg HNO_2-N/L, respectively (Anthonisen *et al.,* 1976). Thus, NOB are more sensitive to FA and FNA than AOB.

The pH of the system has an effect on the nitrification efficiency due to the influence of pH on nitrogen speciation. The optimal range for nitrification is between pH 7.5-8.0 (Grady and Lim., 1980). At a pH less than 6.8 nitrification efficiency begins to drop off rapidly (Grady and Lim., 1980) although nitrification has been demonstrated to occur between pH 6.6-9.7 (Odell *et al.,* 1996). Operating above the optimal pH range may cause accumulation of FA (pKa = 9.3 at 20°C) which has been shown to be inhibitory to NOB at concentrations as low as 0.1 mg NH_3-N/L (Anthonisen *et al.,* 1976). FNA (pKa = 3.4 at 20°C) is not likely to be inhibitory in conventional nitrification processes due to the normal operating pH >7 and low conventional nitrite concentrations (<1 mg NO_2^--N/L); however, in scenarios with elevated nitrite concentrations such as digester centrate, FNA might be present in inhibitory concentrations.

The temperature of the system, like pH, has an effect on the nitrification efficiency due to the influence of temperature on speciation equilibrium constants as well as the impact of temperature on bacterial activity. Equilibrium constants will either increase or decrease with temperature depending if the dissociation is exothermic or endothermic. The pK_a of FA decreases with increasing temperature, meaning that at higher operating temperatures, FA becomes more abundant than at lower temperatures operating at the same pH. Furthermore, increasing

temperature generally increases bacterial activity. Nitrification kinetics generally increase with increasing temperatures; however, AOB and NOB have different optimum operating temperatures. While operating below 27°C the AOB will have a lower activity than the NOB and the AOB will be rate limiting; however, at 28°C and higher the AOB will have higher activity than the NOB and the NOB will be rate limiting (Hunik, 1993; Hellinga *et* al., 1998; Metcalf and Eddy, 2014).

Nitrification can be inhibited by a wide range of toxic compounds at concentrations that would not negatively impact aerobic heterotrophs (Anthonisen *et al.,* 1976; Metcalf and Eddy, 2014). Toxic compounds include: organic solvents, amines, proteins, tannins, phenolic compounds, alcohols, cyanates, ethers, carbonates and benzene. Metals, although beneficial at trace concentrations, have been shown to completely inhibit nitrification at low concentrations of 0.25 mg/L for Ni and Cr and 0.1 mg/L for Cu (Skinner and Walker, 1961).

2.4.4 Copper Toxicity to AOB and NOB

One significant heavy metal of note in mining wastewater is copper. Copper can be found in the environment in two valence states: cuprous (Cu^{1+}) and cupric (Cu^{2+}). In mining wastewater, copper is mostly found as the cupric ion as the presence of an oxidant, such as oxygen, vastly favours cupric production ($E°= 0.52$ V for Cu^{+} vs $E°=0.34$V for Cu^{2+}). Copper is often the focus of research as it tends to interact with bacteria differently than other heavy metals such as zinc, arsenic, nickel or lead. Copper tends to sorb onto bacteria at a greater rate; with sorption constants of K_p = 20.3±0.1 L/g bCOD for Cu vs 0.1-0.4±0.0 L/g bCOD for Zn, Ni, and Cd) and caused greater inhibition at low concentrations; with 13.3±10.3% viable cells after exposure to 1mM Cu while 1mM of Zn, Ni, and Cd resulted in cell viabilities of 72.8±7.5%, 104.8±1.7%, and 84.7±7.0% (with 100% viability in un-inhibited scenario) (Hu *et al.,* 2003).

Copper has been shown to inhibit nitrification at concentrations ranging from 0.08-40 mg Cu/L (Skinner *et al.,* 1961; Cenci *et al.,* 1979; Sato *et al.,* 1988; Gerardi *et al.,* 2002; Juliasti *et al.,* 2003; Çeçen *et al.,* 2010; Ochoa-Herrera *et al.,* 2011). The large range in inhibitory values is due to the difference in the experimental conditions such as: pH; the quantity of suspended solids; whether the experiment was a batch or continuous operation; and whether the experiment was testing pure cultures, AS, or biofilm systems (Sterrit *et al.,* 1980; Sato *et al.,* 1988, Hu *et al.,* 2004; Özbelge *et al.,* 2007; Şengör *et al.,* 2011). Batch test have been shown to overestimate inhibitory concentrations for continuous operations as batch tests, as a single, short operation, do not allow for the long term impacts of growth conditions and contact time that occur in normal, long term operations to become evident (Hu *et al.,* 2004; Özbelge *et al.,* 2007; Şengör *et al.,* 2011). Pure cultures, as compared to treatment processes, have not acclimated to any sort of harmful conditions and so are the most sensitive to adverse environments (Özbelge *et al.,* 2007). Attached growth systems have been shown to be more resilient to harmful contaminants compared to suspended growth systems as will be discussed in Sections 2.6.1-2.6.2.

The ability of copper to inhibit nitrification is thought to be dependent not on the bulk phase copper concentration but dependent on the concentration of free (non-complexed) copper and certain copper-ammonium complexes (Braam *et al.*,1951; Sato *et al.,* 1988; Lee *et al.,* 2009; Çeçen *et al.,* 2010). Therefore, the toxicity of copper to nitrifying bacteria is related to the pH of the wastewater and the contaminants in the wastewater which can influence the distribution of copper between free and complexed states as well as the access the bacteria has to the copper.

2.5 Partial Nitrification/Anammox

PN/A, also known as partial nitritation/anammox or deammonification, is the combined two-step process of incomplete nitritation followed by anaerobic (anoxic) ammonia oxidation

through which ammonia is converted to nitrogen gas through the reduction of nitrite. The anammox process was discovered in a denitrifying fluidized bed reactor by Mulder *et al*. (1995) where it was theorized to be a biological phenomenon based on a theory of Broda (1977) who speculated that there were potential lithotrophs that would use ammonium as an electron donor and nitrite/nitrate as an electron acceptor. The work of van de Graaf *et al.* (1997) confirmed that the anammox process was biological in origin through the use of heavy nitrogen (N^{15}) marked TAN. Furthermore, specific anammox organisms began to be identified as early as 1999 (Strous *et al.*, 1999) and continued to be discovered (Schmid *et al.*, 2003; Kartal *et al.*, 2007).

With the increased knowledge on the anammox process, applications of the anammox process began to be developed and implemented (van Dogen *et al.*, 2001). The first full-scale application was a two-tank PN/A system developed in Rotterdam, Netherlands as part of an EU-sponsored study (Jetten *et al.*, 2002). A single tank PN/A process was explored using TAN and low concentrations of oxygen (<2 mg/L) and revealed that small clumps of anammox bacteria and AOB dominated the reactor, while very few NOB developed, resulting in TAN converted predominantly to N_2 gas. This process is a cost efficient and effective alternative method for the total removal of ammonia nitrogen compared to conventional treatment methods of nitrification-denitrification. PN/A requires 60% less oxygen than conventional nitrification-denitrification and 89-100% less carbon source (Strous *et al.*, 1998; Metcalf and Eddy, 2014).

2.5.1 Anaerobic Ammonia Oxidation

Anaerobic ammonia oxidation, commonly referred to as anammox, is the autotrophic oxidation of TAN to nitrogen gas through the reduction of nitrite. The anammox reaction consumes TAN and nitrite to produce nitrogen gas and small amounts of nitrate as shown in the empirically developed eqns 2.9 and 2.10 (Strous *et al.*, 1998; Lotti *et al.*, 2014, respectively) where eqn 2.9

was the stoichiometry originally developed using independent averaged rates, and eqn 2.10 was developed using original data obtained through long term operations. The TAN:NO_2^- ratio is 1:1.146-1.32 rather than a 1:1 ratio because NO_2^- is the electron acceptor for TAN, but also the electron donor for the reduction of inorganic carbon as CO_2 (Strous *et al.*, 1998).

$$NH_4^+ + 1.32NO_2^- + 0.066HCO_3^- + 0.13H^+ \rightarrow 0.066CH_2O_{0.5}N_{0.15} + 1.02N_2 + 0.26NO_3^- + 2.03H_2O \quad (2.9)$$

$$NH_4^+ + 1.146NO_2^- + 0.07HCO_3^- + 0.057H^+ \rightarrow 0.071CH_{1.74}O_{0.31}N_{0.2} + 0.986N_2 + 0.161NO_3^- + 2.002H_2O \quad (2.10)$$

2.5.2 Partial Nitrification

PN is the partial and incomplete oxidation of TAN to nitrite. To facilitate the anammox process, an ideal TAN: nitrite ratio of 1:1.3 is required for optimal removal. PN is an aerobic process facilitated by AOB and, due to the production of nitrite and oxygen availability, can therefore present favourable conditions for NOB. To prevent the oxidation of nitrite to nitrate, there have been multiple methods and control strategies investigated to suppress the NOB. These methods and control strategies include DO control, pH control, and the use of inhibitors such as FA and FNA (Bartroli *et al.*, 2010; Piculell *et al.*, 2016; Li *et al.*, 2017; Duan *et al.*, 2019). There has been significant research in the area of PN on a variety of treatment systems such as AS, membrane biofilm, aerated granules, and MBBRs (Garrido *et al.*, 1997; Fux *et al.*, 2004; Wang *et al.*, 2009; Isanta *et al.*, 2015; Li *et al.*, 2017).

DO concentration limitation has been used to supress the activity of NOB by taking advantage of the lower oxygen affinity of NOB (K_m = 62 µM) compared to AOB (K_m = 16 µM) and, therefore, oxygen will be preferentially consumed by AOB for nitritation (Schramm *et al.*, 1996). Various strategies have been developed to control the DO concentration including

restricting air-flow, pH controls, and alkalinity controls. The pH control method is dependent on the pH change due to oxidation of TAN and nitrite as well as pH influences on AOB and NOB.

2.5.3 Anammox Bacterial Communities

The anammox process is facilitated by monophyletic anaerobic chemolithoautotrophic bacteria called *Planctomycetales* such as *Candidatus Brocadia animmoxidans* (Strous *et al.,* 1999) *Candidatus Anammoxoglobus propionicus* (Kartel *et al.,* 2007), *Candidatus Keunenia stuttgathiensis* (Strous *et al.,* 2006) and *Candidatus Scalindua* (Schmid *et al.*,2003). Anammox bacteria (AnAOB) are very slow growing with doubling times of 11 days (Strous *et al.,* 1998) and operate optimally at temperatures of 30°C - 40°C (Elgi *et al*., 2001; Jin *et al.,* 2012) and have demonstrated activity within the pH range of 6.5-9 with an optimal pH of 8 (Elgi *et al.,* 2001; Jin *et al.,* 2012).

2.5.4. Toxicity to Partial Nitritation and Anammox Bacteria

The PN/A processes have been a significant topic of research since the process's discovery, and investigating toxicity and inhibitors to AnAOB, AOB, and NOB are imperative to the effective operation of PN/A processes. AnAOB have been shown to be inhibited by FA, FNA, and DO (Jin *et al*., 2012). AnAOB was found to be inhibited by: FA concentrations of 20-40 mg N/L (Fernandez *et al.,* 2012) in suspended growth systems, and at concentration of 57-187 mg N/L in attached growth systems (Tang *et al.,* 2010); FNA concentrations of 11µg N/L (Fernandez *et al*., 2012); and DO concentrations of >0.5 mg O_2/L (Strous *et al*., 1997). While understanding toxicity of AnAOB is important to ensure operating effective anammox systems, NOB toxicity can be beneficial as a strategy to achieve PN through suppression of NOB activity. Toxicity to AOB and NOB has been discussed in Section 2.3.3.

2.6 Nitrogen Removal Wastewater Treatment and Technologies

Biological wastewater treatment technologies were developed to take advantage of natural biological processes for the purpose of contaminant and nutrient removal. Biological wastewater treatment technologies generally come in one of two categories: suspended growth systems where bacteria float freely in the planktonic state, or attached growth (or biofilm) systems, where bacteria attach to a surface in the sessile state.

2.6.1 Suspended Growth

Suspended growth processes are processes in which the bacteria are allowed to flow freely in the bulk liquid. These bacteria are referred to as planktonic bacteria. Planktonic bacteria are highly active individually and produce little extracellular polymeric substance (EPS), which can reduce contact with toxins and substrates; therefore, planktonic bacteria tend to be susceptible to toxicity. The high individual activity produces large amounts of biomass that can significantly contribute to post-treatment solids management and costs. The activity of planktonic bacteria is substrate limited due to the unrestricted access of the bacteria to substrate in the bulk fluid.

As suspended growth bacteria flow freely in the bulk liquid, the biomass is constantly removed from treatment systems in the effluent stream; therefore, there remains a challenge to balance HRT and SRT. To retain significant quantities of bacteria solids and attain a high process activity, thickened solids can be recycled into the treatment system as in the AS system (Metcalf and Eddy, 2014).

Conventional planktonic treatment technologies are treatment technologies that allow bacteria to flow freely throughout the system and include the conventional lagoon (aerated or otherwise), and activated sludge systems. The conventional lagoon system is essentially a large, shallow tank (depths of 1-3m) through which water flows and as such the lagoon acts as a gravity

fed pond. As the bacteria are generated in the system, the rates are low compared to other treatment systems due to acting as a chemostat (where HRT=SRT) resulting in low quantities of biomass and therefore the technology must compensate by having high HRTs of approximately 3-25 days for nitrification (Rittman and McCarty, 2014). This technology has a low operational intensity and is often used by communities that have an abundance of inexpensive land available such as rural communities. As lagoons are generally exposed to the elements, their temperature is dependent on the ambient temperature and thus can reach temperatures of 1°C or less, and become ice covered in cold climates.

The AS system is a CSTR followed by a settling tank that thickens that solids and returns a portion of the thickened solids back to the treatment reactor achieving SRTs of 2-12 days. AS systems are one of the most widely used treatment systems worldwide for the removal of contaminants such as TAN.

There have been a number of applications of suspended growth technologies to achieve PN including the SHARON process, DEaMONification (DEMON) process and Completely Autotrophic Nitrogen-removal Over Nitrite (CANON) process. The SHARON process is a chemostat that takes advantage of the temperature effects on the growth rates and minimum sludge age for AOB and NOB. By operating between the temperature range of 30-35 °C, the AOB has a minimum SRT of 0.5-1 days while NOB had minimum SRT of 1-1.5 days (Hunik, 1993; Hellinga *et al.,* 1998); therefore, by operating a suspended growth system without recycle and a retention time lower than the minimum SRT for NOB, the NOB are constantly washed out before they accumulate in a significant quantity (Hellinga *et al.,* 1998). The CANON process is a single sequencing batch reactor (SBR) to retain the slow growing AnAOB biomass. PN/A treatment were controlled through maintaining a low DO concentration of 0.02 mg O_2/L and an HRT of 24h

(Sliekers, 2002). The DEMON process is a SBR that is controlled by time, pH and DO control (Wett, 2007). A DO concentration of 0.3 mg O_2/L is maintained to limit NOB activity. pH check points were used to determine the extent of PN/A occurring as PN decreases pH through the release of H^+ and the anammox process increases the pH through the production of alkalinity thus, the pH was used to control the duration of aeration (Wett, 2007)

2.6.2 Attached Growth

Bacteria exist in nature in two forms as suspended growth (planktonic) or attached growth/biofilms (sessile). Identical bacteria in the planktonic state are physiologically different from those in a biofilm (Stewart and Franklin, 2008). In suspended growth systems, the bacteria are free to move around the bulk phase as individual cells. Although this allows bacteria to freely access substratum for growth and allows bacteria to achieve high levels of activity, it also exposes bacteria to toxicity and stress factors. Stress can cause planktonic cells to attach to a surface and produce an EPS. This EPS binds the bacteria to the surface and creates a protective biofilm, at the cost of accessibility of substrate. Futhermore, the EPS, through mass transfer limitations, slows the transportation of substrates and toxins which can enable a microbial response and can contribute to the defense of the biofilm. Within the biofilm dwell large, diverse microbial communities containing many different types of bacteria, archaea and protozoa (Flemming *et al.*, 2007).

Operating within EPS modifies how bacteria in attached growth systems interact with the environment. Attached growth system kinetic activities are mass transfer rate limited, unlike planktonic systems that are substrate rate limited, due to the fact that substrate must penetrate the biofilm through diffusion before the bacteria have access to the substrate. Diffusivities of TAN, oxygen, nitrite, and nitrate are 1.86×10^{-9}, 2.0×10^{-9}, 1.7×10^{-9}, and 1.7×10^{-9} m^2/s (Tijhuis, 1994;

Picioreanu, 1997), respectively; thus, the mass transfer limitation caused by diffusion results in a reduction in kinetic activity due to the restriction in substrate accessibility. However, the reduced individual bacterial activity in biofilms is compensated for by the extremely high biomass concentration (10-60 g VSS/L) resulting in overall elevated system activity. Biofilm systems experience increased resilience to toxicity and inhibitors due to reduced activity which allows bacteria to reduce the rate of inhibition; the EPS which can physically entrap contaminants and reduces the rate of toxicity penetration due to mass transfer effects; and communication between bacteria that allows for the horizontal gene transfer of beneficial genes (Flemming *et al.*, 2007; Flemming *et al.*, 2013).

Attached growth treatment technologies are technologies that rely on bacteria operating in a biofilm state attached to a medium such as activated carbon, plastics, or rock rather than bacteria floating freely throughout the system. The carriers for sessile treatment technologies can be stationary, operated through restricted movement on a single plane of action, or moving freely throughout the system. Stationary sessile treatment technologies are technologies where the carriers hosting the biofilm does not move in the system and includes trickling filters: where the water flows slowly over plates; and packed beds: which are reactors filled with stationary materials that may or may not be submerged on which biofilm grows; such as, the submerged attached growth reactor (SAGR) and biological activated filters (BAF). Technologies that operate on a single plane of action include biofilm carriers that move back and forth or rotation such as the rotating biological contactor (RBC). Systems where biofilm-laden carriers move freely are called moving bed systems such as the MBBR.

The RBC is one of the oldest attached growth technologies that is still widely used for TAN removal. The RBC typically consists of a covered system that contains large discs that house the

biofilm and is mounted on horizontal rotating shafts. The biofilm discs are conventionally 40% submerged in the wastewater and have typical TAN loading rates of 0.75 – 1.5 g TAN/m^2·d (Metcalf and Eddy, 2014).

The SAGR are aerated gravel beds that are typically used to supplement lagoon systems due to their ease of setup, operation, and retrofitting. SAGR systems are plug flow systems where the bulk liquid flows through the length of the reactor, as opposed to CSTR systems; therefore, SAGR have the capacity to step feed, where influent can be input at various points in the reactor to achieve both BOD and nitrogen removal (Grady *et al.,* 1999). In the SAGR, gravel acts as the carriers that houses the biofilm. The SAGR has demonstrated the capacity to fully treat TAN during the winter months (Mattson *et al.,* 2018).

The BAF is a submerged media filter that contains carriers on which biofilms can develop. The media can be sunken (SG>1) or floating (SG<1), and can be upflow or downflow. As the liquid flows through the media, the biofilm covered media entraps solids and consumes substrate such as TAN. The entrapment of solids means that BAF have the advantage of not requiring post-treatment clarification to remove suspended solids; however, solids build-up means that the system does require periodic backwashing to ensure adequate performance. Typical TAN loading rates for the BAF are 1.0-1.6 kg TAN/m^3·d at 20°C (Rittman and McCarty, 2014).

The MBBR is a CSTR that is filled with submerged, moving plastic biofilm carriers (SG<1) that act as the surface for biofilm attachment. The carriers move freely within the reactor through aeration or mechanical mixing, which allows for shear forces to minimize excess biofilm build-up and prevents sloughing events. The simplistic design of MBBRs, consisting of the reactor, the carriers and aeration, results in simple operation and a small footprint (Ødegaard, 1999). Typical TAN loading rates for the MBBR are 1-2 g TAN/m^2·d (Ødegaard, 1999).

2.7 MBBR Technology

The MBBR technology, as developed by AnoxKaldnes®, is an attached growth technology consisting of a reactor or series of reactors filled with biofilm carriers. The biofilm carriers are designed with high surface area geometry on which the biofilm can grow, and can be optimized for use in a variety of system loading conditions as well as be optimized for specific biofilm thicknesses. The carriers are agitated and moved throughout the reactor volume through aeration or mechanical mixing. The concept behind the MBBR was to combine the advantages of AS processes and biofilter technologies while avoiding the disadvantages of these technologies (Ødegaard, 1999). This was accomplished through the free flow of the carriers throughout the reactor volume, allowing the system to take full advantage of the reactor volume as compared to other processes where static biofilms or mechanisms only allow for limited effective tank volume to be used for treatment. In essence, the carriers move around the reactor similarly to how planktonic bacteria flow in suspended growth processes such as AS. Unlike the AS; however, the bacteria stay on the carriers in the form of biofilm resulting in an extremely long SRT; thus no sludge recycle is necessary to keep high concentrations of bacteria. As the carriers flow through the system, shear forces (erosion) and carrier on carrier contact (abrasion) remove loose or excess biofilm that becomes suspended and is carried out in the effluent thus allowing the MBBR to be a self-cleaning system, reducing the amount of maintenance required (Ødegaard, 1999).

The MBBR system can be used to treat a variety of constituents such as BOD or nitrogen and can be aerobic, anoxic or anaerobic (Ødegaard, 1999). One of the major benefits of the MBBR system is the customizability for loading rate by manipulating design parameters and the ease of upgrading for higher performance by increasing the carrier fill fraction to compensate for an increase in flowrate. This allows the treatment plant the option to increase treatment capacity to

accommodate a growing population or an increased flow simply by adding additional carriers without having to perform costly infrastructure retrofits or overdesigning the system. Typical bulk fill fractions range from 30-70% of the bulk reactor volume.

Attached growth system kinetics are limited by the mass transfer of substrate into the biofilm. Therefore, the quantity of substrate that can be transferred through the biofilm is dependent on the surface area available for mass transfer if substrate concentration is not being considered. Surface area loading rates (SALRs) (eqn 2.11) and surface area removal rates (SARRs) (eqn 2.12) can be defined as:

$$SALR = \frac{Q \cdot C_{in}}{V \cdot \%_{fill} \cdot S_{ab}} \quad 2.11$$

$$SARR = \frac{Q \cdot \left(C_{in} - C_{eff}\right)}{V \cdot \%_{fill} \cdot S_{ab}} \quad 2.12$$

Where Q is the volumetric flowrate (m^3/d), C_{in} is the influent substrate concentration (g/m^3), C_{eff} is the effluent substrate concentration (g/m^3), V is the reactor volume (m^3), $\%_{fill}$ is the fraction of total volume that is made up by carriers as a bulk volume (volume of carriers plus carrier-pore spaces) (as decimal) and S_{ab} is the specific surface area per bulk carrier volume (m^2/m^3). The SALR represents the substrate concentration normalized to the effective surface area while the SARR represents the quantity of substrate removed per unit of effective surface area.

2.7.1 MBBR Carriers and Biofilm

The carriers used in the MBBR system are small, high density polyethylene cylinders (SG = 0.95) with various inner geometries, such as interconnecting walls, to supply surface area for the bacteria to grow on. Due to shear forces and contact between carriers, biofilm does not easily grow

on the outside of the carriers but rather on the protected surfaces. As the bulk liquid flows across the biofilm surface, loose biofilm is removed and mass transfer between the bulk liquid and the biofilm allows substrate to diffuse into the biofilm. Biofilm thickness is an important parameter for MBBR carriers as the thickness of the biofilm can effect substrate penetration (Rittman and McCarty, 2014) and excess biofilm thickness can result in clogging of the carrier-pores which results in a reduction of mass transfer kinetics. There are a variety of carrier types that can be used depending on the required surface area and probable biofilm thickness. Carriers have different designs, sizes and geometries and as a result have different specific surface areas (ranging from 350-1000 m^2/m^3). Carriers can be optimized for high specific surface area, size, and biofilm thickness.

2.7.1.1 Nitrifying MBBR Systems

The MBBR technology has been used for nitrification purposes for many years and for many functions such as tertiary nutrient removal in municipal WRRF, as an add-on polishing system for lagoon treatment, or in industrial treatment. Nitrification removal rates in nitrifying MBBR systems are limited by the BOD content of the wastewater, as well as the oxygen content of the wastewater (Fig 2.1). The nitrifying MBBR commonly operates at loading rates of 1-2.5 g $TAN/m^2 \cdot d$ at DO concentrations of 4-6 mg O_2/L at temperatures typical to municipal wastewater treatment (Ødegaard, 1999). The MBBR has been proven to reliably perform nitrification at 1°C, where many other nitrifying technologies such as suspended growth technologies have failed to perform (Hoang *et al*., 2014; Young *et al*., 2016).

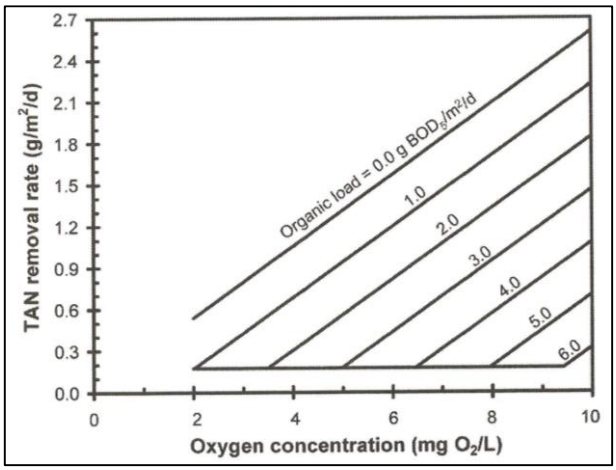

Figure 2.2 Relationship between TAN removal rate, oxygen concentration and organic load at 15°C (Hem *et al*., 1994)

2.7.2 Nitrifying MBBR Reactor Configuration

There are two general types of reactor systems used in wastewater treatment: batch and continuous. Batch systems are systems in which the vessel is filled prior to operations, and drained after operations are completed; therefore, there is no addition or drainage during operation. Batch reactors are filled initially before any reaction takes place and then emptied at the end once the reaction has been completed. Batch systems operate at unsteady state as the conditions shift from their initial concentrations to the final concentrations. Batch systems are often used when performing short term tests. The second type of system is a continuous system where there is a continuous flow into the reactor and out of the reactor. Due to the constant and consistent inflow and outflow, continuous flow systems often operate at steady state providing a consistent product. The steady state designation does not assume that reactions do not occur but rather an equilibrium between the influent, the effluent and the reaction kinetics inside the reactor has been achieved.

Within the continuous system designation, there are two general systems of ideal reactors: the CSTR and the plug flow reactor (PFR). The PFR is, in general, a tank in which the hydraulic

path is much longer than its cross sectional area, preventing sufficient longitudinal diffusion throughout the entire working volume resulting in concentration descending along the length of the reactor. PFRs are largely unsuited to be used as MBBR systems because the PFR tank geometry does not allow for carriers to move throughout the entire reactor volume, as the flow through the proportionally long reactor would force the carriers to the outlet rather than be evenly distributed.

The CSTR is a tank that is completely mixed throughout the working volume due to a method of mechanical mixing, such as aeration or a paddle mixer, that constantly mix the bulk liquid. This mixing causes homogeny within the bulk liquid phase resulting in a uniform concentration throughout the reactor system. As the influent is instantly and uniformly distributed throughout the reactor volume, the concentration within the reactor is identical to the concentration leaving the reactor which results in a low bulk concentration and low reaction kinetics, whereas a PFR is unmixed longitudinally and operates with a concentration gradient along the reactor length, providing areas of higher concentration. This constant mixing of the CSTR is ideal for biofilm as it moves the carriers throughout the entire reactor volume in constant flow, as opposed to having the carriers flow to the end of the reactor and recycled to the beginning as would occur in a PFR.

The bulk liquid inside a CSTR is identical to the effluent leaving the CSTR; therefore, the rates inside the reactor are dependent on the target effluent concentrations. Operating multiple reactors in series causes the reactors proceeding the final reactor to have higher effluent concentrations and therefore higher reaction rates meaning that there is a kinetic advantage to operating multiple CSTRs in series. This benefit is based purely on the bulk phase concentration and does not take in to account any benefit that may result from using a biological biofilm system. The operation of reactors in series may also allow for reactor specialization for specific treatment objectives.

2.7.3 Partial Nitrification MBBR Systems

Achieving PN in attach growth systems has been difficult due to the resilient properties and adaptability of biofilms when using inhibitory-based control methods such as FA and FNA exposure (Fux *et al.,* 2004). Although Fux *et al*. (2004) were able to temporarily achieve PN at elevated loading rates of 5.4 - 7.5 g TAN/m^2·d (influent = 650 mg TAN/L, T = 30°C, DO = 1.5 - 3 mg O_2/L) nitrate accumulation did eventually occur, even with the addition of FA and in the presence of low DO concentration. Rosenwinkel and Cornelius (2005) achieved PN treating reject water through limiting DO to less than 1 mg O_2/L which was successful at suppressing the NOB at the cost of AOB activity. Piculell *et al.* (2016) achieved PN using a combined strategy of thin biofilms and periodic alternating feed between municipal (51 mg TAN/L, T= 15°C, pH = 7.8, DO = 6.6) and sidestream (800 mg TAN/L, T= 30°C, pH = 8.6, DO = 8.6) feeds. The alternating feed would result in periodic exposure to elevated FA and FNA concentrations and a resulting spike in NO_X as NO_2^- averaging around 80%; however, as the experiment proceeded, the time between alternating feeds decreased (Piculell *et al*., 2016).

2.8 References

Acheampong MA, Paksirajan K, Lens PNL (2013) Assessment of the effluent quality from a gold mining industry in Ghana. *Environmental Science and Pollution Research* 20:3799-3811

Anthonisen, AC., Loehr, RC., Prakasam, TBS., Srinath, EG. (1976) Inhibition of nitrification by ammonia and nitrous acid. *Journal of Water Pollution Control Federation* 48(5): 835-852

Bartroli, A., Pérez, J., Carrera, J. (2010) Applying ratio control in a continuous granular reactor to achieve full nitritation under stable operating conditions. *Environmental Science and Technology* 44: 8930-8935

Bengtsson, S., de Blois, M., Wilén, B. M., & Gustavsson, D. (2018) Treatment of municipal wastewater with aerobic granular sludge. *Critical reviews in environmental science and technology* 48(2), 119-166.

Bock, E., Koops, HP., Harms, H. (1986) Cell biology of nitrifying bacteria. In: Prosser JI (ed) Nitrfication. IRL, Oxford, pp 17-38

Braam, F., Klapwijk, A. (1981) Effect of copper on nitrification in activated sludge. *Water Research* 15:1093-1098

Broda, E. (1977) Two kinds of lithotrophs missing in nature. *Zeitschrift für allgemeine Mikrobiologie* 17:491-493

Canadian Environmental Protections Act (1999) S.C. 1999, c. 33

Canadian Fisheries Act (2012) RSC 1985, c F-14

Canada Gazette. (2012). Wastewater Systems Effluent Regulations, Part II (Vol. 145).

Çeçen, F., Semerci, N., Geyik, AG. (2010) Inhibitory effects of Cu, Zn, Ni, and Co on nitrification and relevance of speciation. *Journal of Chemical Technology and Biotechnology* 85:520-528

Cenci, G., and Morozzi, G. (1979) The validity of the TTC-test for dehydrogenase activity of activated sludge in the presence of chemical inhibitors. *Zentralblatt fur Bakteriologie, Parasitenkunde, Infektionskrankheiten und Hygiene* 169:320-330

Clement, B., and Merlin, G. (1995) The contribution of ammonia and alkalinity to landfill leachate toxicity to duckweed. *Science of the Total Environment* 170: 71-79

Di Giulio, RT., Hinton, DE., 2008. The toxicology of fishes, in:, The Toxicology of Fishes, pp. 1–1080.

Ebbs, S. (2004) Biological degradation of cyanide compounds. *Current Opinions in Biotechnology* 15(3): 231-236

Egli, K., Fanger, U., Alvarez, PJJ., Siegrist, H., van der Meer, JR., Zehnder, AJB. (2001). Enrichment and characterization of an Anammox bacterium from a rotating biological contactor treating ammonium-rich leachate. *Archives of Microbiology* 175 (3): 198-207

Emmerson, K., Russo, RC., Lund, RE., Thurston, RV (1975) Aqueous ammonia equilibrium calculation: effect of pH and temperature. *Journal of the Fisheries Research Board of Canada* 32: 2379-2383

Environmental code for practice of metal mines (2009) Environment Canada, Ottawa. https://www.ec.gc.ca/lcpe-cepa/documents/codes/mm/mm-eng.pdf. Accessed 20 April 2017

Erickson, JR. (1985) An evaluation of mathematical models for the effect of pH and temperature on ammonia toxicity to aquatic organisms. *Water Research* 19: 1047-1058

Flemming, H.C., Neu, T.R., Wozniack, D.J., 2007. The EPS matrix: The "house of the biofilm cells". *Journal of Bacteriology* Vol 189 (22), 7945-7947

Fux, C., Huand, D., Monti, A., & Siegrist, H. (2004). Difficulties in maintaining long-term partial nitritation of ammonium-rich sludge digester liquids in a moving-bed biofilm reactor (MBBR). *Water Science and Technology* 49(11-12), 53-60. Doi:10.2166/wst.2004.0803

Garrido, JM., van Benthum, WAJ., van Loosdretcht, MCM., Heijnen, JJ. (1997) Influence of dissolved oxygen concentration on nitrite accumulation in a biofilm airlift suspension reactor.

Biotechnology and Bioengineering. 53(2), 168-178. Doi: 10.1002/(sici)1097-0290(19970120)53:2<168::aid-bit6>3.0.co;2-m

Grady, CPL Jr., and Lim, HC. Biological Wastewater Treatment. Marcel Dekker, NY. 1980

Grady CPL., Daigger GT., Lim HC. Biological Wastewater Treatment. Marcel Dekkar, NY. 1999

Gerardi MH (2002) Nitrification and denitrification in the activated sludge process. Environmental Protection Magazine Series. John Wiley and Sons, Inc. New York.

Harrison, J.J., Cerl, H., Stremick, C. A., Turner, R.J., (2004) Biofilm susceptibility to metal toxicity. *Environmental Microbiology* 6 (12), 1220-1227

He, Q., Chen, L., Zhang, S., Wang, L., Liang, J., Xia, W., & Zhou, J. (2018). Simultaneous nitrification, denitrification and phosphorus removal in aerobic granular sequencing batch reactors with high aeration intensity: Impact of aeration time. *Bioresource technology*, 263, 214-222.

Hellinga, C., Schellen, AAJC., Mulder, JW., van Loosdrecht, MCM., Heijnen, JJ. (1998) The SHARON process: an innovative method for nitrogen removal from ammonium-rich wastewater. *Water Science and Technology* 37: 135-142

Henze, M., Harremoes, P., La Cour Jansen, J., Arvin, E. (2003) Wastewater Treatment: Biological and Chemical Processes 3rd Edition. Springer, Verlag Berlin Heidelberg

Hoang V, Delatolla R, Laflamme E, Gadbois A (2014) An investigation of moving bed biofilm reactor nitrification during long-term exposure to cold temperatures. *Water Environment Research* 86:36-42

Hu Z, Chandran K, Grasso D, Smets BF (2003) Impact of metal sorption and internalization on nitrification inhibition. *Environmental Science and Technology* 37:728-734

Hu, Z., Chandran, K., Grasso D, Smets BF (2004) Comparison of nitrification inhibition by metals in batch and continuous flow reactors. *Water Research* 38:3949-3959

Hunik, JH (1993). Engineering aspects of nitrification with immobilized cells. PhD Thesis, Wageningen Agricultural University.

Isanta, E., Reino, C., Carrera, J., Pérez, J. (2015) Stable partial nitritation for low-strength wastewater at low temperature in an aerobic granular reactor. *Water Research* 80(1): 149-158

Jetten MS., Schmid M., Schmidt I., *et al*., (2002) Improved nitrogen removal by application of new nitrogen-cycle bacteria. *Reviews in Environmental Science and Biotechnology* 1(1) 51-63

Jin, RC., Yang, GF., Yu, JJ., Zheng, P. (2012) The inhibition of the Anammox process: A review. *Chemical Engineering Journal*, 197: 67-79

Juliastuti SR, Baeyens J, Creemers C, Bixio D, Lodewyckx E (2003) The inhibitory effects of heavy metals and organic compounds on the net maximum specific growth rate of the autotrophic biomass in activated sludge. *Journal of Hazardous Materials* B100:271–283

Kartal B., Rattray J., van Niftrik LA., Van de Vossenberg J., Schmid MC., Webb RI., Schouten S., Fuerst JA., Sinninghe Damste J., Jetten MSM, Strous M. (2007) *Candidatus* '*Anammoxoglobus*

propionicus' a new propionate oxidizing species of anaerobic ammonia oxidizing bacteria. *Systemic and Applied Microbiology* 30(1): 39-49

Lee LY, Ong SL, Ng HY, Hu JY, Koh YN (2008) Simultaneous ammonia-nitrogen and copper removal and copper recovery using nitrifying biofilm from the ultra-compact biofilm reactor. *Bioresource Technology* 99: 6614-6620

Li, Y., Wang, Z., Li, J., Wei, J., Zhang, Y., Zhao, B. (2017) Inhibition kinetics of nitritation and half-nitritation of old landfill leachate in a membrane bioreactor. *Journal of Bioscience and Bioengineering* 123(4): 482-488

Lotti, T., Kleerebezem, R., Lubello, C., and Van Loosdrecht, MCM., (2014). Physiological and kinetic characterization of a suspended cell anammox culture. *Water research*, 60, pp.1-14.

Mattson R., Wildman M., Just C. (2018) Submerged attached-growth reactors as lagoon retrofits for cold-weather ammonia removal: performance and sizing. *Water Science and Technology* 78(8):1625-1632

Metcalf and Eddy, Wastewater Engineering: Treatment and Resource Recovery. McGraw-Hill, New York, USA, 5th edition, 2014.

Mulder A., van de Graaf AA., Robertson LA., Kuenen JG. (1995) Anaerobic ammonia oxidation discovered in denitrifying fluidized bed reactor. *FEMS Microbiology Ecology*. 16:177-184

Ochoa-Herrera V, Leon G, Baniban Q, Afield J, Sierra-Alvares R (2011) Toxicity of copper (II) ions to microorganisms in biological wastewater treatment systems. *Science of Total Environment* 412-413: 380-385

Ødegaard H (1999) The moving bed biofilm reactor. *Water Environmental Engineering and Reuse of Water*, Hokkaido Press:250-305

Odell, LH., Kirmeyer, GJ., Wilczak, A., Jacangelo, JG., Marcinko, JP., and Wolfe, RL (1996). Controlling Nitrification in Chloraminated Systems. *Journal AWWA* 88(7):86-98.

Özbelge TA, Özbelge HO, Altinten P (2007) Effect of acclimatization of microorganisms to heavy metals on the performance of activated sludge process. *Journal of Hazardous Materials* 142:332-339

Picioreanu, C., van Loosedrecht, MCM., Heijnen, JJ. (1997) Modelling the effect of oxygen concentration on nitrite accumulation in a biofilm airlift suspension reactor. *Water Science and Technology* 36(1): 147-156

Pianka, ER. (1970) On r- and K- Selection. *The American Naturalist*, 104(940): 592-597

Qin, H., Han, C., Jin, Z., Wu, L., Deng, H., Zhu, G., Zhong, W. (2018) Vertical distribution and community composition of anammox bacteria in sediments of a eutrophic shallow lake. *Journal of Applied Microbiology* 125:121-132

Rittmann, BE., and McCarty, PL. (2014) Environmental Biotechnology: Principles and Applications. McGraw-Hill, Boston.

Rosenwinkel KH., and Cornelius A. (2005) Deammonification in the moving-bed process for the

treatment of wastewater with high ammonia content. *Chemical Engineering and Technology* 28(1):49-52

Sato C, Leung SW, Schnoor JL (1988) Toxic response of *Nitrosomonas europaea* to copper in inorganic medium and wastewater. *Water Research* 22:1117-1127

Schmid, M., Walsh, K., Webb, R., Rijpstra, WIC., van de Pas-Schoonen, K., Verbruggen, MJ., Hill, T., Moffett, B., Fuerest, J., Schouten, S., Damasté, JSS., Harris, J., Shaw, P., Jetten, M., Schramm A, de Beer D, van den Heuvel JC, Ottengraf S, Amann R. (1999) Microscale distribution of populations and activities of Nitrosospira and Nitrospira spp. along a macroscale gradient in a nitrifying bioreactor: quantification by in situ hybridization and the use of microsensors. *Applied and Environmental Microbiology* 65(8):3690–6

Schramm A, Larsen L.H, Revsbech N.P, Ramsing N.B, Amann R, Schleifer K.H (1996) Structure and function of a nitrifying biofilm as determined by in situ hybridization and the use of microelectrodes. *Applied and Environmental Microbiology* 62:4641-4647

Şengör SS, Gikas P, Moberly JG, Peyton BM, Ginn TR (2011) Comparison of single and joint effects of Zn and Cu in continuous flow and batch reactors. *Journal of Chemical Technology and Biotechnology* 87:374-380

Skinner FA, and Walker N (1961) Growth of *Nitrosomonas europaea* in batch and continuous culture. *Archiv für Mikrobiologie* 38:339-349

Sleikers A. (2002) Completely autotrophic nitrogen removal over nitrite in one single reactor. *Water Research* 36(10): 2475-2482

Stephanopoulos GN., Aristidou, AA., Nielsen J. (1998) Metabolic Engineering. *Academic Press*

Sterrit RM, Lester JN (1980) Interactions of heavy metals with bacteria. *The Science of the Total Environment* 14:5-17

Strous, M., Heijnen, JJ., Kuenen, JG., Jetten, MSM. (1998) The sequencing batch reactor as a powerful tool to study very slowly growing micro-organisms. *Applied Microbiology and Biotechnology* 50: 589-596

Strous M., Fuerst JA., Kramer EHM., Logemann S., Muyzer G., van de Pas-Schoonen KT., Webb R., Kuenen JG., Jetten MSM. (1999) Missing lithotroph identified as new planctomycete. *Nature* 400;446-449

Strous, M., Kuenen, J.G., Jetten, M.S.M., (1999) Key physiology of anaerobic ammonium oxidation. *Applied Environmental Microbiology* 65, 3248–3250

Strous, M. (2003) *Candidatus* "Scalindua brodae", sp. nov., *Candidatus* "Scalindua wagneri", sp. nov., Two new species of Anaerobic Ammonium Oxidizing Bacteria. *Systemic and Applied Microbiology* 26 :529-538

Strous M., Pelletier E., Mangenot S., *et al.* (2006) Deciphering the evolution and metabolism of an anammox bacterium from a community genome. *Nature* 440: 790-794

Tijhuis, L. (1994) The biofilm airlift suspension reactor: biofilm formation, detachment, and heterogeneity. Ph. D – dissertation, Delft, The Netherlands. Pg. 123.

Vadivelu, VM., Keller, J., Yuan, Z., (2007). Free ammonia and free nitrous acid inhibition on the anabolic and catabolic processes of Nitrosomonas and Nitrobacter. *Water Science and Technology* 56, 89–97

Van de Graaf AA., deBruijin P., Robertson LA., Jetten MSM., Kuenen JG. (1997) Metabolic pathway of anaerobic ammonium oxidation on the basis of N-15 studies in a fluidized bed reactor. *Microbiology-UK* 143:2415-2421

Van Dogen U., Jetten MSM., van Loosedrecht MCM, (2001) The SHARON-Anammox® process for treatment of ammonium rich wastewater. *Water Science and Technology* 44:153-160

Wang R., Terada, A., Lackner, S., Smets, BF., Henze, M., Xia, S., Zhao, J. (2009) Nitritation performance and biofilm development of co-and counter – diffusion biofilm reactors: Modeling and experimental comparison. *Water Research* 43(10); 2699-2709

Wett B. (2007) Development and implementation of a robust deammonification process. *Water Science and Technology* 56(7): 81-88

Young B, Banihashemi B, Forrest D, Kennedy K, Stinzi A, Delatolla R (2016) Meso and micro-scale response of post carbon removal nitrifying MBBR biofilm across carrier type and loading. *Water Research* 91:235-243

CHAPTER 3 - PARTIAL NITRITATION AT ELEVATED LOADING RATES: DESIGN CURVES AND BIOFILM CHARACTERISTICS

3.1 Context

Chapter 3 presents the research article entitled *Partial nitritation at elevated loading rates: design curves and biofilm characteristics* and has been published in *Bioprocess and Biosystems Engineering* in 2019. This article discusses the high-rate, passive partial nitritation strategy using nitrifying MBBR technology through elevated TAN loading rates, as well as providing justification for the phenomenon through biofilm characteristics (thickness, mass, density, and morphology) and NO_X distribution design curves.

3.2 Abstract

There is a need to develop low operational intensity, cost-effective and small-footprint systems to treat wastewater. Partial nitritation (PN) has been studied using a variety of control strategies; however, a gap in passive operation is evident. This research investigates the use of elevated loading rates as a strategy for achieving low operational intensity PN in a moving bed biofilm reactor (MBBR) system. The effects of loading rates on nitrification kinetics and biofilm characteristics were determined at elevated, steady dissolved oxygen concentrations between 5.5 and 7.0 mg O_2/L and ambient temperatures between 19 and 21˚C. Four elevated loading rates (3, 4, 5 and 6.5 g NH_4^+-N/m^2·d) were tested with a distinct shift in kinetics being observed towards nitritation at elevated loadings. PN was achieved at 6.5 g NH_4^+-N/m^2·d with 100% nitrite accumulation, likely due to thick biofilm (572 µm) and elevated NH_4^+-N load, which resulted in suppression of nitrite oxidation.

3.3 Introduction

The release of nutrients, and in particular nitrogen, into natural receiving waters, such as rivers and oceans, can cause significant adverse effects. These effects include algae growth along with acute and chronic ammonia and nitrate toxicity to aquatic life. Many governments, including the EU, the USA and Canadian have regulated the discharge of nitrogen constituents to receiving bodies (US EPA, 1972; EEC, 1991; Canada Gazette, 2012). Wastewater discharges from municipal rural and urban wastewater treatment plants, such as lagoons and activated sludge facilities, are one of the largest contributors of undesirable nutrients and deleterious substances, such as ammonia, to natural receiving waters (Delatolla and Babarutsi, 2005; WRI, 2018). The conventional method to remove nitrogen from municipal wastewater is the microbially mediated two-step nitrification process followed by the microbially mediated denitrification process. Nitrification is the two-step oxidation of ammonia to nitrite (nitritation) by ammonia oxidizing bacteria (AOB) and the subsequent oxidation of nitrite to nitrate (nitratation) by nitrite oxidizing bacteria (NOB) and is facilitated by aerobic autotrophic bacteria. Denitrification is the reduction of nitrate to nitrogen and is facilitated by anoxic, heterotrophic bacteria. Recently, economical alternatives to conventional nitrification and denitrification in municipal and industrial treatment systems are being explored due to the high operating costs of supplying the aeration required to fully oxidize ammonia to nitrate. Additional operating costs can also exist in the form of an external carbon source to facilitate post nitrification denitrifier activity, along with additional sludge production costs due to high yield of denitrifiers, or in the form of additional capital costs from recycling the nitrified effluent back to the heterotrophic treatment system, larger treatment vessels, and additional infrastructure.

The alternative microbially mediated nitrogen removal process of partial nitritation (PN) followed by anaerobic ammonium oxidation (anammox) is of significant interest to the wastewater treatment community as it can potentially reduce energy requirements for aeration by 60% and operational costs from carbon requirements by 75% (Mulder *et al*., 1995). The anammox process is performed by anaerobic autotrophs that oxidize ammonia with nitrite to produce primarily nitrogen gas (Stous *et al*., 1998). Anammox treatment requires the total ammonia nitrogen (TAN) of municipal wastewaters to first be partially converted to nitrite (PN); with the ammonia concentration being reduced to 40 - 45% of the total nitrogen in the wastewater and the nitrite-nitrogen accumulating to 55 - 60% of the total nitrogen in the wastewater (Strous *et al*., 1998). Anammox treatment has been implemented in over 100 full-scale operations worldwide to ammonia from sidestream wastewaters originating from anaerobic digesters prior to being returned to the head of the facility (Lackner *et al*., 2014). Anammox treatment has been achieved using single stage (single vessel) processes, meaning the PN and anammox processes occur within a single reactor system. These systems have been designed as suspended growth, attached growth, or hybrid systems. Examples of single stage systems include the Completely Autotrophic Nitrogen-removal Over Nitrate (CANON) process, the DEamMONification (DEMON) process, and the ANITA Mox process. Anommox treatment has also been designed as a two stage (two vessel) partial-nitritation/anammox process, with two stage systems being designed as suspended growth conventional activated sludge systems, attached growth moving bed biofilm reactor (MBBR) systems, hybrid integrated fixed film activated sludge (IFAS) systems and granular activated sludge systems (van Dougen *et al*., 2001; Rosenwinkel and Cornelius, 2005; Wett, 2007; Christensson *et al.,* 2013). The Single reactor High activity Ammonia Reaction Oxidation to Nitrite (SHARON) process, for example, is conventionally a suspended growth process that aims

to prevent nitratation through the manipulation of NOB growth via temperature and sludge retention (Hellinga *et al*., 1998; Fux *et al.,* 2004).

NOB sensitivity to inhibition by free ammonia (FA) and free nitrous acid (FNA) has been used as a strategy to enhance attached growth nitritation in various technologies, including the SHARON process, with contradicting results. Some studies have found FA and FNA inhibition effective and suggested inhibition as a control strategy (Brockmann and Morgenroth, 2010; Park *et al*., 2010; Park *et al*., 2014), others have found that there was no significant benefit (Fux *et al*., 2004; Gaul *et al.*, 2005; Bartroli *et al*., 2010), while others have observed some benefit at operation at pH values greater than 8.0 (Wang *et al*., 2009; Huiliñir *et al*., 2010). Therefore, modern PN control strategies have been applied to sidestream attached growth systems with a focus on limiting dissolved oxygen (DO) by using sequencing batch systems, intermittent aeration, constant low DO operation, and controlling biofilm thickness (Hao *et al.,* 2002; Wett, 2007; Gilbert *et al*., 2015; Piculell *et al*., 2016; Laureni *et al*., 2016). Previous studies have postulated that it is not the DO concentration but rather the DO to ammonium ratio that determines the extent of PN. As such, this limiting aeration as a PN strategy has been demonstrated to work best with high influent ammonia concentrations if higher DO concentrations are desired (Bartroli *et al*., 2010; Isanta *et al*., 2015; Bian *et al*., 2017).

There exists the potential of the MBBR technology to be used for mainstream PN treatment of municipal wastewater as success has been observed when limiting DO, controlling the pH or limiting the thickness of the biofilm; however, these control methods are often operationally intensive or demonstrate intermittent nitrate production thus requiring additional control methods to achieve PN (Peng *et al*., 2007; Durián *et al*., 2014; Gilbert *et al*., 2015). PN control strategies based on limited DO are not only operationally intensive, as these strategies require constant

monitoring and adjustment, but also demonstrate limited removal kinetics as nitritation kinetics become oxygen mass transfer rate limited at low oxygen concentrations. Therefore, there is a need for low operational intensity design strategies that do not solely rely on limited DO while providing stable PN without nitrate production events.

Preliminary studies performed on MBBR systems in our laboratory demonstrated that there is potential for PN when operating at elevated TAN loading rates that are significantly higher than conventional operation at ambient temperatures. Hence, operation at elevated TAN loading rates under conventional aeration conditions is a low operational intensity strategy for attached growth systems such as the MBBR to achieve PN. If successfully implemented, attached growth systems will benefit from: elevated removal rates when compared to alternative control systems due to conventional nitrification oxygen concentrations; a reduced footprint of the system due to the elevated loading rate; and more stable nitrite accumulation compared to other strategies. The effects of elevated loading rates on PN have been explored at specific operational conditions such as operation using reject wastewaters at elevated temperatures (30˚C) compared to mainstream municipal treatment; in tandem with alternative control strategies such as limited DO concentrations or SBR operation; using different biofilm technologies such as aerated granules, membrane bioreactors, packed-bed reactors, rotating biological contactors or the SHARON process applied to the MBBR technology; and at elevated influent ammonia concentrations (Fux *et al*., 2004; Gaul *et al*., 2005; Wang *et al*., 2009; Ganigué *et al.*, 2009; Bartroli *et al*., 2010; Huiliñir *et al*., 2010; Zhang *et al*., 2011). Although elevated loading effects have been studied at these conditions, the effects of loading rate on MBBR systems, at unrestricted DO concentrations and conventional pH values without FA and FNA inhibition strategies has yet to be thoroughly explored as a design method of passive PN at ambient temperatures.

The aim of this study is to investigate MBBR systems that are designed for and operated at elevated TAN surface area loading rate (SALR) values ranging from 3 g TAN/m^2·d to 6.5 g TAN/m^2·d, at conventional pH values, and at ambient temperatures to achieve stable, economical and compact PN, using a loading strategy that reduces the operational intensity of these systems by reducing actions required to properly operate, benefits from elevated rates of nitritation, and mitigates the production of nitrate during operation. The novelty of this study is the passivity and low operational intensity of the loading strategy for a pre-treatment step for anammox compared to the active control strategies required in many other PN studies, and to fill the knowledge gap of extremely high loaded biofilm systems at conventional temperatures and pH. The specific objectives include: (i) developing the TAN SALR design curve of stable PN at conventional oxygen concentrations; (ii) quantification of the relation between TAN SALR and nitrite oxidation at elevated SALR operation; and (iii) determining the effects of TAN SALR on biofilm characteristics, morphology and linking these effects to the performance of the PN MBBR system.

3.4 Methods and Materials

3.4.1 Experimental Set-Up

A single bench-scale, continuous-flow MBBR system with an effective volume of 2 L and height of 14 cm was operated for 34 months in order to achieve stable operation (Fig. S3.1). The reactor was initially filled with a total bulk volume of 1.2 L consisting of clean, high density polyethylene AnoxKaldnes^{TM} (Lund, Sweden) K5 carriers (specific bulk surface area = 800 m^2/m^3; carrier mass = 2605 ± 16 mg) mixed with seeded K5 carriers from a biochemical oxygen demand (BOD) removal municipal integrated film activated sludge (IFAS) wastewater treatment system located in Hawkesbury, Ontario, Canada. The ratio of seeded to clean carriers at start-up was 1:25. The biofilm was established over a period of one month using a synthetic wastewater with an

influent ammonia concentration of 50 mg TAN/L until an ammonia removal efficiency of 97% was achieved. The influent ammonia concentration was gradually increased to 125 mg TAN/L at a rate of 25 mg TAN/L per week until the effluent ammonia concentration was greater than 5 mg TAN/L. The target experimental influent ammonium concentration of 125 mg TAN/L was used in this study to originally simulate TAN concentrations seen in mining wastewater; however, it was determined that the results found in this manuscript have potential municipal applications for sidestream or mainstream PN and the results are framed as such.

The reactor was fed with a synthetic wastewater at a flow rate of 1L per hour providing a hydraulic retention time (HRT) of two hours. Mixing in the reactor was provided via fine bubble aeration at a rate of 4 L/min ($G = 214\ s^{-1}$, eqns 9.1 and 9.2) to achieve adequate carrier movement. To reduce the number of experimental variables, the aeration rate was kept at a constant 4 L/min for the duration of the entire experiment. The air supply was connected to a regulator from which the air flow could be controlled and distributed. The reactor was initially operated at a fill fraction of 60% of the bulk volume which resulted in an SALR of 3.2 g TAN/m^2·d. Reactor conditions such as pH, temperature and DO are shown in Table 3.1. The DO concentrations were not limited to reduce operational intensity associated with adjusting of the DO concentration to stimulate PN. Therefore, the DO concentrations used in this study were elevated compared to DO concentrations used for operations at conventional TAN loading rates as a result of the necessary airflow rate and consumption by the AOB and NOB communities at the elevated loadings used in this research. This methodology resulted in higher DO concentrations than those seen in many studies that worked to limit DO (typically <3 mg O_2/L) (Garrido *et al*., 1997; Fux *et al*., 2004; Wang *et al*., 2009; Ganigué *et al*., 2009; Zhang *et al*., 2011; Bian *et al*., 2017; Li *et al*., 2017) although there have been studies that tested similar DO concentrations under operational conditions quite distinct

from the MBBR design used in this study (Bartroli *et al*., 2010; Isanta *et al*., 2015; Zheng *et al*., 2016).

Table 3.1 Operational parameters at various SALRs (average ± 95% confidence interval)

	Target SALR (g TAN/m^2·d)			
	3	**4**	**5**	**6.5**
Fill Fraction (%)	60	50	40	30
pH	8.0 ± 0.1	7.5 ± 0.1	7.9 ± 0.1	7.9 ± 0.3
Dissolved Oxygen (mg O_2/L)	5.8 ± 0.8	5.6 ± 0.2	5.8 ± 0.1	6.7 ± 0.2
Temperature (˚C)	19.6 ± 0.3	19.8 ± 0.5	20.5 ± 0.2	20.9 ± 0.6

To determine the effects of increasing the TAN SALR, the reactor fill fraction was reduced from 60% to 50%, 40% and 30% of the bulk liquid volume, resulting in measured SALRs of 3.16 ± 0.08, 3.99 ± 0.14, 4.91 ± 0.13 and 6.52 ± 0.001 g TAN/m^2·d. Fill fraction was modified in this study as opposed to influent ammonia concentrations or flow rates to enable the SALR to vary while the influent ammonia concentrations and HRT are maintained at all loading conditions. For ease of discussion in this manuscript, the SALR values of this study will be subsequently referred to as 3, 4, 5 and 6.5 g TAN/m^2·d.

A laboratory scale reactor was operated at an SALR of 3 g TAN/m^2·d and with a corresponding fill fraction of 60% for two months until steady state was reached; with steady state defined as ± 10% fluctuations around average values of TAN, nitrite, and nitrate concentrations over five consecutive data set across a minimum of five days. After steady state was attained, a minimum of five triplicated data points were obtained to quantify the kinetics at an SALR of 3 g TAN/m^2·d and the corresponding fill fraction of 60%. The reactor was then operated at an SALR of 4 g TAN/m^2·d and a 50% fill for two months until steady state was reached and the triplicated

data were obtained. The SALR and fill percent were increased to 5 g TAN/m^2·d and 40% fill, and was operated for a period of two years. Kinetic data was obtained for a period of two-years of operation, at a loading rate of 5 g TAN/m^2·d to ensure that there was no significant long term change in the performance of the system and no instability of operation. The fill fraction was lowered to 30% and SALR increased to 6.5 g TAN/m^2·d after the two-year period and operated for a period of six months. The extended periods of operation were to ensure that there would be no delayed changes in kinetics due to adaptation of nitrifying bacteria, specifically the NOB community.

3.4.2 Wastewater Feed

The reactor was fed with a synthetic wastewater (SWW) recipe based on Delatolla *et al.* (2009), Hoang *et al.* (2014), and Tian *et al.* (2017). The SWW was intended to simulate post-carbon removal wastewater and consisted of (per L of SWW) 0.590 g $(NH_4^+)_2SO_4$ (resulting in a concentration of 125 mg NH_4^+-N/L), 1.625 g $NaHCO_3$, 0.071 g $MgSO_4 \cdot 7H_2O$, 0.029 g $CaCl_2 \cdot 2H_2O$, 0.079 g KH_2PO_4, and 0.005 g $FeSO_4 \cdot 7H_2O$. Essential trace elements were added in quantities of (per L of SWW) 0.1 mg $MnCl_2 \cdot 4H_2O$, 0.025 mg $Na_2MoO_4 \cdot 2H_2O$, 0.1025 mg $CuSO_4 \cdot 5H_2O$, 0.001 mg $CoCl_2 \cdot 6H_2O$, and 0.03 mg $ZnSO_4 \cdot 7H_2O$. To provide a 1:5 sCOD: N ratio to simulate residual carbon that would remain after secondary treatment, peptone, sodium acetate ($NaCH_3COO$) and dextrose ($C_6H_{12}O_6$) were added in concentrations of (per L of SWW) 4.86 mg, 2.592 mg and 4.86 mg, respectively, to provide a total sCOD concentration of 25 mg sCOD/L.

3.4.3 Wastewater Analysis

Standard methods were used for the quantification of total ammonia nitrogen (Nessler Method, 4500C-NH_3), nitrite (4500B-NO_2^-), nitrate (4500A-NO_3^-), sCOD (HACH 8000, HACH company, 2014), and, total suspended solids (TSS) and volatile suspended solids (VSS) (2540D)

(AWWA, 1989). The DO concentration and the temperature in the reactors were measured using a HACH Flexi HQ30d DO probe (Loveland, CO, USA). The pH was measured using a SympHony VWR pH probe (Radnor, PA, USA). Airflow rate was measured using a Dwyer VFA-24 Visi-Float® acrylic air flow meter (Michigan City, IN, USA).

3.4.4 Biofilm Analysis

The biofilm characteristics analyzed include biofilm thickness, mass, morphology and density. Biofilm thickness and morphology were characterized using variable pressure scanning electron microscope (VPSEM) imaging utilizing the Tescan USA Inc, Vega II_XMU SEM (Cranberry, PA, USA) at ~40 Pa (Delatolla *et al*., 2015). Four carriers per reactor condition (totalling 16 carriers) were extracted and stored in a container with a damp paper towel to prevent the carriers from drying out. The carriers were analyzed within four hours of harvesting the carriers from the reactor. The carriers were not modified or treated prior or during analysis. To determine biofilm thickness and morphology, five images per carrier were acquired at 60× magnification, totalling 20 images per loading condition (80 images in total) (Delatolla *et al*., 2012; Young *et al*., 2016). The images were acquired at random locations to prevent bias. One image per carrier (totalling four images per condition) was acquired at 6× magnification to provide an overall image of the carrier to identify anomalies in the biofilm. To visualise the biofilm surface morphology, one image per carrier (totalling four images per loading condition) was acquired at 600× magnification at a random location on the carrier (Young *et al*., 2017a).

The biofilm thickness was measured and quantified using the MedCalc Digimizer Image Analysis Software V.4.6.1 (Ostend, Belgium). A minimum of 1000 thickness measurements per reactor per loading condition were acquired as biofilm thickness variance may be significant under specific operating conditions. A thickness measurement was determined by measuring the distance

between the biofilm carrier and the top of the biofilm. The thicknesses of any empty and clogged pores were not quantified and instead were enumerated for each carrier. The number of clogged carrier-pores per carrier was quantified by visually examining 20 harvested carriers for each loading condition.

Biofilm mass was quantified using a modified protocol based on the procedures described in Delatolla *et al.* (2008) and Forrest *et al.* (2016). Three carriers per condition were harvested and the carriers were dried at 105˚C for a minimum of twelve hours. The carriers were then cooled to room temperature a minimum of one hour in a desiccator after which they were weighed. The biofilm on the carriers were removed and the carriers were again dried for a minimum of twelve hours at 105˚C. After cooling for a minimum of one hour in a desiccator the carriers were weighed. The difference in mass between the carrier with biofilm and the clean carrier was recorded as the biofilm mass. Testing was performed to ensure that the biofilm removal method did not significantly change the mass of the biofilm carrier.

3.4.5 Statistical Analyses

Statistical significance was determined using paired student t-tests with a p-value<0.05 indicating statistical significance (Young *et al*., 2017b). Standard error was used when presenting all figures and tables (p-value <0.05). Correlations were determined using Pearson's correlation.

3.5 Results and Discussion

3.5.1 Design Curve for Partial Nitritation at Elevated SALR

Nitritation and nitratation kinetics were quantified at SALRs of 3, 4, 5, and 6.5 g $N/m^2 \cdot d$, with DO concentrations between 5.5 and 7.0 mg O_2/L and operational temperatures of between 19 and 21°C (Table 3.1). The effects of TAN SALR on nitritation are listed in Table S3.1 and are shown as a design curve in Fig. 3.1 which can be used as a guideline for field applications. The

horizontal dashed lines included in Fig. 3.1 indicate the transition from TAN mass transfer rate limited kinetics to what is likely oxygen mass transfer rate limited TAN removal rates (Ødegaard, 1999). The MBBR system loaded with an SALR of 3 g TAN/m^2·d demonstrated a surface area removal rate (SARR) of 2.01 ± 0.05 g TAN/m^2·d, and a TAN removal efficiency of 63.9 ± 0.4 %. This low removal efficiency indicates that the nitrification kinetics at an SALR of 3 g TAN/m^2·d and SARR of 2.01 ± 0.05 g TAN/m^2·d likely operate at zero-order kinetics with respect to the bulk liquid TAN as the system was operated at oxygen mass transfer limited conditions. At SALRs of 4, 5, and 6.5 g TAN/m^2·d the TAN SARRs did not significantly vary from each other and demonstrated an average SARR of 3.52 ± 0.11 g TAN/m^2·d. No statistical correlation (R^2 = 0.27) was observed between SALR and SARR at these elevated loading rates, indicating that the nitrification reactions were, again, likely zero-order with respect to the TAN concentrations and hence the kinetics were oxygen mass transfer rate limited.

A statistically significant increase in TAN oxidation efficiency from 63.9 ± 0.4 to 82.2 ± 2.2% was observed between SALRs of 3 and 4 g TAN/m^2·d with both reactor conditions operating at similar DO concentrations (Fig. 3.1). It is expected that an increase in loading rate would result in a reduction in TAN oxidation efficiency as the removal rate transitions from first-order to mixed order to zero-order kinetics with respect to bulk TAN concentration (Ødegaard, 1999). The observed increase in ammonia oxidation efficiency alongside an increase in loading rate coincided, in this study, with the MBBR system transitioning from nitrification (oxidation of ammonia to nitrite and the subsequent oxidation of nitrite to nitrate) to PN (partial oxidation of ammonia to nitrite).

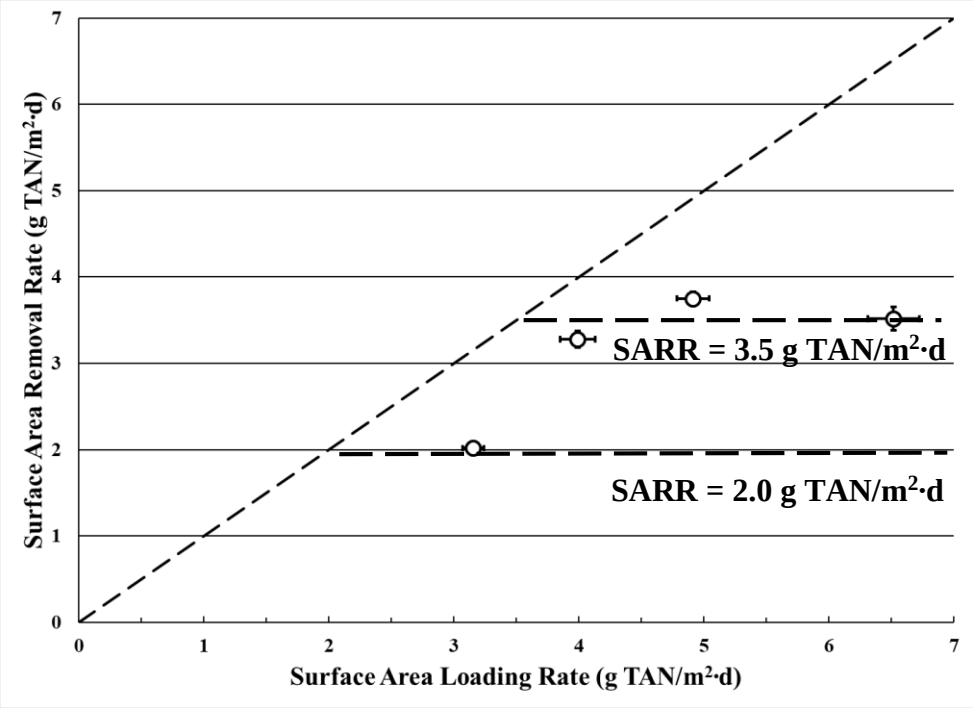

Figure 3.1 TAN SARR across TAN SALR (average ± 95 % CI); 100% removal indicated by diagonal dashed line, and estimated zero-order kinetics conditions at SARR of 2.0 and 3.5 g TAN/m^2·d indicated by horizontal dashed lines

The shift from nitrification to PN was likely due to a shift in the biofilm bacterial community's activity favouring AOB over NOB (Bartroli *et al*., 2010; Ciesielski *et al*., 2010; Isanta *et al*., 2015). As the AOB population outcompetes the NOB population in the biofilm for DO, the shared electron acceptor, the AOB consumption of oxygen will likely increase; resulting in an increase in the observed ammonia oxidation efficiency (Brockmann and Morgenroth, 2008). The fine bubble aeration rate was maintained at 4 L/min at SALRs of 3 and 4 g TAN/m^2·d, with the bulk DO concentration being statistically similar at the two loading conditions. Hence, it is likely that the oxygen consumed for nitrite oxidation by the NOB population at an SALR of 3 g TAN/m^2·d instead contributed to the ammonia oxidizing AOB population at an SALR 4 g TAN/m^2·d. It should be noted that the TAN removal efficiency subsequently decreased to 76.4± 1.5% at a loading rate of 5 g TAN/m^2·d and further decreased to 54.0 ± 2.9% at a loading rate of

6.5 g TAN/m^2·d. The decrease in TAN oxidation efficiency with increasing SALR was due to stagnating SARRs which suggests that the system remained oxygen mass transfer rate limited and continued to perform PN as the SALR increased above 4 g TAN/m^2·d.

3.5.2 Relation between TAN SALR and Nitrite Oxidation at Elevated SALR

The percentage of total oxidized TAN that remained as nitrite (NO_x as nitrite) at an SALR of 3 g TAN/m^2·d was measured at 8.45 ± 0.4%, signifying nitrification. As the SALR increased from 3 g TAN/m^2·d to 4 g TAN/m^2·d the TAN SARR increased from 2.01 ± 0.05 g TAN/m^2·d to 3.28 ± 0.10 g TAN/m^2·d, while the percentage of NO_x as nitrite increased to 44.05 ± 4.7%. At an SALR of 6.5 g TAN/m^2·d the TAN SARR was 3.52 ± 0.001, while the percentage of NO_x as nitrite was 99.8 ± 0.5 % of the total oxidized TAN, indicating the achievement of PN and the likely suppression of nitrite oxidation activity in the biofilm (Fig. 3.2). The complete reduction of nitrification efficiency has also been observed at an SALR of 3.76 g TAN/m^2·d by Ciesielski *et al.* (2010), who operated two nitrifying MBBRs in series treating leachate. Huiliñir *et al.* (2010) found success operating a rotating disk biofilm reactor at very high loading rates, while utilizing high pH values of 8.5 and low DO concentrations during continuous activity. In contrast, Fux *et al*. (2004) and Gaul *et al.* (2005) who operated at temperatures typical to sidestream processes, did not find that elevated loading rates were sufficient to suppress NOB.

In the present study the percentage of NO_x as nitrite was found to be well modelled across SALR (R^2 = 0.9761), with almost complete nitrification of the oxidized TAN occurring at a SALR of less than 3 g TAN/m^2·d and almost complete PN at an SALR of 6.5 g TAN/m^2·d, as demonstrated by the percentage of NO_x as nitrite approaching 100% at elevated loading rates (Fig. 3.2). Hence this relation presents a simple model for describing the influence of SALR on the percentage NOx distribution. The distribution is representative of the shift in biofilm activity from

nitrification to nitritation as the SALR increases beyond conventional rates. Furthermore, there is a strong linear relationship between SALR and the percentage of NO_X as nitrite which shows potential for the relation shown in Fig. 3.2 to be used as a design curve for SALR to achieve PN in MBBR systems. This relationship is significant because it reduces the operational intensity of PN systems and provides a design pathway towards a simple and passive PN system.

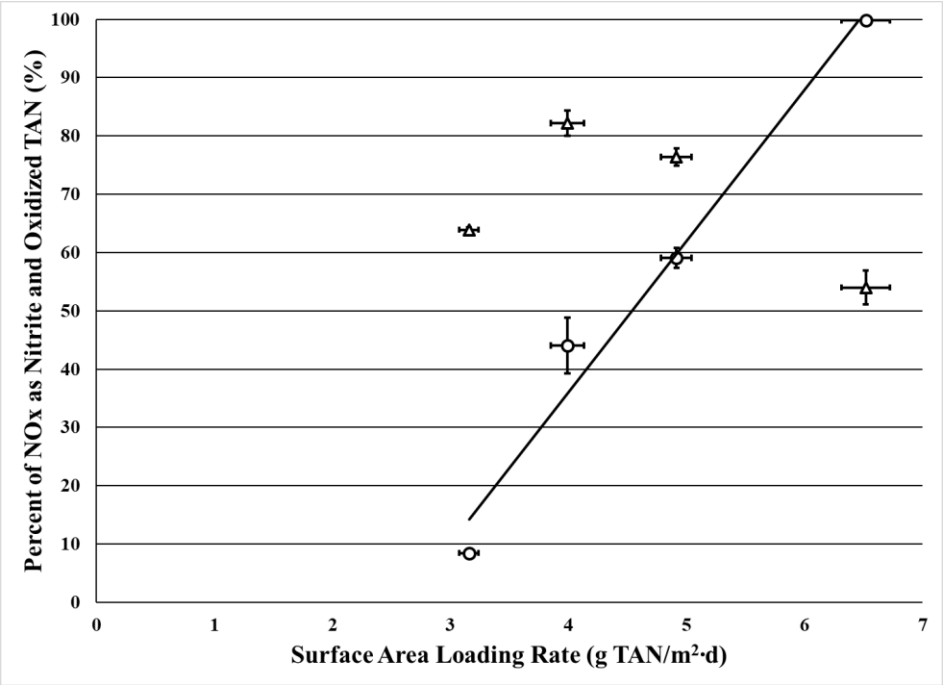

Figure 3.2 Percent of total NO_x as nitrite across SALR(○), and percent of TAN oxidized (△) (average ± 95% CI); projected regression (solid line) with an equation of Percent of NO_x as Nitrite (%) = 25.95(SALR (g TAN/m^2·d) - 2.6) (R^2=0.976)

Effluent TAN concentrations decreased as the loading rate increased from 3 g TAN/m^2·d to 4 g TAN/m^2·d, and then subsequently increased as the SALR continued to increase (Fig. 3.3). Nitrite accumulation increased with increasing SALR and nitrate production decreased as the SALR increased. At an SALR of 6.5 g TAN/m^2·d the effluent TAN concentration was 60.1 ± 3.0 mg TAN/L and the effluent nitrite concentration was 68.6 ± 2.1 mg NO_2^--N/L, demonstrating an appropriate nitrogen speciation for subsequent anammox processes. Hence, the SARR values

measured at elevated SALRs of 4 g TAN/m^2·d to 6.5 g TAN/m^2·d, along with the low concentration of nitrate and the percent NO_x as nitrite demonstrate that SALR loading can be an effective and efficient strategy for achieving PN in a low operational intensive MBBR system without limiting DO.

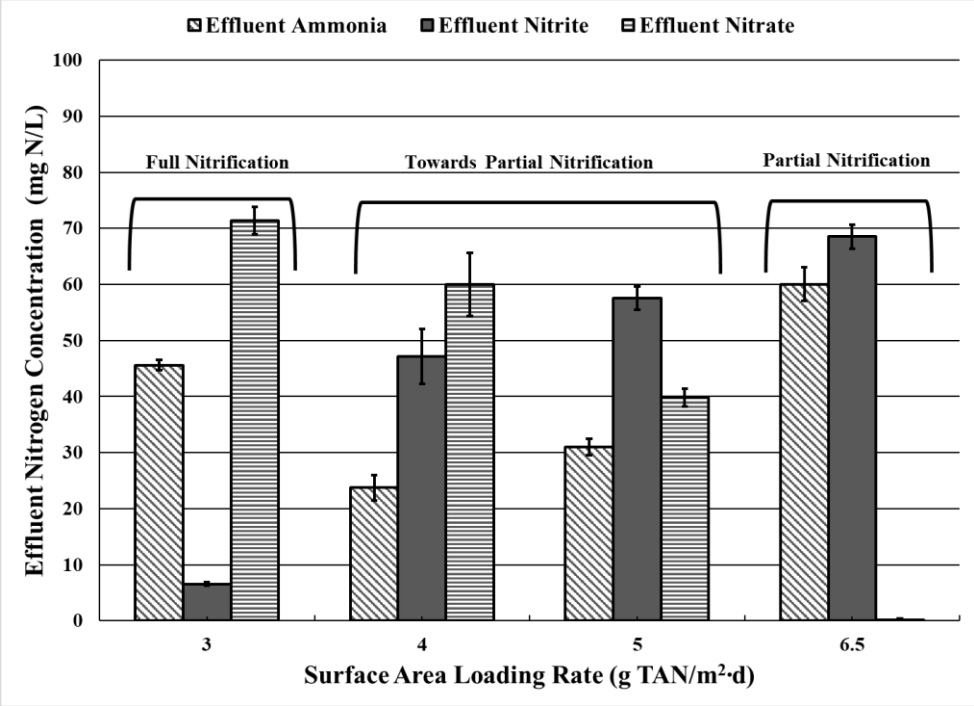

Figure 3.3 Effluent ammonia (diagonal shading), nitrite (solid fill) and nitrate (horizontal shading) concentrations at each loading condition (average ± 95% CI)

3.5.3 TAN SALR Effects on Biofilm Characteristics and Morphology

The meso-scale effects of TAN loading rate on the biofilm were quantified through the analyses of biofilm characteristics such as biofilm thickness, mass, density, morphology, total suspended solids (TSS), and solids retention time (SRT) (Table 3.2). There was a statistically significant increase in the thicknesses of the biofilms as the SALR increased from 3 to 6.5 TAN/m^2·d. The increase in biofilm thickness strongly correlated to an increase in TAN SALR (R^2 =0.995). An increase in biofilm thickness is expected as a result of increased loading rate as the

potential to support greater quantities of nitrifying bacteria increases (Bryers, 1987; Flemming, 1993). The velocity gradient (eqns 9.1 and 9.2) of 214 s^{-1} was constant throughout the experiment; therefore, the mixing did not contribute to the change in biofilm thickness between TAN loading rates.

An increase in biofilm thickness is also shown in previous works to be a result of the bacterial community response to operational factors such as temperature, loading rate, and inhibitor concentrations (Beer *et al*., 1994; White and Gadd, 2000; Bjornberg *et al*., 2009). At a loading rate of 6.5 g TAN/m^2·d, significant clogging of the biofilm carrier-pores was evident with an average of 59 ± 2 clogged carrier-pores out of 64 total carrier-pores. Conversely, at the lower loaded conditions of 3 to 5 g TAN/m^2·d there were no clogged carrier-pores. The clogging of the carrier-pores may have been a result of the specific geometry of the K5 carrier and in particular the pore size of the carrier, as well as the growth of thick biofilm that is associated with high loaded systems.

The masses of the biofilms were not statistically significantly different between loading rates of 3 and 4 g TAN/m^2·d, and between loading rates of 5 and 6.5 g TAN/m^2·d, and was shown to be statistically significantly different among all other loading rates (Table 3.2). The loading rates of 3 and 6.5 g TAN/m^2·d had statistically significantly different densities with no statistically significant difference being observed among the other loading rates. Biofilm morphology, the shape of the biofilm, was qualitatively analysed (Fig. S3.2) and it was found that there was a distinct increase in roughness, heterogeneity and lack of uniformity in the shape of the biofilm correlating with an increase in SALR. Hence, this increased roughness and heterogeneity is shown to be indicative of highly loaded, PN MBBR biofilms.

There was a statistically significant decrease in TSS concentrations from 68.4 ± 18.0 to 33.7 ± 3.4 mg/L between the loading rates of 4 and 5 g TAN/m^2·d. Furthermore, there was a statistically significant increase in SRT from 4.2 ± 1.4 to 9.1 ± 1.5 d, as the loading rate increased from 4 to 5 g TAN/m^2·d. This change in SRT may be due to shifts in the microbiome as well as changes in the duration in experimental phase, where the system operated at an SALR of 4 g TAN/m^2·d for 2 months and operated at an SALR of 5 g TAN/m^2·d for a period of 2 years, which can effect biofilm maturity. It should be noted that the observed SRT values were very low for attached growth systems, where typical SRTs for MBBR systems were around 40 days (Gong *et al*., 2012). The elevated SRTs observed were likely due to the elevated loading rates and activities observed during operations.

Table 3.2 Biofilm characteristics (average ± 95% CI)

	Target SALR (g TAN/m^2·d)			
	3	**4**	**5**	**6.5**
Biofilm Thickness (μm)	167 ± 36	239 ± 56	338 ± 62	572 ± 148
Biofilm Mass (mg /carrier)	22.3 ± 1.7	24.5 ± 3.3	35.6 ± 2.2	39.4 ± 3.0
Biofilm Density (kg/m^3)	54.7 ± 16	42.2 ± 16	43.3 ± 11	28.3 ± 9.5
Avg Clogged Carrier-Pores (Maximum 64 total carrier –pores)	0	0	0	59 ± 2
Total Suspended Solids (mg TSS/L)	68.4 ± 18.0	69.5 ± 24.1	33.7 ± 3.4	27.2 ± 3.1
Solids Retention Time (d)	4.2 ± 1.4	3.9 ± 1.8	9.1 ± 1.5	9.4 ± 1.8

3.6 Discussion on Achieving Partial Nitritation at Elevated Loading Conditions

The operation of the MBBR system to achieve PN at elevated SALRs while maintaining conventional DO concentrations is hypothesized to be a result of multiple contributing factors

resulting from the elevated TAN loading rate, including: the resultant large biofilm thickness, the resultant morphology of the biofilm, and the mass transfer effects affecting the embedded AOB and NOB populations. Previous studies have suggested alternative control strategies for NOB suppression, including: FA, FNA, DO/TAN ratio and limited bulk DO concentrations (Brockmann and Morgenroth, 2010; Park *et al*., 2010; Park *et al*., 2014; Bartroli *et al*., 2010; Isanta *et al*., 2015; Bian *et al*., 2017). One of the objectives of this study was to refrain from restricting the DO concentration; hence, the strategy of limited bulk DO concentration did not contribute to PN. While it is possible that FA, FNA and the DO/TAN ratio can contribute to the suppression of NOB, it is unlikely that these are the primary pathways for suppression during this study due to the lack of correlation of these parameters across the four loading conditions (Table 3.3).

FA and DO/TAN in this study correlate to an increase in percent nitrite accumulation only after a significant over-loading took place, resulting in a shift of removal kinetics towards nitritation. Although Bartroli *et al.* (2010) were able to achieve full nitritation with very little nitrate accumulation at DO/TAN ratios of 0.25 g O_2/g TAN or lower using aerated granules while operating at 30˚C; in this study PN, with no nitrate production, was only achieved once the DO/TAN ratio was 0.11 g O_2/g TAN at the highest SALR and was not achieved at the lowest loading rate despite having a DO/TAN ratio of 0.14 g O_2/g TAN. Likewise, in this study FA was highest at the lowest loading rate of 3 g TAN/m^2·d where very little oxidized TAN remained as nitrite and, due to the pH values of this study the FNA was consistently very low. It has also been shown that over time NOB can become resilient to the inhibitory effects of FA and FNA (Duan *et al*., 2019). Therefore, these alternative control strategies were likely not the controlling factor causing PN. Conversely, high loading rate has not shown to be sufficient as a method to achieve PN on its own (Fux *et al*., 2004), therefore the effect of high loading rates in this study along with

the excess biofilm thickness relative to the porosity and structure of the carriers was likely able to limit DO uptake by NOB, suppress their activity and hence achieve stable and long term PN with no oxygen control necessary. While the excess biofilm thickness may limit the oxygen available to the microbiome as a whole, the AOB dwell in the upper layers and thus have the most immediate access to oxygen. This means that the AOB would be less affected by the overall oxygen restriction than the NOB that live deeper in the biofilm and only have access to the oxygen that was allowed to penetrate deeply. MBBR carriers with appropriate pore sizes are hence likely necessary to achieve the large biofilm thickness and the clogged biofilm structure that is likely necessary for PN that was observed in this study.

Table 3.3 Parameters that may effect NOB suppression

	Target SALR (g TAN/m^2·d)			
	3	**4**	**5**	**6.5**
Free Ammonia (FA) (mg N/L)	1.53	0.22	0.719	1.39
Free Nitrous Acid (FNA) (mg N/L)	$3.58x10^{-5}$	$9.59x10^{-4}$	$4.55x10^{-4}$	$5.55x10^{-4}$
DO/TAN (mg O_2/mg TAN)	0.14	0.23	0.19	0.11

3.7 Conclusion

This study investigated the potential of achieving PN using the MBBR technology via a passive loading rate design strategy. An increase in TAN oxidation efficiency was observed as SALR increased from 3 to 4 g TAN/m^2·d, while also demonstrating a shift in nitrification kinetics towards partial nitrification. This shift in kinetics was hypothesized to be due to the unconventionally elevated TAN SALR and reduced mass transfer across elevated biofilm thicknesses as opposed to the restriction or active limitation of DO conventionally used in previous PN systems. Operations at an SALR of 6.5 g TAN/m^2·d and a DO concentration of 6.7 ± 0.2 mg

O_2/L, demonstrated 100% nitrite accumulation and a desirable stoichiometric ratio of ammonium and nitrite (45% NH_4^+-N and 55% NO_2^--N) for the anammox process from a PN MBBR system. As such, the results have the potential to provide a basis for the design of small footprint, low operation intensity and high removal rate PN systems. This knowledge base can be further expanded by the investigation of high loading rate as a passive design strategy at municipal ammonium concentrations with the intention of moving to pilot scale.

3.8 Supplemental Material

Table S3.1 Influent and effluent nitrogen concentrations

	Target SALR (g TAN/m^2·d)			
	3	**4**	**5**	**6.5**
Measured SALR (g TAN/m^{2}d)	3.16 ± 0.08	3.99 ± 0.14	4.91 ± 0.13	6.52 ± 0.001
SARR (g TAN/m^{2}d)	2.01 ± 0.05	3.28 ± 0.10	3.75 ± 0.09	3.52 ± 0.001
Effluent TAN (mg TAN/L)	45.6 ± 0.9	23.7 ± 2.3	31.0 ± 1.5	60.1 ± 3.0
Percent of TAN Oxidation (%)	63.9 ± 0.4	82.2 ± 2.2	76.4 ± 1.5	54.0 ± 2.9
Effluent Nitrite (mg NO_2^--N/L)	6.6 ± 0.3	47.2 ± 4.9	57.6 ± 2.1	68.6 ± 2.1
Effluent Nitrate (mg NO_3^--N/L)	71.4 ± 2.5	60.0 ± 5.6	39.8 ± 1.6	0.1 ± 0.2
Percent NO_X as Nitrite (%)	8.4 ± 0.4	44.1 ± 4.7	59.1 ± 1.7	99.8 ± 0.2
Influent Nitrogen (mg/L)	127.4 ± 4.4	134.1 ± 6.0	132.1 ± 4.1	131.1 ± 5.5
Effluent Nitrogen (mg/L)	123.6 ± 3.4	130.9 ± 7.2	128.4 ± 3.9	128.7 ± 6.4
Nitrogen Balance (%)	97.1	97.6	97.2	98.2

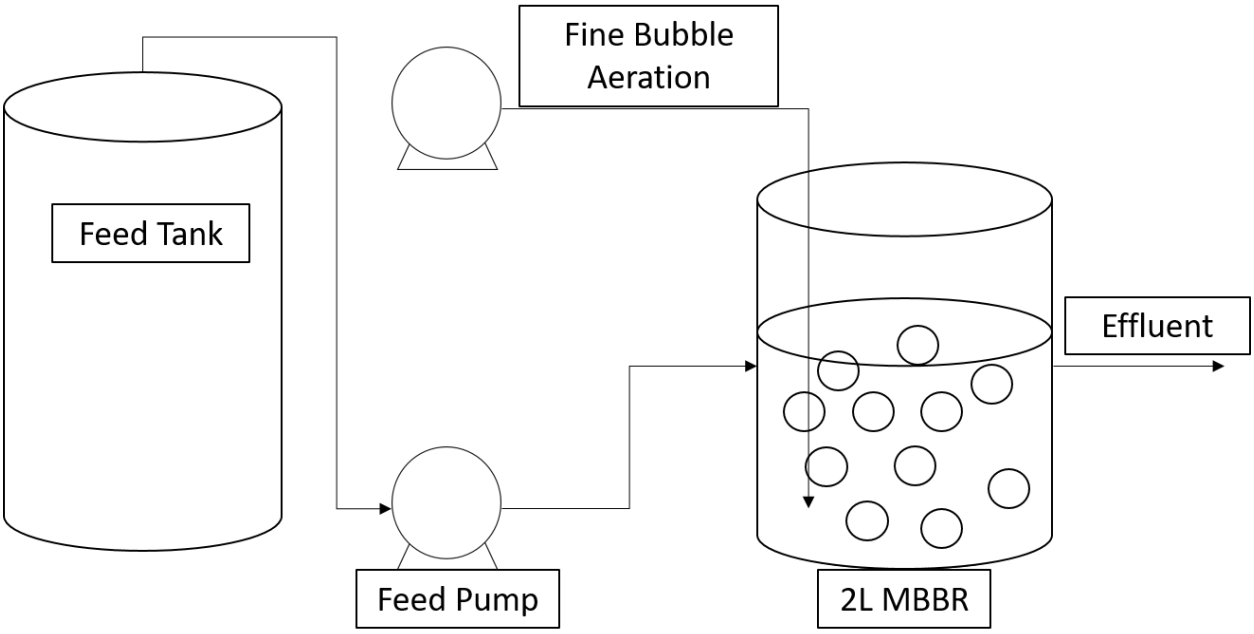

Figure S3.4 Basic system diagram consistent of a feed tank, a centripetal pump to transport the feed solution, fine bubble aeration, and a 2L moving bed biofilm reactor filled with AnoxK^{TM}5 carriers.

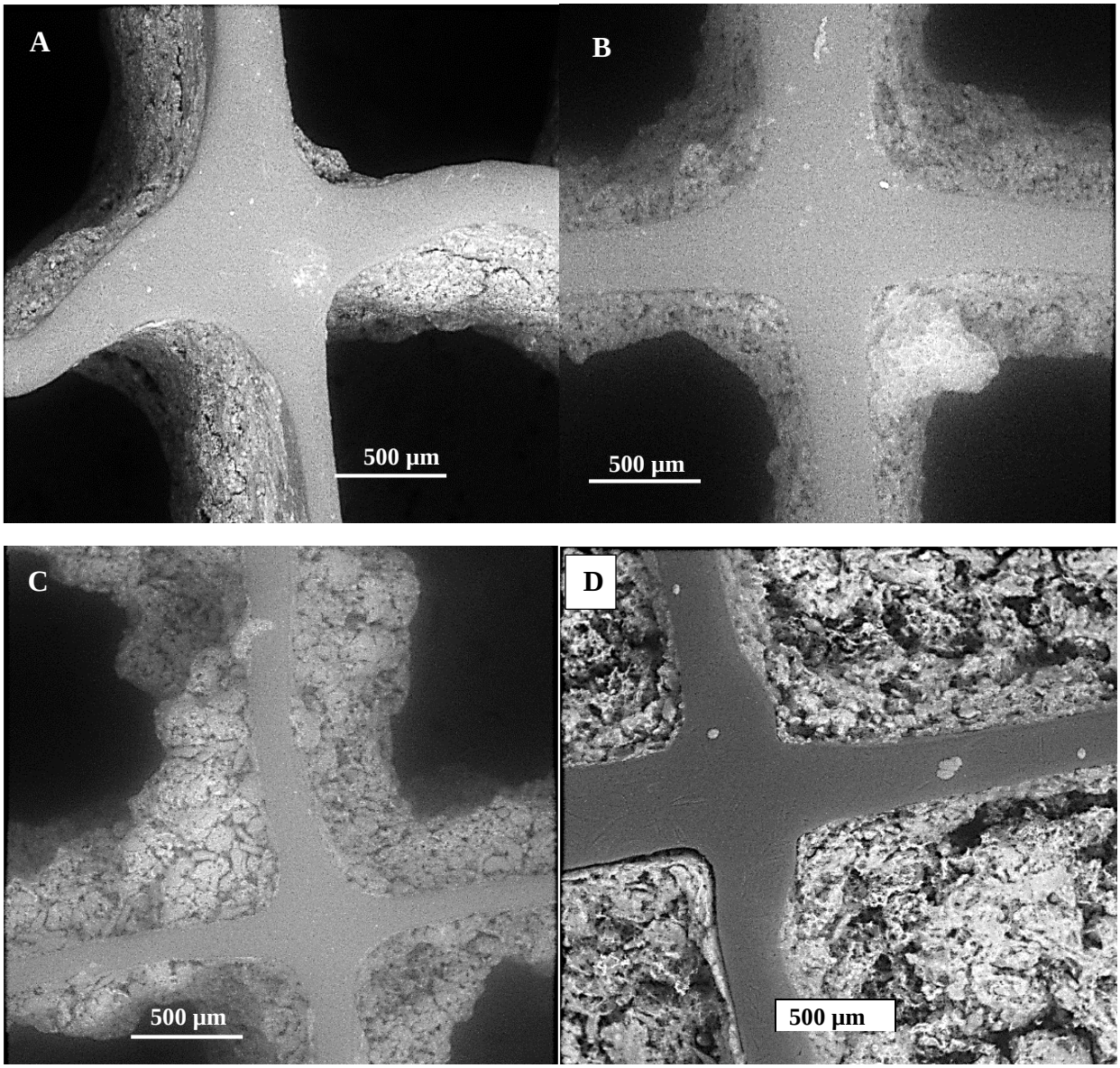

Figure S3.5 VPSEM images for biofilm thickness and morphology analyses acquired at 60× magnification at SALR of a) 3 g TAN/m^2·d, b) 4 g TAN/m^2·d, c) 5 g TAN/m^2·d and d) 6.5 g TAN/m^2·d

3.9 References

APHA, AWWA, WEF. (1989) *Standard methods for examination of water and wastewater.* Washington, D.C., 17th edition, 1989

Bartroli, A., Pérez, J., Carrera, J. (2010) Applying ratio control in a continuous granular reactor to achieve full nitritation under stable operating conditions. *Environmental Science and Technology* 44: 8930-8935

Beer, DD., Stoodley, P., Roe, F., Lewandowski, Z. (1994) Effects of biofilm structures on oxygen distribution and mass transport. *Biotechnology and Bioengineering* 43: 1131-1138

Bian, W., Zhang, S., Zhang, Y., Li, W., Kan, R., Wang, W., Zheng, Z., Li J. (2017) Achieving nitritation in a continuous moving bed biofilm reactor at different temperatures through ratio control. *Bioresource Technology* 226:73-79

Bjornberg, C., Lin, W., Zimmerman. RA. (2009) Effect of temperature on biofilm growth dynamics and nitrification in a full-scale MBBR system. *Proceedings of the Water Environment Federation, WEFTEC: Session 61 through 70*: 4407-4426

Brockmann, D., Morgenroth, E. (2008) 'Partial nitrification in biofilms: inhibition versus competition. *Outline paper for IWA world water congress*, Sept 7-12

Brockmann, D., Morgenroth, E. (2010) Evaluating operating conditions for outcompeting nitrite oxidizers and maintaining partial nitrification in biofilm systems using biofilm modeling and Monte Carlo filtering. *Water Research* 44(6): 1995-2009

Bryers, JD. (1987) Biologically active surfaces: processes governing the formation and persistence of biofilms. *Biotechnology Progress* 3: 57-68

Canadian Fisheries Act: Wastewater Systems Effluent Regulations. 2012. Canada Gazette Part II, 146(15). Retrieved from the Canada Gazette website: http://www.gazette.gc.ca/rp-pr/p2/2012/2012-07-18/html/sor-dors139-eng.html (Accessed May 2018)

Christensson, M., Ekström, S., Chan, AA., Le Vaillant, E., Lemarie, R. (2013) Experience from start-ups of the first ANITA Mox plants. *Water Science and Technology* 67:2677-2684

Ciesielski, S., Dorota, K., Ewelina, K., Przenyslaw, K. (2010) Characteriszation of Bacterial Structures in a two-stage moving bed biofilm reactor (MBBR) during nitrification of landfill leachate. *J. Microbiol. Biotechnol* 20: 1140-1151

Council Directive 91/271/EEC of 27 May 1991 concerning urban waste water treatment. https://www.ecolex.org/details/legislation/council-directive-91271eec-concerning-urban-waste-water-treatment-lex-faoc013224. (Accessed May 2018)

Delatolla, R., Babarutsi, S. (2005) Parameters effecting hydraulic behaviour of aerated lagoons. *Journal of Environmental Engineering* 131(10): 1404-1413

Delatolla, R., Berk, D., Tufenkji, N. (2008) Rapid and reliable quantification of biofilm weight and nitrogen content of biofilm attached to polystyrene beads. *Water Research* 42:3082-3088

Delatolla, R., Tufenkji, N., Comeau, Y., Gadbois, A., Lamarre, D., Berk, D. (2009) Kinetic analysis of attached growth nitrification in cold climates. *Water Science and Techology* 60:1173-1184

Delatolla, R., Tufenkji, N., Comeau, Y., Gadbois, A., Lamarre, D., Berk, D. (2012) Effects of long exposure to low temperatures on nitrifying biofilm and biomass in wastewater treatment. *Water Environment Research* 84: 328-338

Delatolla, R., Séguin, C., Springthorpe, S., Gorman, E., Campbell, A, I. Douglas. (2015) Disinfection byproduct formation during biofiltration cycle: implications for drinking water production. *Chemosphere* 136: 190-197

Duan, H., Ye, L., Lu, X., Yuan, Z. (2019) Overcoming nitrite oxidizing bacteria adaptation through alternating sludge treatment with free nitrous acid and free ammonia. *Environ. Sci. Technol*. DOI: 10.1021/acs.est.8b06148

Durián, U., del Val Rio, A., Campos, JL., Mosquera-Corral, A., Méndez, R. (2014) Enhanced ammonia removal at room temperature by pH controlled partial nitrification and subsequent anaerobic ammonium oxdation. *Environmental Technology* 35: 383-390

Flemming, HC. (1993) Biofilms and environmental protection. *Water Science and Technology* 27: 1-10

Forrest, D., Delatolla, R., Kennedy, K. (2016) Carrier effects on tertiary nitrifying moving bed biofilm reactor: An examination of performance, biofilm and biologically produced solids. *Environmental Technology* 37: 662-671

Fux, C., Huang, D., Monti, A., Siegrist, H. (2004) Difficulties in maintaining long-term partial nitritation of ammonium-rich sludge digester liquids in a moving-bed biofilm reactor (MBBR). *Water Science and Technology* 49: 53-60

Ganigué, R., Gaborró, J., Sànchez-Melsió, A., Ruscalleda, M., López, H., Vila, X., Colprim, J., Balaguer, MD. (2009) Long-term operation of a partial nitritation pilot plant treating leachate with extremely high ammonium concentration prior to an anammox process. *Bioresource Technology* 100(23): 5624-5632

Garrido, JM., van Benthum, WAJ., van Loosdretcht, MCM., Heijnen, JJ. (1997) Influence of dissolved oxygen concentration on nitrite accumulation in a biofilm airlift suspension reactor.

Biotechnology and Bioengineering 53(2): 168-178. Doi: 10.1002/(sici)1097-0290(19970120)53:2<168::aid-bit6>3.0.co;2-m

Gaul, T., Märker, S., Kunst, S. (2005) Start-up of moving bed biofilm reactors for deammonification: the role of hydraulic retention time, alkalinity and oxygen supply. *Water Science and Technology* 52(7): 127-133

Gilbert, EM., Agrawal, S., Schwartz, T., Horn, H., Lackner, S. (2015) Comparing different reactor configurations for partial nitritation/anammox at low temperatures. *Water Research* 81: 92-100

Gong, L., Jun, L., Yang, Q., Wang, S., Ma, B., Peng, Y. (2012) Biomass characteristics and simultaneous nitrification-denitrification under long sludge retention time in an integrated reactor treating rural domestic sewage. *Bioresource Technology* 119: 277-284

Hao, X., Heijnen, JJ., van Loosedrecht, MCM. (2002) Sensitivity analysis of a biofilm model describing a one-stage completely autotrophic nitrogen removal (Canon) process. *Biotechnology and Bioengineering* 77: 266-277

Hellinga, C., Schellen, AAJC., Mulder, JW., van Loosdrecht, MCM., Heijnen, JJ. (1998) The SHARON process: an innovative method for nitrogen removal from ammonium-rich wastewater. *Water Science and Techology* 37: 135-142

Hoang, V., Delatolla, R., Laflamme, E., Gadbois, A. (2014) An investigation of moving bed biofilm reactor nitrification during long-term exposure to cold temperatures. *Water Environment Research* 86:36-42

Huiliñir, C., Romero, R., Muñoz, C., Bornhardt, C., Roeckel, M., Antileo, C. (2010) Dynamic modeling of partial nitrification in a rotating disk biofilm reactor: Calibration, validation and simulation. *Biochemical Engineering Journal* 52(1): 7-18

Isanta, E., Reino, C., Carrera, J., Pérez, J. (2015) Stable partial nitritation for low-strength wastewater at low temperature in an aerobic granular reactor. *Water Research* 80(1): 149-158

Lackner, S., Gilbert, EM., Vlaeminck, SE., Joss, A., Horn, H., van Loosdrecht, MCM. (2014) Full-scale partial nitritation/anammox experiences–an application survey. *Water Research* 55: 292–303

Laureni, M., Falâs. P., Robin, O., Wick, A., Weissbrodt, DG., Nielsen, JL., Ternes, TA., Morgenroth, E., Joss, A. (2016) Mainstream partial nitritation and anammox: long-term process stability and effluent quality at low temperatures. *Water Research* 101: 628-639

Li, Y., Wang, Z., Li, J., Wei, J., Zhang, Y., Zhao, B. (2017) Inhibition kinetics of nitritation and half-nitritation of old landfill leachate in a membrane bioreactor. *Journal of Bioscience and Bioengineering* 123(4): 482-488

Mulder, A., Van de Graaf, AA., Robertson, LA., Kuenan, JG. (1995) Anaerobic ammonium oxidation discovered in a denitrifying fluidized bed reactor. *FEMS Microbiology Ecology* 16: 177-184

Ødegaard H (1999) The moving bed biofilm reactor. *Water Environmental Engineering and Reuse of Water*, Hokkaido Press:250-305

Park, S., Wookeun, B., Rittmann, BE. (2010) Operational boundaries for nitrite accumulation in nitrification based on minimum/maximum substrate concentrations that include effects of oxygen limitation, pH, and Free Ammonia and Free Nitrous acid inhibition. *Environmental Science and Technology* 44: 335-342

Park, S., Chung, J., Rittmann, BE., Wookeun, B. (2014) Nitrite accumulation from simultaneous free-ammonia and free-nitrous-acid inhibition and oxygen limitation in a continuous flow biofilm reactor. *Biotechnology and Bioengineering* 112(1): 43-52

Peng, Y., Gao, S.,Wang, S., Bai, L. (2007) Partial nitrification from domestic wastewater by aeration control at ambient temperature. *Chinese Journal of Chemical Engineering* 15: 115-121

Piculell, M., Christensson, M., Jönsson, K., Welander, T. (2016) Partial nitrification in MBBRs for mainstream deammonification with thin biofilms and alternating feed supply. *Water Science and Technology*. 73: 1253-1260

Rosenwinkel, K., and Cornelius, A. (2005) Deammonification in the moving-bed process for the treatment of wastewater with high ammonia content. *Chemical Engineering and Technology* 28: 49-52

Strous, M., Heijnen, JJ., Kuenen, JG., Jetten, MSM. (1998) The sequencing batch reactor as a powerful toll to study very slowly growing micro-organisms. *Applied Microbiology and Biotechnology* 50: 589-596

Tian, X., Ahmed, W., Delatolla, R. (2017) Nitrifying bio-cord reactor: performance optimization and effects of substratum and air scouring. *Environmental technology* DOI: 10.1080/09593330.2017.1397760

U.S. Clean Water Act, 33 U.S.C. § 1251 et seq. 1972. U.S Environmental Protections Agency, Washington. https://www.epa.gov/laws-regulations/summary-clean-water-act. (Accessed February 2018)

van Dongen, U., Jetten, MSM., van Loosdrecht, MCM. (2001) The SHARON-Anammox process for treatment of ammonium rich wastewater. *Water Science and Technology* 44: 153-160

Wang R., Terada, A., Lackner, S., Smets, BF., Henze, M., Xia, S., Zhao, J. (2009) Nitritation performance and biofilm development of co-and counter – diffusion biofilm reactors: Modeling and experimental comparison. *Water Research* 43(10): 2699-2709

Wett, B. (2007) Development and implementation of a robust deammonification process. *Water Science and Technology* 56: 81-88

White, C., Gadd, GM. (2000) Copper accumulation by sulfate reducing bacterial biofilms. *FEMS Microbiology Letter* 183: 313-318

World Resources Institute, http://www.wri.org/our-work/project/eutrophication-and-hypoxia/sources-eutrophication (Accessed May 2018)

Young, B., Delatolla, R., Ren, B., Kennedy, K., Laflamme. E., Stintzi, A. (2016) Pilot-scale tertiary MBBR nitrification at 1°C: characterization of ammonia removal rate, solids settleability and biofilm characteristics. *Environmental Technology*. 37: 2124-2132

Young, B., Delatolla, R., Kennedy, K., Laflamme, E., Stintzi, A. (2017a) Low temperature MBBR nitrification: microbiome analysis. *Water Research* 111: 224-233

Young, B., Delatolla, R., Abujamel, T., Kennedy, K., Laflamme, E., Stintzi, A. (2017b) Rapid start-up of nitrifying MBBRs at low temperatures: nitrification, biofilm response and microbiome analysis. *Bioprocess and Biosystems Engineering* 40: 731-739

Zhang, L., Yang, J., Hira, D., Fuji, T., Furukawa, K. (2011) High-rate partial nitrification treatment of reject water as a pretreatment for anaerobic ammonium oxidation (anammox). *Bioresource Technology* 102(4): 3761-3767

Zheng, Z., Li, Z., Ma, J., Chen, G., Bian, W., Li, J., Zhao, B. (2016) The nitritation performance of biofilm reactor for treating domestic wastewater under high dissolved oxygen. *Journal of Environmental Science* 42: 267-274

CHAPTER 4 – MICROBIAL COMMUNITY ANALYSIS OF PARTIAL NITRITATION ACHIEVED USING ELEVATED LOADING RATES

4.1 Context

Chapter 4 presents the research article entitled *Microbial community analysis of partial nitritation achieved using elevated loading rates*. This article is in preparation for submission for publication. This study investigates the meso-, micro-, and molecular-scale response of the biofilm to elevated TAN SALR values as a passive, low operational intensity strategy to achieve partial nitritation. This article discusses changes in kinetics, biofilm characteristics, cell viability, and the microbiome to propose the method of suppression of the NOB as activity suppression or population suppression.

4.2 Abstract

There is an urgent need to develop cost-effective, low operational intensity, and efficient ammonia treatment systems to meet stringent wastewater discharge regulations. A moving bed biofilm reactor (MBBR) system operated at elevated total ammonia nitrogen (TAN) loading rates ranging from 3 to 6.5 g TAN/m^2·d has shown promise as a design strategy to achieve robust partial nitritation (PN) without the need for intense operational measures to inhibit the nitrite oxidizing microbial population. An investigation of the biofilm, the viability of the embedded cells and the microbial ecology is necessary to fully understand this low operational intensity design. The mechanism responsible for the system to attain robust PN is shown to be the suppression of nitrite oxidizing bacteria (NOB) activity, as there was a statistically significantly similar NOB count per reactor at various loading rates; however, there was a decrease of two orders of magnitude in the NOB activity. This decrease in NOB activity is likely due to numerous factors, including an increase in thickness of the biofilm, as well as the relative increase in ammonia oxidizing bacteria

(AOB) that preferentially uptake oxygen compared to NOB. The AOB to NOB ratio increased by a factor of 1:2.6 to 8.7:1 at loading rates of 3 to 6.5 g TAN/m^2·d, respectively. As such, the elevated loading rates of this design strategy results in the suppression of the NOB population due to limited access to oxygen via mass transfer limitations through thick biofilm and competition with an augmented AOB population in the biofilm.

4.3 Introduction

Nitrification, the oxidation of total ammonia nitrogen (TAN) to nitrite (nitritation) by ammonia oxidizing bacteria (AOB) followed by the oxidation of nitrite to nitrate (nitratation) by nitrite oxidizing bacteria (NOB), in combination with denitrification is the most common treatment method to remove TAN from wastewater. The modern alternative treatment process of partial nitritation (PN) in combination with anaerobic ammonia oxidation (anammox), also referred to as PN/A, has commercial and environmental benefits over nitrification and denitrification. These benefits include 60% lower oxygen requirements, 89-100% less carbon requirements, and 78% less biomass production (Strous *et al.,* 1998; Metcalf and Eddy, 2014). Many PN studies have shown a significant decrease in the NOB population when exposed to adverse conditions and inhibitors (Joo *et al.,* 2000; Yun and Kim, 2003; Ganigué *et al.,* 2009; Dosta *et al.,* 2015; Connan *et al.,* 2018; Duan *et al.,* 2019b); however, many of these studies were performed for short operational periods of time while longer term studies have shown that the NOB population either recovers or experiences a change in dominant NOB (Fux *et al.,* 2004; Duan *et al.,* 2019a). Therefore, many control strategies that aim to directly inhibit NOB are unsuccessful in the long term, or require complex, continual control strategies to provide stable PN in PN/A systems.

There has been significant research to achieve stable PN/A, either as a pair of processes or in a single process, using either suspended growth or attached growth technologies. Achieving

PN/A has been successful in a single vessel as these systems operate under low dissolved oxygen (DO) conditions of less than 0.5 mg O_2/L to avoid inhibiting the anammox bacteria. Single reactor technologies include the, DEMON, and CANON systems (Sliekers *et al.,* 2002; Wett., 2006) which are suspended growth systems, and the Anita MOX system (Christensson *et al.,* 2013), which is an integrated fixed film activated sludge system using the moving bed biofilm reactor (MBBR) technology. NOB have been shown to be inhibited by low oxygen concentrations of 0.5 mg O_2/L (Gilbert *et al*., 2015) and at low DO concentrations, the anammox bacteria outcompete NOB for nitrite, thus single reactor PN/A systems do not need to actively inhibit nitratation.

An alternative treatment strategy is to perform the PN/A processes in separate vessels. There have been many control strategies developed to perform PN using suspended growth and attached growth technologies including operating at low DO (0.5-1.5 mg O_2/L), pH control, limiting alkalinity, biofilm thickness, intermittent exposure to high strength sidestream wastewater, limiting DO using TAN/DO ratios, and exposing biomass to inhibitors such as free ammonia (FA) or free nitrous acid (FNA) (Hao *et al.,* 2002; Fux *et al*., 2004; Wett, 2007; Lackner *et al*., 2014; Metcalf and Eddy, 2014; Dosta *et al*., 2015; Gilbert *et al.,* 2015; Piculell *et al.,* 2016; Laureni *et al.,* 2016; Duan *et al.,* 2019a). Many of these control strategies use complex, and operationally intensive strategies that require constant adjustment to achieve PN and have not been shown to achieve stable PN in biofilm systems, such as the MBBR technology, due to the adaptation of NOB (Fux *et al.,* 2004; Duan *et al.,* 2019a). Therefore, it is important to develop a passive design strategy and to understand the impact of the design strategy on the bacteria and the biofilm system as a whole to attain a robust and steady treatment system.

A passive, low operational intensity, and robust PN design strategy has been shown to achieve PN via elevated TAN loading rates using the MBBR technology (Schopf *et al*., 2019). it

was found that PN was achieved at a design TAN loading rate of 6.5 g TAN/m^2·d for a period of 10 months operating at room temperature and without restricting DO. Although there have been studies on PN that have investigated operations at elevated loading rates (Joo *et al.,* 2000; Yun and Kim, 2003), these studies took advantage of alkalinity restriction or operated at significantly higher influent TAN concentrations which contributed to FA as a cause for NOB inhibition. The study by Schopf *et al.* (2019) implies that neither FA, FNA, nor low DO were possible sources of inhibition, with the elevated loading rate and resulting impact on the biofilm morphology were thought to suppress the NOB. It remains unclear whether the method of PN was due to NOB population suppression or NOB activity suppression, with investigations into the bacterial viability and microbiome being required to demonstrate the viability and bacterial abundances of the biofilm system, thus demonstrating the method of NOB suppression.

A comprehensive analysis of the elevated TAN loading rate PN design strategy, including the nitritation and nitratation kinetics, biofilm characteristics, viability, and microbiome, is essential to optimize and gain a thorough understanding of the interactions at the macro-, meso-, micro-, and molecular-scale. This study aimed to investigate the biofilm and microbiome of the MBBR system that has been operated at elevated loading rates, at ambient temperatures and conventional pH values with the objective of achieving steady and robust PN. The specific objectives are to determine the changes in biofilm, embedded biomass and microbiome across increasing higher loading rates, and investigate how these changes contributed to the achievement of PN. This study contributes new information on the effects of elevated loading rates, multiple times higher (1.5 – 6×) than conventional loading rates (1 – 2.5 g TAN/m^2·d), on the MBBR biofilm, biomass and microbiome and ultimately provides an increased understanding of a design

strategy that does not require operational intensity during the system operation to achieve robust and stable PN.

4.4 Methods

4.4.1 Experimental Set-up

The experimental set-up consisted of a single, bench scale 2 L (h = 14 cm) acrylic cylindrical reactor that was operated as a continuous-flow MBBR for a period of 34 months. The reactor was filled with AnoxK^{TM}5 carriers (Specific Gravity = 0.95, Bulk Surface Area = 800 m^2/m^3) from AnoxKaldnes (Lund, Sweden) at an initial fill fraction of 60% by bulk volume (1.2 L bulk volume) of clean carriers and seeded carriers (at a ratio of 1 seeded carrier per 25 clean carriers). The seeded carriers were harvested from a municipal biochemical oxygen demand (BOD) removal integrated fixed film activated sludge (IFAS) system at the Hawkesbury, Ontario WRRF. The clean and seeded carriers were fed with a synthetic wastewater solution with an influent TAN concentration of 50 mg/L for a period of one month until biofilm developed on all carriers and 97% TAN removal was achieved. The influent TAN concentration was increased by 25 mg TAN/L per week until an influent of 125 mg TAN/L was achieved. 125 mg TAN/L was chosen to simulate mine wastewater; however, the results are framed for municipal applications due to the potential for mainstream and side-stream PN.

The reactor influent flow rate was 1 L/h of feed which resulted in a hydraulic retention time (HRT) of 2 h. The fine bubble aeration was supplied using an air regulator at a constant airflow rate of 4 L/min (G = 214 s^{-1}) as it was the minimum air flow rate to provide sufficient movement for the carriers within the reactor. The aeration was supplied at 4 L/min for the length of the experiment to reduce the number of experimental variables. The reactor was initially operated at a target surface area loading rate (SALR) of 3 g TAN/m^2·d with a fill fraction of 60%.

The reactor was further operated at target loading rates of 4, 5, and 6.5 g TAN/m^2·d at fill fractions of 50, 40, and 30%, respectively. System characteristics including pH, DO, temperature, fill fraction, target and measured TAN loading rates, and influent TAN concentration are presented in Table 4.1. The DO levels present in this study were significantly higher than conventional DO concentrations (~ 4 mg O_2/L) to ensure that oxygen was not a limiting variable in achieving PN. Additionally, as the air supply was supplied at an identical, constant flow rate at each condition to provide sufficient agitation, DO was not explicitly controlled and was the result of the reactor kinetics.

Table 4.1 System characteristics at various SALRs (average ± 95% confidence interval)

	Target SALR (g TAN/m^2·d)			
	3	**4**	**5**	**6.5**
Influent TAN Concentration (mg/L)	126.3 ± 1.9	133.1 ± 3.0	131.1 ± 2.0	130.4 ± 2.4
Measured SALR (g TAN/m^2·d)	3.16 ± 0.1	3.99 ± 0.1	4.91 ± 0.1	6.52 ± 0.0
Fill Fraction (%)	60	50	40	30
pH	8.0 ± 0.1	7.5 ± 0.1	7.9 ± 0.1	7.9 ± 0.3
Dissolved Oxygen (mg O_2/L)	5.8 ± 0.8	5.6 ± 0.2	5.8 ± 0.1	6.7 ± 0.2
Temperature (˚C)	19.6 ± 0.3	19.8 ± 0.5	20.5 ± 0.2	20.9 ± 0.6

Fill fraction was determined through bulk volume approximation. A clear, 2 L plexiglass beaker was filled with clean carriers until the level of carriers was at the desired volume indication mark (i.e., 1.2 L for 60% fill). It has been acknowledged that due to the relative sizes of the 2 L beaker and the carrier, the bulk surface area approximation used for large-scale installations and the actual available surface area may differ. However, the bulk surface area approximation of 800

m^2/m^3 of bulk carrier volume will be used for consistency with previous literature (Schopf *et al.*, 2019). Fill fraction was chosen as the variable to control SALR, rather than HRT or influent TAN concentration, to maintain identical hydraulic conditions, and influent concentrations affecting TAN concentration effects.

After the biofilm was fully developed, the reactor was operated at a loading rate of 3 g TAN/m^2·d for two months until steady state was reached. Steady state was defined by fluctuations of ± 10% or less of TAN, nitrite, and nitrate concentrations over the course of five consecutive sampling days. To ensure that steady state data were obtained, triplicate samples analyzed for each parameter unless stated otherwise in the methods. A triplicate, for the purpose of this study, consisted of three independent samples obtained from the reactor at a single time point to determine experimental error. A set of triplicated data points was obtained per day over a minimum of five consecutive days to act as a representative sample of steady state. The reactor was then operated at an SALR of 4 g TAN/m^2·d, by reducing the fill fraction to 50%, for a period of two months. After the two-month period, steady state was achieved and triplicate testing was performed. The system loading rate was changed to SALR of 5 g TAN/m^2·d by reducing the fill fraction to 40% and was operated for a period of two years. The reactor was operated at this condition for an extended period of time to confirm that, after any adaptation had occurred and steady state was achieved, the system would still achieve PN unlike what has been observed with other control strategies (Fux *et al.,* 2004; Piculell *et al.,* 2016; Duan *et al*., 2019). Triplicate data were taken after six months of operations and again after the two years of operation to confirm that there was no statistically significant difference in the results. After the two-year period, the loading rate was increased to 6.5 g TAN/m^2·d by reducing the fill fraction to 30%, half of the initial

fill fraction. The reactor was operated at the loading rate of 6.5 g TAN/m^2·d for six months to ensure that adaptation did not impact achieving PN using elevated TAN loading rates.

4.4.2 Wastewater Feed

The synthetic wastewater (SWW) used to feed the reactor was a based on a recipe used in previous studies (Delatolla *et al*., 2009; Hoang *et al.,* 2014; Tian *et al.,* 2017). The SWW simulated post-carbon removal wastewater and consisted of (per L of SWW) 0.590 g $(NH_4^+)_2SO_4$ (resulting in a concentration of 125 mg NH_4^+-N/L), 1.625 g $NaHCO_3$, 0.071 g $MgSO_4 \cdot 7H_2O$, 0.029 g $CaCl_2 \cdot 2H_2O$, 0.079 g KH_2PO_4, and 0.005 g $FeSO_4 \cdot 7H_2O$. Essential trace elements were added in quantities of (per L of SWW) 0.1 mg $MnCl_2 \cdot 4H_2O$, 0.025 mg $Na_2MoO_4 \cdot 2H_2O$, 0.1025 mg $CuSO_4 \cdot 5H_2O$, 0.001 mg $CoCl_2 \cdot 6H_2O$, and 0.03 mg $ZnSO_4 \cdot 7H_2O$. To provide a 1:5 sCOD: N ratio to simulate residual carbon that would remain after secondary treatment, peptone, sodium acetate ($NaCH_3COO$) and dextrose ($C_6H_{12}O_6$) were added in concentrations of (per L of SWW) 4.86 mg, 2.592 mg and 4.86 mg, respectively, to provide a total sCOD concentration of 25 mg sCOD/L.

4.4.3 Chemical Analyses

To quantify the macro-scale kinetics in the reactors the following standard methods were used: 4500C-NH_3 (Nessler method for TAN), 4500B-NO_2^- (nitrite), 4500A-NO_3^- (nitrate), HACH 8000 (sCOD, HACH Company, 2014) and 2540D (total suspended solids and volatile suspended solids) (APHA 1989). COD contribution of nitrite (NO_2^--N) was determined to be 1.14 g O_2/g N. To quantify the temperature and DO in the reactor, the HACH Flexi HQ30d DO probe (Loveland, CO, USA) was used. The airflow rate was quantified using the Dwyer VFA-24 Visi-Float ® air flow meter (Michigan City, IN, USA). To determine the pH a SympHony pH probe (Radnor, PA, USA) was used.

4.4.4 Biofilm Characterisation

The biofilm characteristics analyzed include biofilm thickness, mass, morphology and density. Biofilm thickness and morphology were characterized using variable pressure scanning electron microscope imaging utilizing the Tescan USA Inc, Vega II_XMU SEM (Cranberry, PA, USA) at ~40 Pa (Delatolla *et al*., 2015). Four carriers per reactor condition (totalling 16 carriers) were extracted and analyzed within four hours of harvesting the carriers from the reactor. To determine biofilm thickness and morphology, five images per carrier were acquired at 60× magnification, totalling 20 images per loading condition (80 images in total) (Delatolla *et al*., 2012; Young *et al.*, 2016). The images were acquired at random locations to prevent bias. One image per carrier (totalling four images per condition) was acquired at 6× magnification to provide an overall image of the carrier to identify anomalies in the biofilm. To visualise the biofilm surface morphology, one image per carrier (totalling four images per loading condition) was acquired at 600× magnification at a random location on the carrier (Young *et al.*, 2017).

The biofilm thickness was measured and quantified using the MedCalc Digimizer Image Analysis Software V.4.6.1 (Ostend, Belgium). A minimum of 1000 thickness measurements per reactor per loading condition were acquired as biofilm thickness variance may be significant under specific operating conditions. The thicknesses of any empty and clogged pores were not quantified and instead were enumerated for each carrier. The number of clogged carrier-pores per carrier were quantified by visually examining 20 harvested carriers for each loading condition.

Biofilm mass was quantified using a modified protocol based on the procedures described in Delatolla *et al.* (2008) and Forrest *et al.* (2016). Three carriers per condition were harvested and the carriers were dried at 105˚C for a minimum of twelve hours. The carriers were then cooled to room temperature a minimum of one hour in a desiccator after which they were weighed. The

biofilm on the carriers were removed and the carriers were again dried for a minimum of twelve hours at 105˚C. After cooling for a minimum of one hour in a desiccator the carriers were weighed. The difference in mass between the carrier with biofilm and the clean carrier was recorded as the biofilm mass. Testing was performed to ensure that the biofilm removal method did not significantly change the mass of the biofilm carrier.

4.4.5 Cell Viability and Cell Coverage

Cell viability (live/dead) analysis was completed using Confocal Laser Scanning Microscope imaging. The biofilm was stained with three different dyes; the SYTO®9 and propidium iodide from the FilmTracer™ Live/Dead Biofilm Viability Kit (Life Technologies, CA, US) and the 18909 Calcofluor White Stain (Sigma-Aldrich, MO, US). The images were taken using a ×63 water immersion objective with the 510/Axiolmager confocal laser scanning microscope (Zeiss, VA, US). The images were acquired with the Zen 2 software (Zeiss, VA, US). A minimum of four sets of images were taken per condition. Each set of images consists of a stack of five images (for a minimum of 20 images) over a depth of 35µm to determine the number of viable and nonviable cells throughout the biofilm depth. The images were analysed for cell viability and cell abundance using the Nikon NI Vision Assistant Software (National Instruments, LabView, v8.0). Note that the Calcofluor stain was not used for analysis at a loading rate of 6.5 g TAN/m^2·d; however, the SYTO®9 dye stains the biofilm, permitting the biofilm area to be quantified.

$$Cell\ Covereage = \frac{SA_{cells}}{SA_{biofilm}} \qquad (Eq.\ 4.1)$$

Cell coverage was defined as the percentage of biofilm area that is occupied by cells. The total biofilm area ($SA_{biofilm}$) is calculated by quantifying the total biofilm area per image as pixels.

The area occupied by cells (SA_{cells}) is the total area covered by cells per image as pixels. The cell coverage is calculated as the ratio between pixels representing cells and the pixels representing biofilm.

4.4.6 Next Generation Gene Sequencing and Analysis

The microbiome communities were determined by 16S Next Generation DNA sequencing. The protocol used was based on Young *et al.* (2016). Five replicate carriers per condition were randomly selected at the end of each testing stage, and 25 mg of wet biofilm was collected from each carrier and stored in a 1.5 mL sterilized Eppendorf tube. DNA was extracted using the FastDNA Spin Kit (MP Biomedicals, CA, US) from the detached wet biofilms of the MBBR carriers. The samples were stored at –80°C. The V6 hyper-variable region of the 16S rRNA gene was targeted for DNA amplification using two-step polymerase chain reaction (PCR) with a Phusion ® High-Fidelity PCR Master Mix (Thermo-Fisher Scientific Inc., Waltham, MA). The primers used in the PCR were based on a barcode approach from Abujamel *et al.* (2013). Electrophoresis on a 2% agarose gel was used to inspect the PCR amplicons. The amplicons were purified using a Montage PCR96 cleanup kit (EMD Milipore, Billerica, MA). The extracted DNA was quantified using Quanti-iTTM dsDNA HS Assay kits (Life Technologies, Burlington, Canada) and pooled with 200 ng of DNA from each sample. The samples were sequenced using an Illumina Hiseq2500 at the center for applied genomics (TCAG, Toronto, Canada)

The sequencing analysis was performed using the operating platform BioLinux. The 2x100 base paired-end reads were assembled using the Fast Length Adjustment of Short reads (FLASH) software (Magoc and Salzberg, 2011) then quality filtered using the fastq_quality_filter command from the Fastx toolkit with a minimum quality score of 20 over 90% of the sequences. Reads that passed the quality filter were demultiplexed and the barcodes were trimmed using Novobarcode

(Goecks *et al.*, 2010). The Quantitative Insights Into Microbial Ecology (QIIME) software, version 1.8 (Caporaso *et al.*, 2011), was used to compute operational taxonomical unit (OTU) clustering with closed reference strategy at 97% sequence similarity. QIIME aligned the OTUs against the Greengenes database 13.8 utilizing UCLUST algorithm. Then, the relative abundance of the bacterial taxa present in the biofilm was determined following removal of singleton OTUs. Converting OTUs to gene profiling used the PiCrust bioinformatics tool (Langille *et al.*, 2013). The samples were analyzed for differential abundance of bacterial taxa using metagenomeSEQ (Paulson *et al.*, 2013). Differences in bacterial relative abundance and gene profiles were identified using Linear Discriminate Analysis (LDA) with the galaxy software (Giardine *et al.*, 2005; Blankenberg *et al.*, 2010; Goecks *et al.*, 2010).

R Studio was used to determine the alpha diversity, beta diversity, and to generate heat maps. Species alpha diversity was determined using rarefication (n=100000 reads) and the Simpson diversity index to account for both abundance and presence of species. Beta diversity was determined through the use of principal coordinate analysis (PCoA) through the use of both unweighted and weighted unifrac distancing.

4.4.7 Calculations of Reactor Activity, Bacterial Counts, and Bacterial Activity

The following equations are used to approximate reactor activity, bacterial counts, and bacterial activity and are modified and adapted from Young *et al.* (2017). Note that the bacterial counts and bacterial activity are approximations and are used for comparison purposes and should not be considered as exact values. Reactor activity is used in this study to represent the total removal capacity of the reactor and was determined using the SARR as well as taking into account the surface area available. Reactor nitritation activity is the overall activity representing the

oxidation of TAN. Reactor nitratation activity is the overall activity representing the production of nitrate.

$$Reactor\ Nitritation\ Activiy\left(\frac{g\ N}{d}\right) = Q\ \times\ \left(C_{TAN\ in}\ -\ C_{TAN\ eff}\right) \qquad (Eq.\ 4.2)$$

Where Q is reactor flow rate (L/d), $C_{Tan\ in}$ is the influent TAN concentration (mg TAN/L), and $C_{Tan\ eff}$ is the effluent TAN concentration (mg TAN/L).

$$Reactor\ Nitratation\ Activity\ \left(\frac{g\ N}{d}\right) = Q\ \times\ \left(C_{NO3\ eff}\ -\ C_{NO3\ in}\right) \qquad (Eq.\ 4.3)$$

Where Q is reactor flow rate (L/d), $C_{NO3\ eff}$ is the effluent nitrate concentration (mg NO_3^--N/L), and $C_{NO3\ in}$ is the influent nitrate concentration (mg NO_3^--N/L).

Bacterial counts, the approximate number of a specific bacteria in each reactor, were determined using the following equation.

$$Bacterial\ Counts\ \left(\frac{bacteria}{reactor}\right) = \frac{BT \times \%fill \times S_{AB} \times Vol \times POP\% \times Cell_{coverage} \times Cell_{viable}}{Vol_{bacteria}} \qquad (Eq.\ 4.4)$$

Where BT is biofilm thickness (m), %fill is the fill fraction of bulk volume occupied by carriers (%), S_{AB} is the bulk surface area of the carrier (m^2/m^3), Vol is the volume of the reactor (m^3), POP% is the relative abundance of the target bacteria (%), $Cell_{coverage}$ is the percentage of biofilm volume that is bacteria (%), $Cell_{viable}$ is the percentage of cells that are live (%), and $Vol_{Bacteria}$ is the approximate volume of a bacteria (3.378E−19 m^3/bacteria) based on the average dimensions of *Nitrosomonas* (1.76 µm × 064µm) and *Nitrobacter* (1.5 µm × 0.7 µm) (Pillay *et al*., 1989), and *Nitrospira* (1.55 µm × 0.3 µm) (Ehrich *et al*., 1995).

Bacterial activity, the approximate kinetic activity per bacteria, was determined using the following equation.

$$Bacterial\ Activity\ \left(\frac{g\ N}{bacteria}\right) = \frac{Reactor\ Activity}{Bacterial\ Counts} \quad (Eq.\ 4.5)$$

Where Reactor Activity is the total mass of the target substrate removed per day per reactor (g N/reactor·d) and Bacterial Counts is the total number of the target bacteria per reactor.

4.4.8 Statistics

The student T-test (p<0.05) was used to determine statistical significance. Linear regression was used to determine linear slopes and the equation of the line. Error values for data were determined with 95% confidence.

Error for calculated values including; AOB and NOB counts, reactor activity, and bacterial activity was determined through the following equation:

$$\delta E = |E| \times \sqrt{(\frac{\delta A}{A})^2 + (\frac{\delta B}{B})^2 + \cdots} \quad (Eq.\ 4.6)$$

Where E is calculated value, δE is the 95% confidence error (α = 0.05) of the calculated value, A and B are variables in the equations (either numerator or denominator), and δA and δB are error values associated with variables A and B, respectively.

4.5 Results and Discussion

4.5.1 Nitritation and Nitratation Kinetics

TAN oxidation kinetics and nitrite oxidation kinetics are quantified in this study at SALRs of 3, 4, 5, and 6.5 g TAN/m^2·d (Table S4.1). The TAN SARR values are 2.01 ± 0.05, 3.28 ± 0.10, 3.75 ± 0.09, and 3.52 ± 0.01 g TAN/m^2·d, respectively, and the fraction of oxidized TAN remaining

as nitrite was 8.4 ± 0.4, 44.1 ± 4.7, 59.1 ± 1.7, and 99.8 ± 0.2%, respectively, translating to nitrite SARR values of 1.78 ± 0.04, 1.81 ± 0.05, 1.49 ± 0.03, and 0.005 ± 0.0002 g NO_2^--N/m^2·d, respectively. These results coincide with overall daily TAN removal of 1.93 ± 0.06, 2.62 ± 0.10, 2.40 ± 0.06, 1.69 ± 0.08 g TAN/d, respectively, and overall daily NO_2^- removal of 1.71 ± 0.06, 1.44 ± 0.14, 0.955 ± 0.04, and 0.002 ± 0.005 g NO_2^-- N/d, respectively. The daily TAN removal values demonstrate that there is a slight decrease in TAN removal as the TAN SALRs increase from 4 to 5 g TAN/m^2·d despite the increase in TAN SARR. Furthermore, there is a significant decrease in daily TAN removal as the TAN SALR increases from 5 to 6.5 g TAN/m^2·d despite marginal decrease in TAN SARR. The nitritation and nitratation SARR kinetics, as previously discussed by Schopf *et al.* (2019), demonstrated that PN was achieved via a simple design modification to the MBBR technology to operate at a design load of SALR of 6.5 g TAN/m^2·d. A strong linear relation (R^2 = 0.97) is shown to exist between TAN SALR and nitrite accumulation, demonstrating the potential to use SALR as a design tool to determine nitrite accumulation to achieve PN. Furthermore, the systems operated at an elevated TAN SALR of 6.5 g TAN/m^2·d, achieving PN, for over 10 months, demonstrating a robust and stable performance.

4.5.2 Biofilm Characteristics

Biofilm characteristics, defined as the biofilm thickness, dry-mass, dry-density, total suspended solids, and morphology, were quantified at TAN loading rates of 3, 4, 5, and 6.5 g TAN/m^2·d (Figure 4.1, Table S4.2). There is a statistically significant increase in biofilm thickness at each loading rate, with over 80% of carrier pores being clogged at a TAN SALR of 6.5 g TAN/m^2·d, thus demonstrating a strong positive correlation with loading rate and biofilm thickness. There is no statistically significant increase in biofilm mass between SALR 3 and 4 g TAN/m^2·d, and SALR 5 and 6.5 g TAN/m^2·d; however, there is a statistically significant increase

in biofilm mass between SALR 4 and 5 g TAN/m^2·d (Figure 4.1). The change in biofilm mass between SALR 4 and 5 g TAN/m^2·d occurs when the biofilm does not experience a significant shift from nitrification to PN, whereas a shift from nitrification to PN occurs between an SALR of 3 to 4 g TAN/m^2·d, where there is no statistically significant change in biofilm mass; however, there is a potential shift in microbiome. There is a significant decrease in biofilm density between SALR 3 and 4 g TAN/m^2·d, and between SALR 5 and 6.5 g TAN/m^2·d; however, there is no statistically significant change in biofilm density between SALR 4 and 5 g TAN/m^2·d. There is a qualitative increase in roughness of the biofilm morphology with increasing SALR which is indicative of an increase of stress on the biofilm system (Schopf *et al.*, 2019). Shear forces were identical at each loading rate as identical aeration was supplied at each loading rate; therefore, shear forces were discounted as a contributor to changes in biofilm thickness and morphology.

4.5.3 Cell Viability and Cell Coverage

Cell coverage, the fraction of biofilm covered by cells, and cell viability, the fraction of cells that have intact cell membranes and are therefore considered viable cells, were analyzed to determine the effects of elevated TAN loading rates on the viability of the bacteria in the microbiome (Figure 4.2). There is no statistically significant difference in cell coverage or cell viability between TAN SALR values of 3, 4, and 6.5 g TAN/m^2·d; however, there was a statistically significant decrease in cell coverage and cell viability observed at a TAN SALR of 5 g TAN/m^2·d compared to TAN SALRs of 3, 4, and 6.5 g TAN/m^2·d. The decrease in cell coverage and cell viability observed at a TAN SALR of 5 g TAN/m^2·d could be due to a shift in the microbiome towards a specialized TAN oxidation biofilm. Although a TAN SALR of 6.5 g TAN/m^2·d is an even higher load than 5 g TAN/m^2·d, the increased biofilm thickness could provide

a suitable environment to cultivate a more diverse biofilm, thereby supporting bacteria that are not selected solely for nitritation specialization.

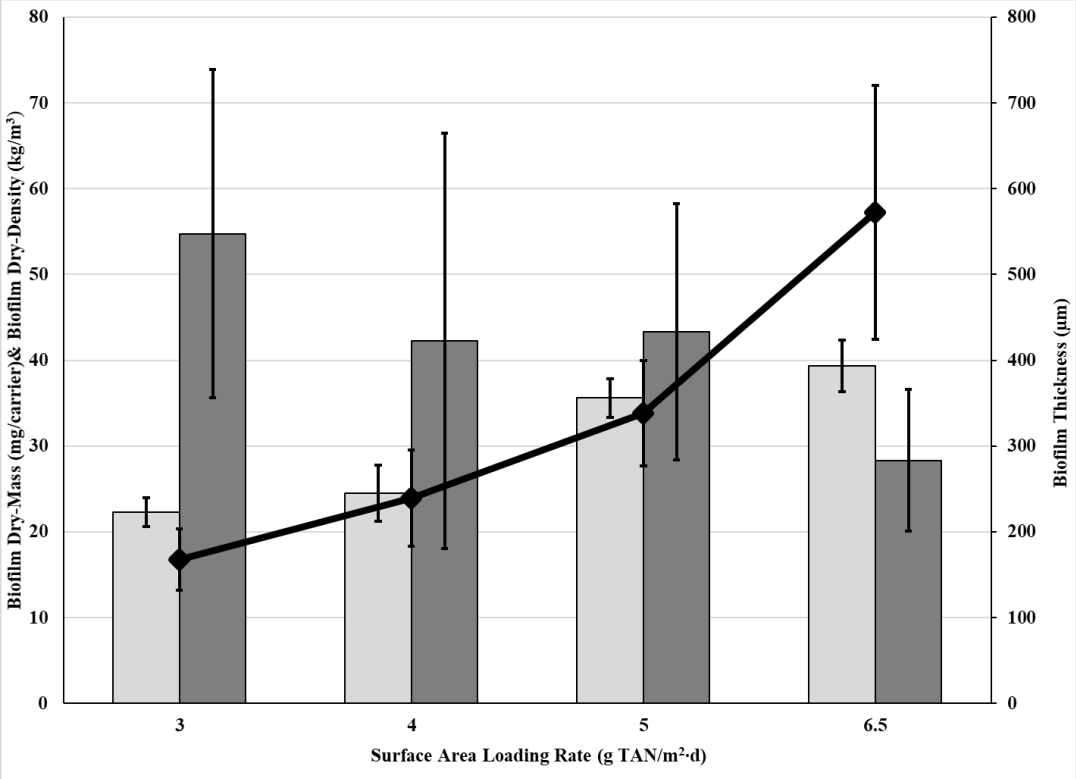

Figure 4.1 Biofilm dry-mass (light grey, left axis), dry-density (dark grey, left axis), and biofilm thickness (diamond line, right axis) across loading rate (95% confidence)

4.5.4 Microbiome and Diversity

The microbiome at each loading rate was analyzed by sequencing the V6 hyper-variable region of the 16S gene of the collected biofilm at the various SALR conditions. The top 10 most abundant taxa at each loading rate are presented in Table 4.2. At TAN SALRs of 3 and 4 g TAN/m^2·d, the ammonia oxidizing *Nitrosomonadaceae* is present at a relative abundance of 2.26% and 1.01%, respectively, while at TAN SALRs of 5 and 6.5 g TAN/m^2·d, the relative abundance increases to 26.79% and 17.34%, respectively, which demonstrates a significant increase in relative population of AOB with increasing TAN SALR values. At TAN SALR values of 3 and 4

g TAN/m^2·d, the *β-Proteobacteria*-related species are present at relative abundances of 12.50 and 13.43%, respectively, which decreases to 1.47 and 0.31% as the TAN SALR increases to 5 and 6.5 g TAN/m^2·d.

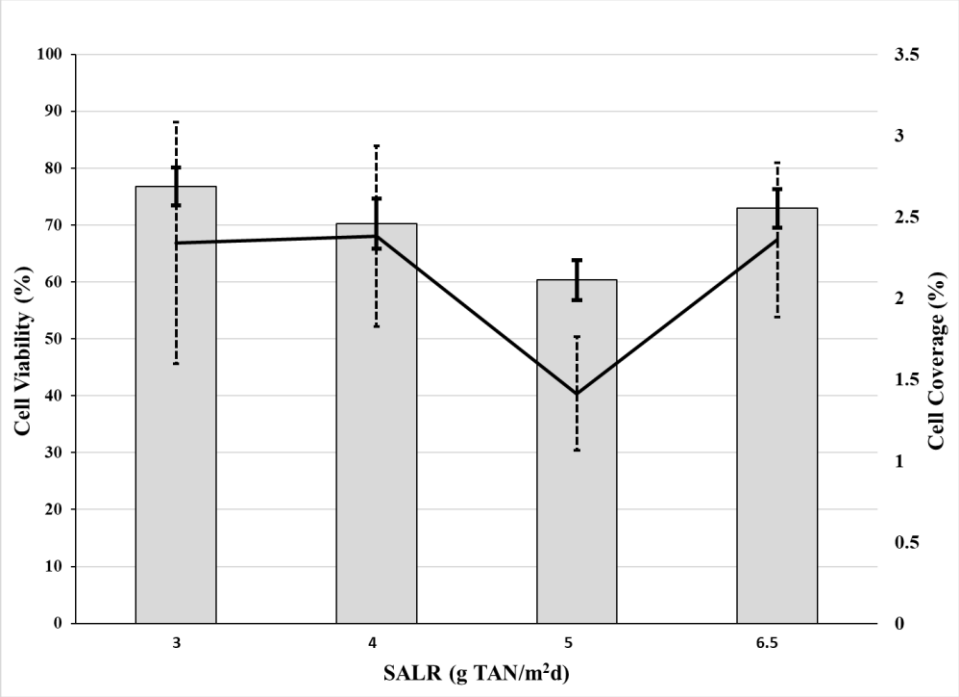

Figure 4.2 Cell viability (light grey, left axis) and cell coverage (line, right axis) with loading rate (95% confidence)

The class "*β-Proteobacteria"* consists of orders such as *Nitrosomonadales* which are mainly chemolithoautotrophic bacteria including the family *Nitrosomonadaceae,* a family of known AOB. However, *β-Proteobacteria* contain heterotrophic bacteria; thus, it is difficult to determine the functionality of autotrophic or heterotrophic at the resolution of class (Boden *et al*., 2017). *Comamonadaceae* and *Xanthamonadaceae* are two taxa that have been identified as being present in the biofilm, and both are identified as bacteria that can potentially contribute to nitritation and have been shown to be abundant in PN systems (Fitzgerald *et al.,* 2015; Dosta *et al.,* 2015; Connan *et al.,* 2019). *Comamonadaceae* and *Xanthamonadaceae* were abundant at total

relative populations of 16.1, 13.1, 4.2, and 12.3% and 0.75, 1.25, 13.53, and 22.43%, respectively, at loading rates of 3, 4, 5, and 6.5 g TAN/m^2·d, respectively. These bacterial families however, have a variety of functionalities; therefore, it is difficult to attribute nitritation kinetics to the activity of *Comamonadaceae* and *Xanthamonadaceae*. Thus, while *β-Proteobacteria, Comamonadaceae,* and *Xanthamonadaceae* are present in the biofilm and have the potential to contribute to the nitritation kinetics observed in this study, there is insufficient specificity resolution to adequately determine which specific bacteria these bacteria represent and cannot determine the specific functionality; thus, *Nitrosomonadaceae* is considered the only likely AOB in this study.

At TAN loading rates of 3, 4, 5, and 6.5 g TAN/m^2·d the dominant NOBs were identified as *Nitrospiraceae, Nitrospira* and an unidentified genus of *Nitrospiraceae.* As the resolution needed to distinguish between the two dominant NOBs is lacking, for the purpose of this study the relative abundances are combined into a single NOB referred to as the shared family name of "*Nitrospiraceae".* The relative abundance of *Nitrospiraceae* is 5.85, 4.62, 14.99, and 2.00% at loading rates of 3, 4, 5 and 6.5 g TAN/m^2·d, respectively. The AOB to NOB ratios are 1:2.6, 1:4.6, 1.8:1, and 8.7:1 at TAN loading rates of 3, 4, 5, and 6.5 g TAN/m^2·d, respectively. The presence of *Nitrospiraceae* has been observed in many nitrifying wastewater treatment systems and also in operations where oxygen restriction was deemed to be the method for NOB suppression. Similar AOB to NOB abundance ratios of 12.4:1 (Joo *et al*., 2000) and 5.6:1 (Yun and Kim, 2003) were observed; therefore, it is reasonable to have presence of NOB at a TAN SALR value of 6.5 g TAN/m^2·d despite the lack of nitrite oxidation observed.

Table 4.2 Top 10 most abundant bacteria (% of total abundance) at each loading rate designated at highest resolution. Designations: C-class, O-order, F-family, G-genus.

	3 g TAN/m^{2}d	**4 g TAN/m^{2}d**	**5 g TAN/m^{2}d**	**6.5 g TAN/m^{2}d**
1	F_Comamonadaceae 16.1%	F_Comamonadaceae 13.1%	F_Nitrosomonadaceae 26.8%	F_Nitrosomonadaceae 17.3%
2	C_Betaproteobacteria 12.5%	C_Betaproteobacteria 13%	F_Nitrospiraceae 13.1%	G_Thermomonas 13.5%
3	G_Rhodobacter 7.5%	F_Microbacteriaceae 10.9%	F_Xanthomonadaceae 6.8%	G_Hydrogenophaga 10.1%
4	O_Rhizobiales 5%	O_Rhizobiales 7.5%	G_Cryocola 6.8%	F_Xanthomonadaceae 6.7%
5	F_Rhodospirillaceae 5%	G_Flavobacterium 6.6%	F_Rhodocyclaceae 4.4%	F_Cytophagaceae 4.9%
6	F_Caulobacteraceae 3.9%	F_Rhodospirillaceae 3.8%	C_Chloracidobacteria 4.2%	F_Rhydocyclaceae 4.2%
7	F_Rhodocyclaceae 3.9%	F_Caulobacteraceae 3.8%	G_Thermomonas 3.6%	O_Rhizobiales 3.9%
8	G_Flavobacterium 3.3%	F_Nitrospiraceae 3.2%	F_Cytophagaceae 3.2%	G_Cryocola 3.4%
9	G_Nitrospira 3.2%	C_Gammaproteobacteria 3.2%	G_Rhodobacter 3.1%	C_Chloacidobacteria 3.1%
10	F_Nitrospiraceae 2.6%	G_Rhodobacter 2.7%	G_Hydrogenophia 2.8%	F_Comamonadaceae 2.3%
AOB	F_Nitrosomonadaceae 2.3%	F_Nitrospiraceae 3.2%	F_Nitrosomonadaceae 26.8%	F_Nitrosomonadeaceae 17.3%
NOB	G_Nitrospira 3.2%	G_Nitrospira 1.26%	G_Nitrospira 1.86%	G_Nitrospira 0.30%
NOB	F_Nitrospiraceae 2.6%	F_Nitrospiraceae 3.2%	F_Nitrospiraceae 13.1%	F_Nitrospiraceae 1.70%

To properly understand the effects of elevated loading rate on the microbiome, alpha-diversity analysis, the diversity within a microbiome, and beta-diversity analysis, the diversity between microbiomes is used. The alpha-diversity (Figure 4.3) is presented using the Simpson diversity index, where a value of 1 indicates an extremely diverse microbiome and a value of 0 indicates a single bacteria microbiome. The alpha-diversities found in this study are similar to other PN biofilm studies (Wang *et al*., 2018; Jia *et al*., 2018). The alpha-diversities at TAN SALR values of 3 and 4 g TAN/m^2·d are statistically significantly similar (p = 0.623) with index values of 0.955 ± 0.02 and 0.958 ± 0.004, respectively, demonstrating diverse populations. There is a statistically significant decrease (p = 1.7 ×10^{-8}) in index values from 0.958 ± 0.004 to 0.893 ±

0.005 as the TAN SALR values increases from 4 to 5 g TAN/m^2·d. Conversely there is a statistically significant increase (p = 0.0035) in diversity with an increase in TAN SALR values from 5 to 6.5 g TAN/m^2·d as the Simpson diversity index values increase from 0.893 ± 0.005 to 0.928 ± 0.016. The decrease in diversity index at a TAN SALR of 5 g TAN/m^2·d is aligned with the significant relative abundance of *Nitrosomonadaceae* and *Nitrospiraceae* which account for over 40% of the total abundance, which suggests a specialized biofilm with a nitrifying microbiome. The increase in alpha-diversity observed as the TAN SALR increased from 5 to 6.5 g TAN/m^2·d is due to the decrease in relative populations of AOB and NOB, demonstrating that the microbiome became less focused on PN.

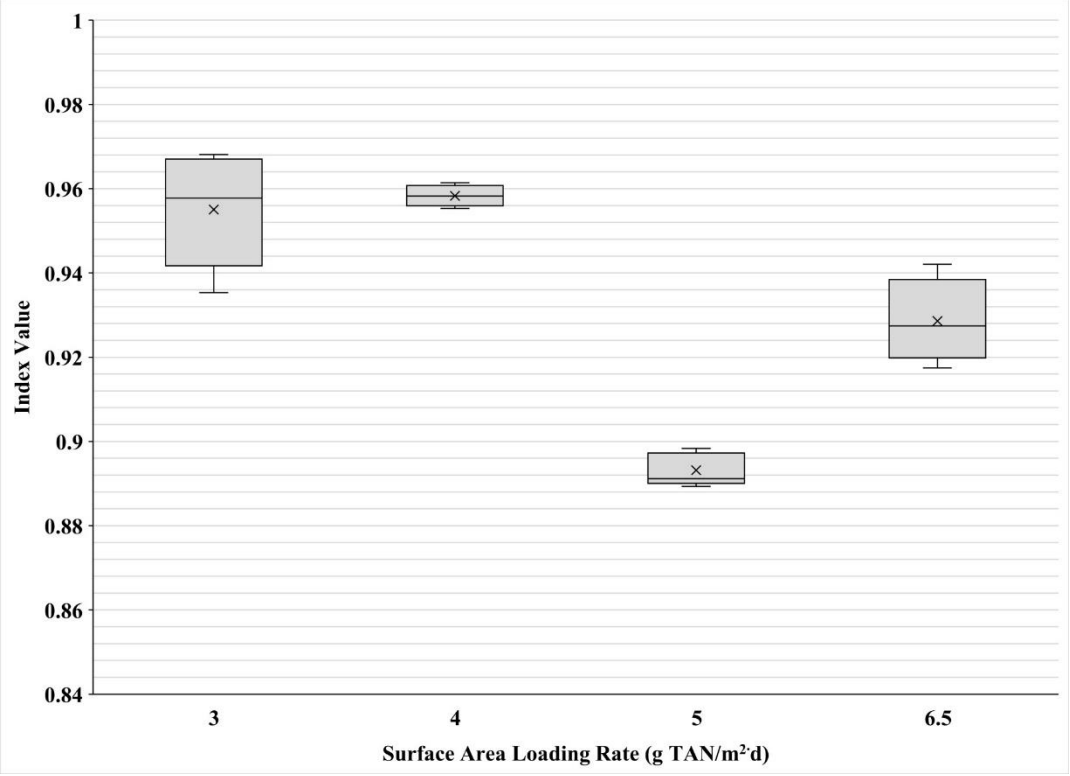

Figure 4.3 Simpson's Index alpha diversity across loading rates where x denotes the average, the upper bar is the highest value, the middle bar is the median, the lowest bar is the lowest value, and the upper and lower edges of the box denotes the value closest to 25th and 75th percentiles

Beta diversity (Figure 4.4) is the representation of the similarities, dissimilarities and diversity between multiple microbiomes. Weighted unifrac principle coordinate analysis (PCoA) is used to attain the beta-diversity. C1 (x-axis) represented 68.3% of the similarity between data points, while C2 (y-axis) represented 14.4% of the similarity between data points, for a total of 82.7% of the total variability. The microbiome communities at TAN SALR values of 3 and 4 g TAN/m^2·d are clustered closely together along C1 and the microbiome communities at TAN SALR values of 5 and 6.5 g TAN/m^2·d are again clusters closely together along C1; however, there is a clear division along C1 groupings of the microbiome communities at TAN SALR values 3 and 4 g TAN/m^2·d compared to the microbiome communities at TAN SALR values of 5 and 6.5 g TAN/m^2·d. Along C2, the microbiome communities at TAN SALRs of 3 and 5 g TAN/m^2·d are clustered closely, while there is a general progression from lower loading to higher loading along C2. In addition to the alpha-diversity and beta-diversity, the effects of TAN SALR on the microbiomes are visualized using a heat map at the family level (Figure S4.1). The heat map at the family level demonstrates a clear shift in the microbiomes between TAN SALRs of 4 and 5 g TAN/m^2·d. The results of the heat map align with the beta-diversity results in which there is a significant divide along the x-axis between the lower TAN SALRs (3 and 4 g TAN/m^2·d), the TAN SALR of 5 g TAN/m^2·d and the TAN SALR of 6.5 g TAN/m^2·d.

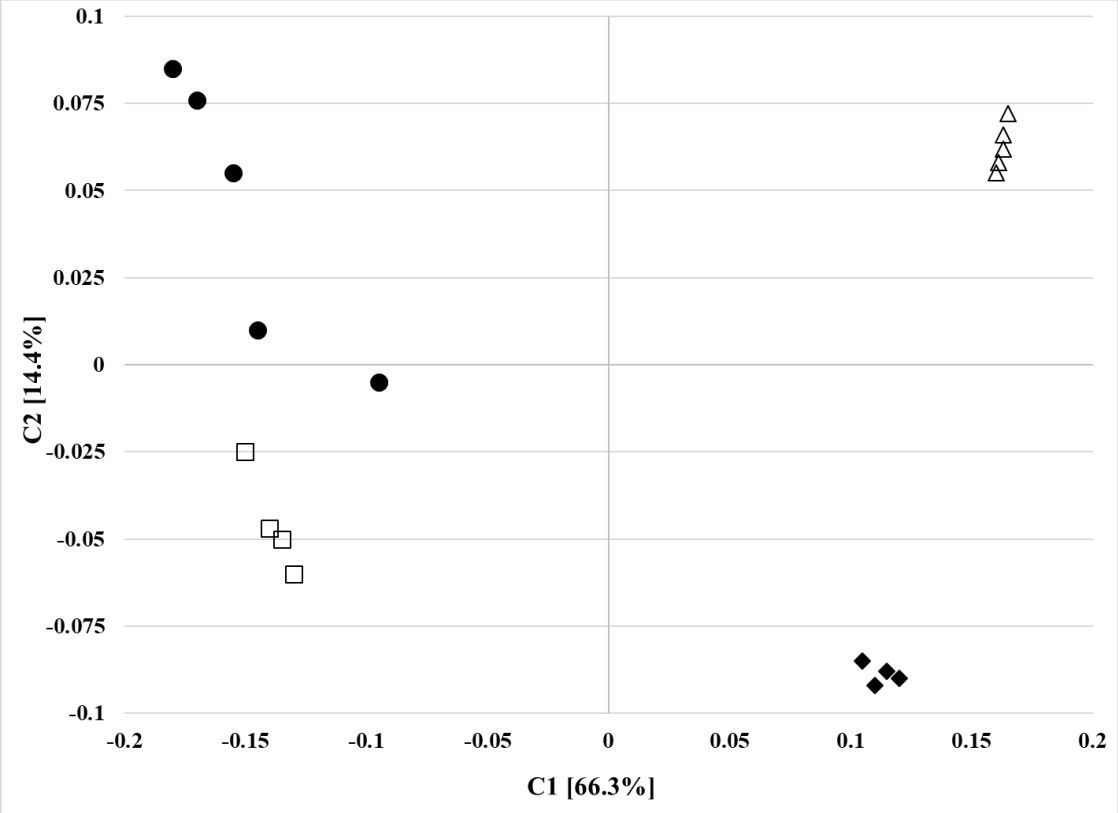

Figure 4.4 Unifrac weighted beta diversity across loading rates ● – 3 g TAN/m^2·d, □ – 4 g TAN/m^2·d, △ – 5 g TAN/m^2·d, and ◆ – 6.5 g TAN/m^2·d)

4.5.5 Bacterial Counts and Bacterial Kinetics

To attain a holistic understanding of the effects of elevated loading rate on PN, the kinetic, biofilm, microbial, and molecular results are examined together. To attain an in-depth understanding of the biofilm system, approximate AOB and NOB bacterial counts per reactor and the activity of the AOB and NOB are calculated at each loading rate, similar to Young *et al.* (2017). The AOB and NOB bacterial counts were calculated to compare the effects of TAN SALR within the study and are approximations rather than real counts. The AOB counts and AOB activity per bacteria at TAN SALR values of 3, 4, 5, and 6.5 g TAN/m^2·d were presented in Table S4.3 (Figure 4.5a). There is no statistically significant difference in AOB counts between TAN SALR values of 3 and 4 g TAN/m^2·d and there is no statistically significant difference between AOB counts

between TAN SALR values of 5 and 6.5 g TAN/m^2·d; however, there is a significant increase in AOB counts between TAN SALR values of 4 and 5 g TAN/m^2·d. There is a significant increase in AOB activity from TAN SALR values of 3 to 4 g TAN/m^2·d and a significant decrease in activity from TAN SALR values of 4 to 5 g TAN/m^2·d and a further decrease from TAN SALR values of 5 to 6.5 g TAN/m^2·d. There is a positive trend of increasing AOB counts with increasing TAN SALR values and, apart from the system at a loading rate of 4 g TAN/m^2·d, there is a negative trend of decreasing AOB activity with increasing TAN SALR values. The increase in AOB activity as the TAN SALR values increases from 3 to 4 g TAN/m^2·d is likely due to the shift from nitrification towards PN.

There is no statistically significant difference in the AOB counts between TAN SALR values of 5 and 6.5 g TAN/m^2·d; however, there is a statistically significant increase in the alpha-diversity index value from 0.893 ± 0.005 to 0.928 ± 0.016, as well as an increase in biofilm thickness. This could be due to the capacity of the biofilm to support AOB having reached capacity at an elevated TAN SALR value of 5 g TAN/m^2·d; therefore, other non-AOB bacteria are able to grow and thrive at a TAN SALR of 6.5 g TAN/m^2·d where there is a statistically significantly thicker biofilm and thus a greater biofilm volume. The capacity for the biofilm to support more bacteria at a TAN SALR of 6.5 g TAN/m^2·d is supported by the statistically significant increase in alpha-diversity from TAN SALR values of 5 to 6.5 g TAN/m^2·d, as well as the fact that although the AOB counts did not statistically significantly change from TAN SALR values of 5 to 6.5 g TAN/m^2·d, there was a statistically significant decrease in *Nitrosomonadaceae* abundance from TAN SALR values of 5 to 6.5 g TAN/m^2·d meaning that there was an increase in the number of bacteria that were not *Nitrosomonadaceae* or AOB.

The NOB counts per reactor and NOB activity per bacteria (Figure 4.5b) at SALRs 3, 4, 5 and 6.5 g TAN/m^2·d were presented in Table S4.3. There is no statistically significant difference between NOB counts at TAN SALR values of 3, 4, 5 and 6.5 g TAN/m^2·d. Conversely, there is no statistically significant difference in NOB activity at TAN SALR values of 3 and 4 g TAN/m^2·d; however, there is a significant 3-fold decrease from TAN SALR values of 4 to 5 g TAN/m^2·d and a statistically significant decrease of more than 100-fold from TAN SALR values of 5 to 6.5 g TAN/m^2·d. There is no statistically significant difference in NOB populations at a TAN SALR of 3 g TAN/m^2·d, where nitrite accumulation was 8% or at a TAN SALR of 6.5 g TAN/m^2·d, where the nitrite accumulation was 100%; therefore, the decrease in reactor nitratation kinetics is due to a suppression effect on NOB rather than an inhibitory effect or a toxic effect. This is also supported by the viabilities at TAN SALR values of 3, 4, and 6.5 g TAN/m^2·d.

The mechanism of suppression is likely oxygen deprivation through the preferential uptake of oxygen by the increasing AOB populations with an increase of TAN SALR values and the restricted access to oxygen by the increasing thickness of the biofilm restricting oxygen penetration; therefore, there is an insufficient concentration of oxygen present for the NOB population to be active. By depriving the NOB of oxygen, without restricting airflow and influent oxygen, the system has full nitrite accumulation while still achieving high TAN removal kinetics. The reactor was operated at a loading rate of 6.5 g TAN/m^2·d for a period of 10 months during which NOB activity remained suppressed unlike with Fux *et al*. (2004) who used inhibitors as a control strategy and the NOB activity recovered after a period of 6 months as demonstrated by nitrate production.

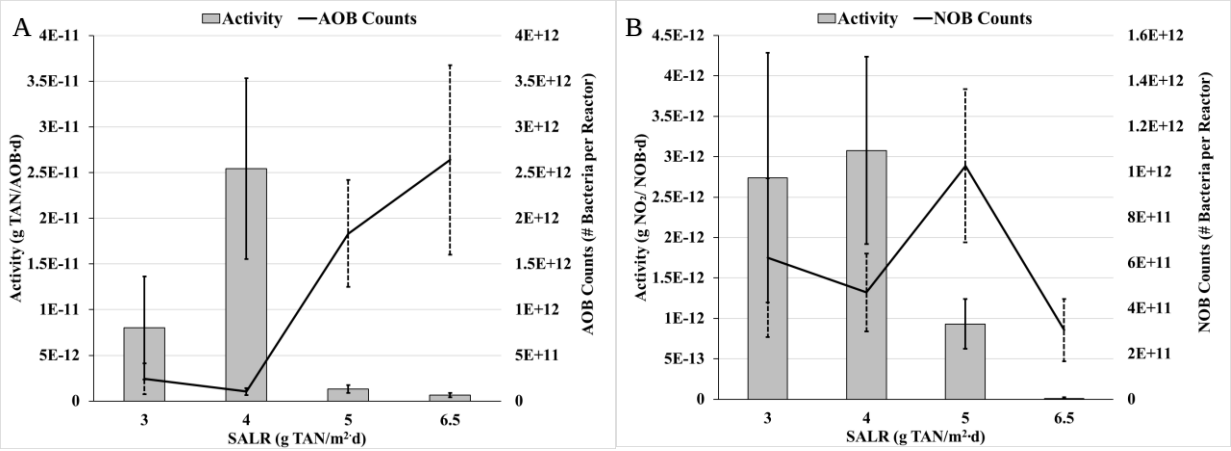

Figure 4.5 Nitrogen removal activity per bacteria (solid bar, left axis) and bacterial counts per reactor (line, right axis) for a) TAN and AOB, and b) Nitrite (NO_2^--N) and NOB

4.5.6 Oxygen Demand

In this study, the cause for NOB suppression due to elevated TAN loading rates is likely due to the AOB preferentially uptaking oxygen, thus depriving the NOB of oxygen. By depriving the NOB of sufficient oxygen, even if the NOB population is present, the NOB cannot oxidize nitrite to nitrate. Joo *et al.* (2000) suggested that an oxygen concentration gradient in the biofilm, generated by diffusion resistance, could selectively limit nitratation due to the differences in oxygen saturation affinity of AOB and NOB. The total oxygen consumed per day, the total oxygen consumed for TAN oxidation, the total oxygen for nitrite oxidation, and the total oxygen consumed for sCOD were calculated (Table S4.4), and the total oxygen per day was normalized as oxygen demand per carrier. Oxygen demand was determined through the stoichiometric requirements for the oxidation, where oxygen demand refers to the oxygen consumed.

The overall oxygen demands at TAN SALR values of 3 and 6.5 are statistically significantly different from all other loading rates while the oxygen demand at TAN SALR values of 4 and 5 are statistically significantly similar. The overall oxygen consumed per day is 6861, 8120, 7149, and 4371 mg O_2/d for TAN SALR values of 3, 4, 5, and 6.5 g TAN/m^2·d, respectively. The oxygen consumption for TAN oxidation and nitrite oxidation is 4279, 5875, 5343, and 3769

mg O_2/d and 1958, 1646, 1092, and 3 mg O_2/d for TAN SALR values of 3, 4, 5, and 6.5 g TAN/m^2·d, respectively, and the oxygen consumption due to sCOD is 600 mg O_2/d at each TAN SALR value. The overall oxygen consumption per carrier is 17.3, 24.3, 26.5, and 22 mg O_2/carrier·d for TAN SALR values of 3, 4, 5, and 6.5 g TAN/m^2·d, respectively. Although the greatest overall daily oxygen consumption occurs at a TAN SALR value of 4 g TAN/m^2·d, the greatest oxygen consumption per carrier occurs at a TAN SALR value of 5 g TAN/m^2·d which corresponds to the overall higher TAN SARR values observed. Therefore, there is a strong trend with the oxygen demand per carrier and SALR; however, there is a decrease in oxygen demand at the highest loading rate due to a reduction in kinetics.

4.6 Conclusion

This study is an in-depth investigation into the meso, micro and molecular-scale response of biofilms exposed to elevated TAN SALRs to achieve PN. It is demonstrated that PN is achieved at a TAN SALR value of 6.5 g TAN/m^2·d with a TAN SARR of 3.5 g TAN/m^2·d and nitrite accumulation of greater than 99% of the oxidized TAN. The 500-fold decrease in NOB activity from TAN SALR values of 3 to 6.5 g TAN/m^2·d, alongside the statistically similar NOB counts between TAN SALR values of 3 and 6.5, suggests that operating at an elevated loading rate suppresses the NOB activity as opposed to reducing the population of the NOB in the biofilm as has been observed in other PN control strategies. There is a trend of increasing AOB populations relative to the NOB populations as the TAN loading rate increases, as demonstrated by the shift in AOB to NOB ratios of 1:2.6 to 8.7:1 at TAN SALR values of 3 and 6.5 g TAN/m^2·d, respectively.

The proposed mechanism of NOB suppression is the preferential uptake of oxygen by the increasing AOB populations in the presence of sufficient TAN at elevated TAN loading, as well as the maintenance of a thick biofilm that reduces oxygen penetration and results in depriving the

embedded NOB of oxygen, thus preventing NOB activity. As the method of NOB suppression is essentially oxygen restriction within the biofilm, adaptation of the NOB does not take place. Adaptation to other forms of NOB suppression is a characteristic of biofilms that has made implementing many PN control strategies a significant challenge. In this study, adaptation of the NOB to elevated TAN SALRs has not been demonstrated across an operational period of over 10 months. Hence, designing systems at elevated TAN SALRs is a potential robust, passive design strategy to achieve high rate PN and as such is a passive design strategy that is ideal for communities where simplified operation is an asset.

4.7 Supplemental Material

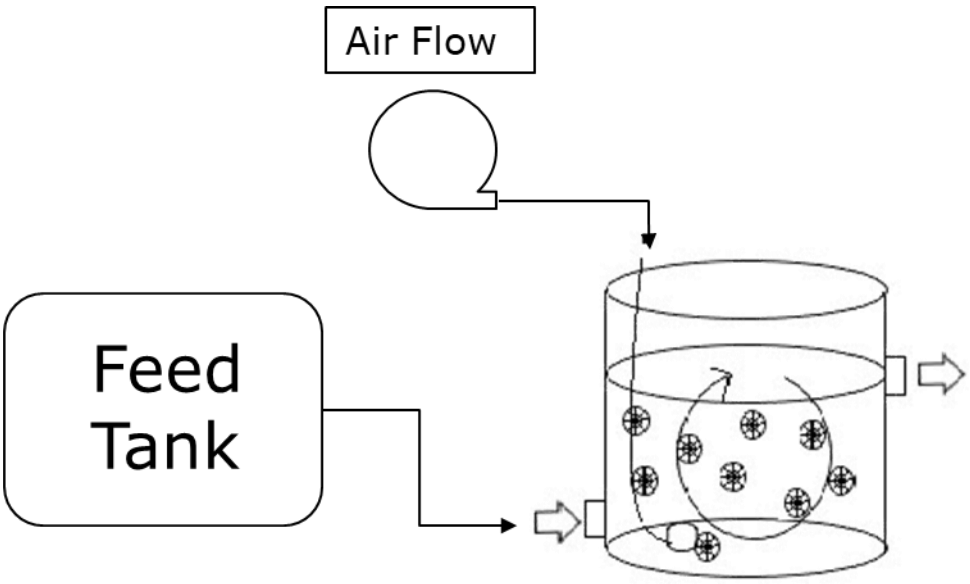

Figure S4.1 Experimental Schematic

Table S4.1 Influent and effluent nitrogen concentrations

	Target SALR (g TAN/m^2·d)			
	3	**4**	**5**	**6.5**
Measured SALR (g TAN/m^{2}d)	3.16 ± 0.08	3.99 ± 0.14	4.91 ± 0.13	6.52 ± 0.001
SARR (g TAN/m^{2}d)	2.01 ± 0.05	3.28 ± 0.10	3.75 ± 0.09	3.52 ± 0.001
Influent TAN (mg TAN/L)	126.3 ± 4.4	133.1 ± 6.1	131.1 ± 4.0	130.4 ± 5.4
Effluent TAN (mg TAN/L)	45.6 ± 0.9	23.7 ± 2.3	31.0 ± 1.5	60.1 ± 3.0
Effluent Nitrite (mg NO_2^--N/L)	6.6 ± 0.3	47.2 ± 4.9	57.6 ± 2.1	68.6 ± 2.1
Effluent Nitrate (mg NO_3^--N/L)	71.4 ± 2.5	60.0 ± 5.6	39.8 ± 1.6	0.1 ± 0.2
Percent NO_X as Nitrite (%)	8.4 ± 0.4	44.1 ± 4.7	59.1 ± 1.7	99.8 ± 0.2
Influent Nitrogen (mg/L)	127.4 ± 4.4	134.1 ± 6.0	132.1 ± 4.1	131.1 ± 5.5
Effluent Nitrogen (mg/L)	123.6 ± 3.4	130.9 ± 7.2	128.4 ± 3.9	128.7 ± 6.4
Nitrogen Balance (%)	97.1	97.6	97.2	98.2

Table S4.2 Biofilm Characteristics, Cell Coverage, and Cell Viability (average ± 95% confidence)

	Target SALR (g TAN/m^2·d)			
	3	**4**	**5**	**6.5**
Biofilm Thickness (μm)	167 ± 36	239 ± 56	338 ± 62	572 ± 148
Biofilm Mass (mg /carrier)	22.3 ± 1.7	24.5 ± 3.3	35.6 ± 2.23	39.4 ± 3.0
Biofilm Density (kg/m^3)	54.7 ± 16	42.2 ± 16	43.3 ± 11	28.3 ± 9.5
Total Suspended Solids (mg/L)	68.4 ± 37.9	69.5 ± 37.8	33.7 ± 6.6	27.2 ± 11.9
Average number of clogged pores per carrier	0	0	0	59 ± 2
Cell Coverage (% of total biofilm area)	2.34 ± 0.74	2.38 ± 0.55	1.41 ± 0.35	2.36 ± 0.48
Cell Viability (% of total bacteria that are viable)	76.8 ± 3.3	70.2 ± 4.4	60.4 ± 3.5	73.0 ± 3.4

Table S4.3 AOB and NOB bacterial counts and bacterial activities (± 95% confidence)

	Target SALR (g TAN/m^2·d)			
	3	**4**	**5**	**6.5**
AOB bacterial counts (AOB/reactor)	2.41E+11 ± 1.69E+11	1.03E+11 ± 4.01E+10	1.83E+12 ± 5.83E+11	2.63E+12 ± 1.03E+12
NOB bacterial counts (NOB/reactor)	6.23E+11 ± 3.49E+11	4.69E+11 ± 1.72E+11	1.03E+12 ± 3.37E+11	3.04E+11 ± 1.36E+11
AOB bacterial activity (g TAN/AOB·d)	8.0E-12 ± 5.6E-12	2.54E-11 ± 9.9E-12	1.31E-12 ± 4.17E-13	6.4E-13 ± 2.54E-13
NOB bacterial activity (g NO_2^--N/NOB·d)	2.74E-12 ± 1.54E-12	3.07E-12 ± 1.16E-12	9.30E-13 ± 3.08E-13	7.90E-15 ± 1.94E-14

Table S4.4 Oxygen demand at each loading rate per constituent

	Target SALR (g TAN/m^2·d)			
	3	**4**	**5**	**6.5**
Total oxygen consumed (Nitrite, Nitrate, Carbonaceous sCOD) (mg O_2/d)	6861	8120	7149	4371
Oxygen consumed for nitrite production (mg O_2/d)	4279	5875	5343	3769
Oxygen consumed for nitrate production (mg O_2/d)	1958	1646	1092	3
Carbonaceous sCOD consumed (mg O_2/d)	624	600	600	600
Oxygen consumed per carrier (mg O_2/carrier·d)	17.3	24.5	26.5	22.0

4.8 References

Abujamel, T., Cadnum, J. L., Sunkesula, V. C., Kundrapu, S., Jump, R. L., Stintzi, A. C., Donskey, C. J., (2013). Defining the vulnerable period for re-establishment of Clostridium difficile colonization after treatment of C. difficile infection with oral vancomycin or metronidazole. *PLOS ONE* 8(10):e76269

APHA, AWWA, WEF. (1989) *Standard methods for examination of water and wastewater*. Washington, D.C., 17th edition, 1989

Blankenberg, D., Kuster, G. Von, Coraor, N., Ananda, G., Lazarus, R., Mangan, M., Nekrutenko, A., Taylor, J. (2010). Galaxy: A Web-Based Genome Analysis Tool for Experimentalists. In *Current Protocols in Molecular Biology* (Vol. Chapter 19, p. Unit 19.10.1-21). Hoboken, NJ, USA: John Wiley & Sons, Inc.

Boden, R., Hutt, LP., Rae, AW. (2017) Reclassification of *Thiobacillus aqueaesculis* (Wood & Kelly, 1995) as *Annwoodia aquaesulis* gen. nov., comb. nov., transfer of *Thiobacillus* (Beijernick, 1904) from *Hydrogenophilales* to the *Nitrosomonadales*, proposal of *Hydrogenophilalia* class, nov. within the 'Proterobacteria', and four new families within the orders *Nitrosomonadales* and *Rhodocyclales*. *International Journal of Systemic and Evolutionary Microbiology* 67(5): 1191-1205

Canadian Fisheries Act: Wastewater Systems Effluent Regulations. (2012). Canada Gazetter Part II, 146(15). Retrieved from the Canada Gazette website: http://www.gazette.gc.ca/rp-pr/p2/2012/2012-07-18/html/sor-dors139-eng.html (Accessed June 2020)

Caporaso, G. J., Lauber, C. L., Walters, W. A., Berg-Lyons, D., Lozupone, C. A., Turnbaugh, P. J., Fierer, N. Knight, R., (2010). Global patterns of 16S rRNA diversity at a depth of millions of sequences per sample. *Proceedings of the National Academy of Sciences of the United States of America*. 4516-4522

Christensson, M., Ekström, S., Andersson Chan, A., Le Vaillant, E., Lemaire, R. (2013). Experience from start-ups of the first ANITA Mox plants. *Water Sci. Technol*., 67(12): 2677-2684

Connan, R., Dabert, P., Moya-Espinosa, M., Bridoux, G., Béline, F., & Magrí, A. (2018). Coupling of partial nitritation and anammox in two- and one-stage systems: Process operation, N2O emission and microbial community. *Journal of Cleaner Production*, 203, 559–573. doi:10.1016/j.jclepro.2018.08.258

Council Directive 91/271/EEC of 27 May 1991 concerning urban waste water treatment (1991). Official Journal L 135, 30.5, p. 40-55

Delatolla, R., Babarutsi, S. (2005) Parameters effecting hydraulic behaviour of aerated lagoons. *Journal of Environmental Engineering* 131(10): 1404-1413

Delatolla, R., Berk, D., Tufenkji, N. (2008) Rapid and reliable quantification of biofilm weight and nitrogen content of biofilm attached to polystyrene beads. *Water Research* 42:3082-3088

Delatolla, R., Séguin, C., Springthorpe, S., Gorman, E., Campbell, A, I. Douglas. (2015) Disinfection byproduct formation during biofiltration cycle: implications for drinking water production. *Chemosphere* 136: 190-197

Delatolla, R., Tufenkji, N., Comeau, Y., Gadbois, A., Lamarre, D., Berk, D. (2009) Kinetic analysis of attached growth nitrification in cold climates. *Water Science and Technology* 60:1173-1184

Delatolla, R., Tufenkji, N., Comeau, Y., Gadbois, A., Lamarre, D., Berk, D. (2012) Effects of long exposure to low temperatures on nitrifying biofilm and biomass in wastewater treatment. *Water Environment Research* 84: 328-338

Dosta, J., Vila, J., Sancho, I., Basset, N., Grifoll, M., Mata-Álvarez, J. (2015) Two-step partial nitritaton/Anammox process in granulation reactors: Start-up operation and microbial characterization. *Journal of Environmental Management* 164: 196-205

Duan, H., Ye, L., Lu, X., Yuan, Z. (2019a) Overcoming nitrite oxidizing bacteria adaptation through alternating sludge treatment with free nitrous acid and free ammonia. *Environmental Science and Technology*. DOI: 10.1021/acs.est.8b06148

Duan, H., Ye, L., Wang, Q., Zheng, M., Lu, X., Wang, Z., Yuan, Z. (2019b) Nitrite oxidizing bacteria (NOB) contained in influent deteriorate mainstream NOB suppression by sidestream inactivation. *Water Research* 162: 331-338

Ehrich, S., Behrens, D., Lebedeva, E, Ludwig, E., Bock, E. (1995) A new obligatory chemolithoautotrophic, nitrite-oxidizing bacterium, *Nitrospira moscoviensis* sp. nov. and its phylogenic relationship. *Archives of Microbiology*. 164: 16-23

Fitzgerald, C.M., Cemjo, P., Oshlag, J.Z., Noguera, D.R. (2015) Ammonia-oxidizing microbial communities in reactors with efficient nitrification at low-dissolved oxygen. *Water Research* 70: 38-51

Forrest, D., Delatolla, R., Kennedy, K. (2016) Carrier effects on tertiary nitrifying moving bed biofilm reactor: An examination of performance, biofilm and biologically produced solids. *Environmental Technology* 37: 662-671

Fux, C., Huang, D., Monti, A., Siegrist, H. (2004) Difficulties in maintaining long-term partial nitritation of ammonium-rich sludge digester liquids in a moving-bed biofilm reactor (MBBR). *Water Science and Technology* 49: 53-60

Giardine, B., Riemer C., Hardison, R. C., Burhans, R., Elnitski, L., Shah, P., Mekrutenko, A. (2005). Galaxy: A platform for interactie large-scale genome analysis. *Genome Research*, 15(10): 1451-1455

Gilbert, EM., Agrawal, S., Schwartz, T., Horn, H., Lackner, S. (2015). Comparing different reactor configurations for partial nitritation/anammox at low temperatures. *Water Research* 81: 92-100

Goecks, J., Nekrutenko, A., Taylor, J., & Galaxy Team, T. (2010). Galaxy: a comprehensive approach for supporting accessible, reproducible, and transparent computational research in the life sciences. *Genome Biology*, 11(8): R86

Goecks, J., Nekrutenko, A., Taylor, J., Team, T. G., (2010). Galaxy: a comprehensive approach for 599 supporting accessible, reproducible, and transparent computational research in the life sciences. *600 Genome Biology* 11(R86)

Hao, X., Heijnen, JJ., van Loosedrecht, MCM. (2002) Sensitivity analysis of a biofilm model describing a one-stage completely autotrophic nitrogen removal (Canon) process. *Biotechnology and Bioengineering* 77: 266-277

Hoang, V., Delatolla, R., Laflamme, E., Gadbois, A. (2014) An investigation of moving bed biofilm reactor nitrification during long-term exposure to cold temperatures. *Water Environment Research* 86: 36-42

Jia, W., Chen, Y., Zhang, J., Li, C., Wang, Q., Li, G., Yang, W. (2018) Response of greenhouse gas emissions and microbial community dynamics to temperature variation during partial nitrification. *Bioresource Technology* 261: 19-27

Joo, SH., Kim, DJ., Yoo, IK., Park, K., Cha, GC. (2000) Partial nitritation in an upflow biological aerated filter by O_2 limitation. *Biotechnology Letters* 22: 937-940

Lackner, S., Gilbert, EM., Vlaeminck, SE., Joss, A., Horn, H., van Loosdrecht, MCM. (2014) Full-scale partial nitritation/anammox experiences–an application survey. *Water Research* 55: 292–303

M. Laureni, P. Falâs, O. Robin, A. Wick, D. G. Weissbrodt, J. L. Nielsen, T. A. Ternes, E. Morgenroth, A. Joss. (2016) Mainstream partial nitritation and anammox: long-term process stability and effluent quality at low temperatures. *Water Research* 101: 628-639

Metcalf and Eddy, *Wastewater Engineering: Treatment and Resource Recovery*. McGraw-Hill, New York, USA, 5th edition, 2014.

Paulson, J., Stine, O., Bravo, H., Pop, M., 2013. Differential abundance analysis for microbial 645 marker-gene surveys. *Nature Methods* 10(12), 1200-1202

Pillay, B., Roth, G., Ollermann, RA. (1989) Cultural characteristics and identification of marine nitrifying bacteria from a closed prawn-culture system in Durban. *South African Journal of Marine Science* 8(1): 333-341

Piculell, M., Christensson, M., Jönsson, K., Welander, T. (2016) Partial nitrification in MBBRs for mainstream deammonification with thin biofilms and alternating feed supply. *Water Science and Technology* 73: 1253-1260

Schopf, A., Delatolla, R., Kirkwood, K.M. Partial nitritation at elevated loading rates: design curves and biofilm characteristics. *Bioprocess and Biosystems Engineering* **42,** 1809–1818 (2019). https://doi.org/10.1007/s00449-019-02177-8

Sliekers A.O., Derwort, N., Campos Gomez, JL., Strous, M., Kuenen, JG., Jetten, MSM. (2002) Completely autotrophic nitrogen removal over nitrite in one single reactor. *Water Research* 36(10): 2475-2482

Tian, X., Ahmed, W., Delatolla, R. (2017) Nitrifying bio-cord reactor: performance optimization and effects of substratum and air scouring. *Environmental technology* DOI: 10.1080/09593330.2017.1397760

U.S. Clean Water Act, 33 U.S.C. § 1251 et seq. 1972. U.S Environmental Protections Agency, Washington. https://www.epa.gov/laws-regulations/summary-clean-water-act

Wang, C., Liu, S., Xu, X., Zhang, C., Wang, D., Yang, F. (2018) Achieving mainstream nitrogen removal through simultaneous partial nitrification, anammox, and denitrification process in an integrated fixed film activated sludge reactor. *Chemosphere* 203: 457-466

Wett B. (2007) Development and implementation of a robust deammonification process. *Water Science and Technology* 56(7): 81-88

World Resources Institute, http://www.wri.org/our-work/project/eutrophication-and-hypoxia/sources-eutrophication (Accessed May 2018)

Young, B., Delatolla, R., Abujamel, T., Kennedy, K., Laflamme, E., Stintzi, A. (2017) Rapid start-up of nitrifying MBBRs at low temperatures: nitrification, biofilm response and microbiome analysis. *Bioprocess and Biosystems Engineering* 40: 731-739

Young, B., Delatolla, R., Ren, B., Kennedy, K., Laflamme. E., Stintzi, A. (2016) Pilot-scale tertiary MBBR nitrification at 1°C: characterization of ammonia removal rate, solids settleability and biofilm characteristics. *Environmental Technology*. 37: 2124-2132

Yun, HJ., and Kim, DJ. (2003) Nitrite accumulation characteristics of high strength ammonia wastewater in an autotrophic nitrifying biofilm reactor. *Journal of Chemical Technology and Biotechnology* **78**: 377-383

Zhang, L., Yang, J., Hira, D., Fuji, T., Furukawa, K. (2011) High-rate partial nitrification treatment of reject water as a pretreatment for anaerobic ammonium oxidation (anammox). *Bioresource Technology* 102(4): 3761-3767

CHAPTER 5 – DEFINED MAXIMAL BIOFILM THICKNESS TO ACHIEVE PARTIAL NITRITATION USING FREE NITROUS ACID

5.1 Context

Chapter 5 presents the research article entitled *Defined maximal biofilm thickness to achieve partial nitritation using free nitrous acid* and is in preparation for submission for publication. This article discusses the impact of the carrier design choice of defined maximal biofilm thickness and undefined biofilm thickness on nitrification kinetics, biofilm characteristics, the microbiome and free nitrous acid inhibition to achieve partial nitritation.

5.2 Abstract

Ammonia is a deleterious pollutant present in municipal wastewater that can be hazardous if released into the environment. There is a need for the development of novel processes to advance ammonium removal technologies. Partial nitritation (PN) and anammox are modern treatment processes that can be combined to provide energy efficient ammonia removal; however, these processes have been shown to be challenging to implement as a two-stage system. New methods to achieve steady PN need to be discovered. Free nitrous acid (FNA) exposure has been explored as a possible strategy for achieving PN; however, exposure time and dosage is variable depending on the treatment system. For biofilm technologies, such as the moving bed biofilm reactor, biofilm characteristics, including biofilm thickness, can cause inconsistent results. Therefore, this study compares defined maximal biofilm thickness with undefined biofilm thickness and their capacity to achieve PN using FNA. This study found that a defined maximal biofilm thickness designed carrier maintained a thin biofilm capable of achieving PN after FNA exposure while the undefined biofilm thickness designed carrier was not suitable for stable PN.

5.3 Introduction

Nitrogen, specifically in the form of ammonium and ammonia which is collectively referred to as total ammonia nitrogen (TAN), can be harmful to the natural environment including bodies of water such as rivers, lakes, and oceans. A primary source of TAN discharge to receiving waters is the effluent from municipal wastewater resource recovery facilities (WRRF). To avoid discharging nitrogen into the environment, raw wastewater undergoes various treatment processes. Conventional TAN treatment consists of the nitrification process followed by the denitrification process. Nitrification is the autotrophic, aerobic oxidation of TAN to nitrite and nitrate while denitrification is the heterotrophic, anoxic reduction of nitrate to nitrogen gas by organic carbon. Nitrification and denitrification lack synergy as the nitrification process can be inhibited by organic carbon while the subsequent denitrification process requires an organic carbon source. The addition of external organic carbon sources to achieve the commonly installed post-anoxic denitrification results in additional costs.

Nitrification is a two-step process consisting of nitritation, the oxidation of TAN to nitrite by ammonia oxidizing bacteria (AOB) and is conventionally the rate limiting step; and nitratation, the oxidation of nitrite to nitrate by nitrite oxidizing bacteria (NOB). Modern nitrogen removal is the combination of partial nitritation (PN) and anaerobic ammonia oxidation (anammox) and has been demonstrated to have the capacity to adequately treat nitrogen in both sidestream and mainstream wastewater treatment. PN is the oxidation of a portion of TAN to nitrite while maintaining as little nitrate production as possible as a pretreatment for anammox whereas the anammox process is the anoxic oxidation of TAN by nitrite (Strous *et al*., 1998). The combined PN and anammox (PN/A) processes requires 60% less oxygen, requires no additional carbon source, and produces 90% less biomass than conventional nitrification and denitrification and

therefore has significant economic benefits (Mulder, 2003; Van Loosdretch and Salem, 2006; Siegrist *et al*., 2008). PN/A can be performed in a single reactor system or in a multiple reactor system. Single reactor systems, such as the DEMON (Shalini *et al.*, 2012), CANON (Wang *et al.*, 2013), and ANITA™ Mox systems (Christensson *et al.*, 2013), operate at low dissolved oxygen (DO) concentrations as anammox bacteria are inhibited by DO (above 0.5 mg O_2/L). At low DO concentrations, the anammox bacteria are capable of outcompeting the NOB for nitrite (Strous *et al.*, 1998; Third *et al.*, 2005). At TAN concentrations typical to mainstream and sidestream wastewater treatment, nitritation is oxygen rate limited (Rusten *et al.*, 2006); therefore, operating at low DO concentrations required for anammox treatment results in low PN rates and so, combined PN/A systems require larger operating volumes to compensate for the lower rates of PN.

Multi-reactor systems that split the PN and anammox processes into different reactors can be optimized for each of the distinct processes, resulting in higher nitritation and anammox rates. However, there have been difficulties shown in the suppression of NOB activity, which resulted in the development of various control strategies to supress NOB activity. NOB activity control strategies that have been implemented to achieve NOB suppression in PN reactors include; operating with DO restriction, alkalinity restriction, sequencing batch operations, chemostat operations (no solids retention), and NOB inhibition through free ammonia (FA) and free nitrous acid (FNA) (Hellinga *et al.*, 1998; Fux *et al.*, 2004; Lackner *et al.*, 2014; Dosta *et al.*, 2015; Gilbert *et al.*,2015; Piculell *et al.*, 2016a; Piculell *et al.*, 2016b; Duan *et al.*, 2019).

FA and FNA have been shown to be inhibitory to both AOB and NOB, and NOB have demonstrated greater sensitivity to FA and FNA than AOB (Anthonisen *et al*., 1976). Exposure to FA and FNA to achieve PN has been accomplished through elevated TAN and nitrite

concentrations from sidestream centrate that typically have elevated TAN and nitrite concentrations compared to mainstream municipal wastewaters (Lackner *et al*., 2014). The TAN and nitrite concentrations present in typical municipal wastewaters are insufficient at typical municipal temperatures and pH values to inhibit NOB. Periodic exposure of the bacteria in the mainstream system to sidestream wastewater has been investigated as a strategy to inhibit NOB, through exposure to elevated FA and FNA concentrations, by either periodically changing the feed or transporting the biomass to a point of contact with sidestream wastewater (Lemaire *et al.*, 2014; Wang *et al*., 2014; Piculell *et al.*, 2016b).

Planktonic and sessile technologies have both been shown to be able to achieve PN; however, sessile technologies have various advantages over planktonic technologies such as lower sludge production, longer solids retention, and a smaller land footprint. The moving bed biofilm reactor (MBBR) is a sessile technology that consists of a tank that is filled with carriers with attached biofilm and the carriers moving through the bulk liquid. High density polyethylene carriers have been used as carriers in MBBR systems and many carrier geometries have been developed to optimise aspects such as size, loading rate, surface area, and potential biofilm thickness. Carriers designed to control biofilm thickness have been used to compare a thin biofilm to a thicker biofilm, and the thin biofilm has been shown to enhance the inhibition of NOB activity using periodic exposure to high strength wastewater compared to a thicker biofilm (Piculell et al., 2016b). This work studies the potential for the use of carriers with defined maximal biofilm thickness to be used for improved PN performance. A current gap of knowledge exists with respect to the direct comparison of defined maximal biofilm thickness designed carriers to undefined biofilm thickness designed carriers, based on carrier geometry, for the purpose NOB population growth or activity inhibition and enhanced PN.

In this study, the AnoxK^{TM}Z-style carrier (z-prototype) and the AnoxK^{TM}M-style prototype carrier (chip-prototype) are used to compare a carrier designed to define a maximal biofilm thickness (z-prototype) and a carrier that was not designed to define a biofilm thickness (chip-prototype) for PN. This study aims to compare defined and undefined maximal biofilm thickness for achieving PN using intermittent exposure to FNA to inhibit NOB activity or population growth. This study also aims to determine the effect of length of FNA exposure on nitritation and nitratation inhibition with both defined and undefined maximal biofilm thickness. The biofilm characteristics and microbiome are analysed to compare the z-prototype and the chip-prototype.

5.4 Methods and Materials

5.4.1 Carrier Geometry

To quantify the effects of maximum defined biofilm thickness compared to undefined maximum defined biofilm thickness on FNA inhibition to achieve PN, two carrier types were used: the z-prototype and the chip-prototype. The z-prototype (Fig. S5.1) is a thin, flat, solid disk with small, 50 µm high walls hatched on each side and a specific surface area of 1200 $m^2/10^6$ carriers. The 50 µm walls protect the biofilm that is within the small cells; however, the biofilm that grows outside of the walls is eroded and detached, thus maintaining a thin biofilm. The chip-prototype (Fig. S5.2) is a thin disk that has many carrier-pores and a specific surface area of the chip-prototype is 1100 $m^2/10^6$ carriers. The biofilm grows within the carrier pores; however, the biofilm growth is unrestricted within the carrier-pore and does not maintain a consistent thickness. The z-prototype carriers and the chip-prototype carriers are not commercially available at the time of writing.

5.4.2 Batch Test Protocol and Setup

To quantify the impact of FNA exposure contact time and carrier design choices, a series of batch tests were performed. The impact of each test condition was quantified through two batch tests; a nitratation batch test to determine NOB activity, followed by a nitritation batch test to determine AOB activity. The order of batch tests is to individually quantify the effects of exposure time on NOB and AOB separately. Nitritation produces nitrite which would provide substrate to the NOB and potentially allow the NOB to be active prior to the nitratation batch test; thus, the nitratation batch test would need to be performed prior to the nitritation batch test.

To perform the batch tests, 20 carriers of the same design (either z-prototype or chip-prototype) were extracted from the maintenance reactor and lightly rinsed with distilled water. The carriers were then placed into the FNA reactor for 0, 1, 2, 3, or 4 hours. The 0-hour exposure was used to quantify the uninhibited AOB and NOB activities and establish a baseline to compare the inhibition batch trial data to. After the target exposure time, the carriers were removed from the FNA exposure solution and gently rinsed with distilled water to remove any excess exposure solution.

The batch reactor was filled with 500 mL (h = 15 cm) of the nitratation test solution, and the carriers were added. A 1.5 mL sample was taken simultaneously to the addition of the carriers at t = 0 min. The batch test took place over a 2-hour period with extraction of 1.5 mL samples occurring every 20 minutes. After the last sample was taken, the carriers were removed and rinsed gently in distilled water, and the reactor was emptied and rinsed. The reactor was then filled with 500 mL of nitritation solution and the carriers were re-added. A 1.5 mL sample was taken as the carriers were added as t = 0 min. Samples with a volume of 1.5 mL were taken every 20 minutes over a 2-hour period. The carriers were disposed of after batch testing. The TAN and

NO_2^--N concentrations and associated nitrogen balances from the batch tests for the z-prototype and chip-prototype are presented in Tables 9.1-9.8, respectively.

The batch reactor (Fig. S5.4) was a single 2 L glass reactor with a temperature controlled water jacket. The batch reactor was operated at a constant temperature of 20°C using the temperature control water jacket. DO was maintained at a constant 4 mg/L through oxygen and nitrogen bubbled in from the bottom of the reactor at a combined flow rate of 1 L/min to providing consistent mixing. The pH was maintained at 7.5 through consistent monitoring and adjustment using 0.05 M H_2SO_4 or 0.05 M NaOH.

The FNA reactor was a single 8 L metal reactor with a temperature controlled water jacket. The reactor was filled with 5 L of FNA exposure solution and operated at a temperature of 30°C and a pH of 6. The pH was controlled using a buffer solution and titrated using 1 M H_2SO_4 and 1 M NaOH. Aeration was provided at a rate of 0.5 L/min to promote movement within the reactor. The reactor operated with a TAN concentration of 400 mg TAN/L and a nitrite concentration of 500 mg NO_2^--N/L, proving a FNA concentration of 0.88 mg N/L.

5.4.3 Carrier Preparation and Maintenance

The z-prototype and chip-prototype carriers were prepared and maintained in an 8 L metal reactor. The temperature was maintained using a temperature control jacket attached to a hot water bath. Large bubble aeration was provided through the bottom of the reactor to provide oxygen and mixing. The aeration was hydrated by bubbling the air through water to prevent water vaporization within the reactor. The reactor was fed at a rate of 81.6 L/d with a solution that was made from diluted high strength waste water; providing an influent TAN concentration

of 43.7 ±1.1 mg/L and an average surface area loading rate (SALR) of 2.83 ± 0.05 g TAN/m^2·d. The maintenance reactor operated at a DO of 6 mg/L and a pH of 7.8 ± 0.2 mg/L.

The maintenance reactor was initially filled with unseeded z-prototype and chip-prototype carriers and seeded using effluent from a nitrifying MBBR system and sludge from a nitrifying activated sludge system. The maintenance reactor was initially operated at an SALR of 0.9 g TAN/m^2·d and a temperature of 25°C to facilitate biofilm growth. The SALR was increased to 2.5 ± 0.03 g TAN/m^2·d over the course of two weeks. After a further 2 weeks of operation the temperature was reduced to 20°C to simulate municipal treatment and the SALR was further increased to 2.83 ± 0.05 g TAN/m^2·d as carriers were removed for a separate study.

5.4.4 Feed Solutions

The wastewater feed solution for the system consisted of centrate from the Sjölunda wastewater treatment plant (approx. 1000 mg TAN/L) that was diluted to an average of 43.7 ± 1.1 mg TAN/L using tap water. The average influent nitrite concentration was 1.34 ± 0.59 mg NO_2^--N/L. To ensure that there was sufficient alkalinity, 300 mg $CaCO_3$/L as $NaHCO_3$ was added. Due to the use of centrate as the basis for the feed, additional nutrients and carbon were not added.

The FNA exposure solution consisted of 7.642 g NH_4Cl (1.5284 g/L), and 12.321 g $NaNO_2$ (2.4642 g/L) as substrates, and 68 g KH_2PO_4 (13.6 g/L) as a buffer resulting in concentrations of 400 mg NH_4^+-N/L, and 500 mg NO_2^-- N/L, with KH_2PO_4 acting as a buffer to keep the pH stable.

The nitratation kinetic test solution for the baseline and the inhibition tests consisted of 1.125 g $NaHCO_3$, 0.2218 g $NaNO_2$, and 0.4 mL of PO_4 solution (12.75 g P/L) dissolved in 1.5 L of distilled water. The nitratation kinetic test solution had a substrate concentration of 30 mg NO_2^--N/L.

The nitritation kinetic solution for the baseline and the inhibition tests consisted of 1.125 g $NaHCO_3$, 0.257 g NH_4Cl, and 0.4 mL of PO_4 solution (12.75 g P/L) dissolved in 1.5 L of distilled water. The nitritation kinetic test solution had a substrate concentration of 45 mg NH_4^+-N/L. The solutions were titrated to a pH of 7.5 using 0.5M H_2SO_4.

5.4.5 Chemical Analysis Methods

Chemical analyses for batch test TAN, nitrite, and nitrate concentrations were performed using HACH vial test kits: Ammonia LCK 303, Nitrite LCK 342, and Nitrate LCK 339, respectively (HACH, CO, USA). To compensate for the interference of nitrite on the Nitrate LCK 339 HACH test, a standard curve was developed and a correction factor of 0.31 × [mg NO_2^--N/L] was subtracted from the corresponding nitrate value.

5.4.6 Biofilm Mass

Biofilm mass was quantified using a modified version of the method used in Piculell *et al.* (2016a). Twenty carriers extracted from the continuous reactor, placed in an aluminium weighing dish and dried at 105°C for a minimum of 8 hours. After this period the carriers were cooled in a desiccator for a minimum of 1 hour. Once the carriers were cooled to room temperature, the carriers and the weighing boat were weighed. The carriers were removed from the weighing boat and placed in 500 mL of 1 M NaOH for a minimum of 8 hours. The carriers were rinsed with distilled water and gently scrubbed with a soft bristle brush to ensure all of the biofilm was removed. The rinsed carriers were returned to the same aluminum weighing boat as before and dried in an oven at 105°C for a minimum of 8 hours. After this period the carriers and weighing boat were placed in the desiccator for a minimum of 1 hour and weighed. The difference in weight was the weight of the biofilm removed. The weight of the biofilm removed was divided by 20 to obtain the average biofilm mass of the carrier.

5.4.7 Biofilm Thickness Image Acquisition and Analysis

To quantify the thickness of the biofilm and analyze the biofilm morphology, images were taken using the OLYMPUS SZ-ET (Olympus Corporation, Japan) and analyzed using the ImageJ program (LOCI University of Wisconsin, USA). To quantify the thickness of the chip-style carriers, 8 top-down images at 2x magnification were acquired. The length of one side of the carrier pores was used to set the scale for the ImageJ program and over 200 biofilm measurements were taken. The results were exported into Microsoft Excel where the results were analyzed. To quantify the biofilm thickness of the z-style carriers, the carriers were cut in half and oriented such that the inside of the carrier was directed towards the camera. Ten images were acquired at 8× magnification with added scale bars. The ImageJ program was used to quantify biofilm thickness using a minimum of 150 individual measurements.

5.4.8 Microbiome Acquisition and Analysis

To quantify the microbiome, two 1.5 mL Eppendorf tubes per carrier per condition were filled with fresh biofilm extracted from carriers obtained from the continuous flow reactor. The samples were labeled and stored in a $-30^{\circ}C$ freezer until further analysis.

The samples were analysed by DNASense (Aalborg, Denmark) with the 16S rRNA gene amplicon sequencing targeting the V1-3 bacterial variable region. The raw sequencing data were processed at DNASense using the UPARSE workflow (Edgar, 2013). Data were analysed through Rstudio using the ampvis2 package (Aalborg University, Denmark) and the MiDAS database. The subsequent sections describe the protocol used by DNASense (Denmark).

5.4.9 DNA Extraction

The standard protocol for the FastDNA Spin kit for Soil (MP Biomedicals, USA) was used for DNA extraction. The following exceptions to the standard protocol were applied; 120 µL of

MT buffer, 500 µL of sample, and 480 µL sodium phosphate buffer were added to the Lysing Matrix E tube; DNA concentration was quantified using the Qubit dsDNA HS/BR Assay kit (Thermo Fisher Scientific, USA); bead beating was performed at 6 m/s for 4 sets of 40 s (Albertsen *et al.*, 2015); and to validate the purity of a subset of DNA extracts and the product size, gel electrophoresis was used using Tapestation 2200 and Genomic DNA screentapes (Agilent, USA).

5.4.10 Library Preparation

A custom protocol based on Caporaso *et al.* (2012) was used to prepare the bacteria 16S V1-3 rRNA gene sequencing libraries. To make a template for the PCR amplification of the bacteria 16S V1-3 rRNA gene amplicon, up to 10 ng of extracted DNA was used. Each 25 µL PCR reaction contained 1.5 mM of $MgSO_4$, 100 µM of each dNTP, Platinum High Fidelity buffer (1X) (Thermo Fisher Scientific, USA), 400 nM of each forward and reverse barcoded library adaptors, and 0.5 U of Platinum Taq DNA polymerase HF. PCR was conducted with the following program: Initial denaturation at 95°C for 2 min, 30 cycles of amplification (95°C for 20 s, 56°C for 30 s, 72°C for 60 s) and a final elongation at 72°C for 5 min. For each sample, duplicate PCR reactions were performed and after the PCR the duplicates were pooled. The adaptors contain 16S V1-3 specific primers: [27F] AGAGTTTGATCCTGGCTCAG and [534R] ATTACCGCGGCTGCTGG (Jumpstart Consortium., 2012). The standard protocol for Agencourt Ampure XP Beads (Beckman Coulter, USA) was used to purify the resulting amplicon libraries with a sample to bead ration of 5:4. The DNA was eluted to 25 µL of nuclease free water (Qiagen, Germany). A Qubit dsDNA HS Assay kit (Thermo Fisher Scientific, USA) was used to measure the DNA concentration and gel electrophoresis was used to validate the product size and purity of a subset of the sequencing library. Gel electrophoresis was performed using Tapestation 2200 and D1000/High sensitivity D1000 screentapes (Agilent, USA).

5.4.11 DNA Sequencing

The purified sequencing libraries were diluted to 6 nM after being pooled in equimolar concentrations. A Miseq (Illumina, USA) was used to pair-end sequence the samples (2x300 bp) using a MiSeq Reagen kit v3 (Illumina, USA) following the standard guidelines for preparing and loading samples on the MiSeq. To overcome low complexity issues with amplicon samples, a >10% PhiX control library was spiked in.

5.4.12 Bioinformatic Processing

The Trimmomatic v.0.32 (Bolger *et al*., 2014), using a SLIDINGWINDOW setting of :5:3 and a MINLEN setting of :275, was used to trim the forward and reverse reads. The trimmed forward and reverse reads were merged using FLASH v.1.2.7 (Magoc and Salzberg, 2011) with the settings – m 10 – M 200. The UPARSE workflow (Edgar, 2013) was used to dereplicate and format the trimmed reads. The dereplicated reads were clustered, using the usearch v.7.0.1090 – cluster_otus command with default settings. OUT abundances were estimated using the usearch v.7.0.1090 –usearch_global command with –id 0.97 –maxaccepts 0 – maxrejects 0. The RDP classifier (Wang *et al.*, 2007) was implemented in the parallel_assign_taxonomy_rdp.py script in QIIME (Caporaso *et al.*, 2010) was used to assign the taxonomy, using –confidence 0.8 and the MiDAS database v. 123 (McIlroy *et al.*, 2017), which is a curated database based on the SILVA database, release 123 (Quast *et al.*, 2013). The results were analysed using the ampvi package v.2.4.10 (Albertsen *et al.*, 2015) in R v.3.5.1 (R Core Team, 2017) using the Rstudio IDE.

5.4.13 Batch Test Surface Area Removal Rate

The surface area removal rate (SARR) for the baseline and inhibited batch tests was calculated using the following equation:

$$SARR_{batch\ test} = \frac{V \times (C_0 - C_t)}{SA_{carrier} \times t} \quad (Eq. 5.1)$$

Where V is the volume of solution, C_0 is the concentration of substrate at t = 0, C_t is the concentration of substrate at t = t, $SA_{carrier}$ is the combined surface area of all of the carriers in the vessel, and t is the time that has passed during the batch test.

For the batch tests: V = 0.5 L; C_0 = 45 mg TAN/L or 30 mg NO_2^--N/L; C_t is the concentration at time t; $SA_{carrier}$ = 0.024 m^2 for the z-prototype or 0.022 m^2 for the chip-prototype; and t = time at which the sample was taken (0 – 0.0833 d).

5.4.14 Percent Inhibition

Percent inhibition is defined by fraction of baseline activity that is demonstrated after exposure to the synthetic exposure solution.

$$Percent\ Inhibition = \frac{SARR_{Baseline} - SARR_{Inhibited}}{SARR_{Baseline}} \times 100\% \quad (Eq. 5.2)$$

Where $SARR_{Baseline}$ is the TAN or NO_2^- SARR quantified from the kinetic batch tests using carriers that were not exposed to the synthetic exposure solution, and $SARR_{Inhibition}$ is the TAN or NO_2^- SARR quantified from the kinetic batch tests using carriers that were exposed to the synthetic exposure solution for a set period of time.

5.5 Results and Discussion

5.5.1 Batch Test Kinetics

Batch kinetic testing was used to quantify the effects of FNA exposure time on nitrifying biofilms at 20°C for the z-prototype carriers and the chip-prototype carriers. This is to quantify the effects of biofilm thickness control strategies on AOB and NOB inhibition due to FNA. The SARR

of the z-prototype and chip-prototype for both nitritation and nitratation are shown in Figure 5.1 and Table 5.1. The baseline AOB nitritation kinetic rates (TAN SARR) were 1.43 ± 0.05 and 2.56 ± 0.09 g TAN/m^2·d for the z-prototype and chip-prototype, respectively, and the baseline NOB nitratation kinetic rates (NO_2^-–N SARR) were 1.39 ± 0.06 and 6.05 ± 0.28 g NO_2^- -N/m^2·d for the z-prototype and chip-prototype, respectively. Note that as the nitritation and nitratation kinetics were determined separately, using solutions that contain either ammonia or nitrite; the nitratation rates were not limited by the nitritation rates as would normally be seen in conventional nitrification. The chip-prototype had higher baseline TAN and NO_2^--N SARR kinetic rates than the z-prototype, similar to what was seen when comparing carriers of different thicknesses (Suarez *et al*., 2019). The chip-prototype also displayed greater overall resilience to FNA exposure than the z-prototype. Although the z-prototype and the chip-prototype experienced similar NO_2^-–N SARR percent inhibition, the higher baseline NO_2^--N SARR of the chip-prototype meant that significant nitratation (1.68 ± 0.08 g NO_2^--N/m^2·d) was still occurring. Furthermore, beyond the NO_2^--N SARR inhibition experienced at 1 hour of exposure, the chip-prototype NO_2^--N SARR was not correlated with exposure time and even after 4 hours of exposure the NO_2^--N SARR inhibition was 77.5% with an NO_2^- SARR of 1.36 ± 0.06 g NO_2^- -N/m^2·d which is still a significant NO_2^--N SARR. Both the z-prototype and the chip-prototype experienced TAN SARR inhibition after 1 hour of exposure and while the z-prototype had a moderate trend of increased TAN SARR inhibition with exposure time, there was no correlation between TAN SARR inhibition and exposure time for the chip-prototype. The optimal exposure time for the z-prototype was 3 hours as the NO_2^--N SARR was 0.09 ± 0.004 g NO_2^- -N/m^2·d with an NO_2^--N SARR inhibition of 94% which is sufficient for PN; however, there was no optimal exposure time for chip-prototype as the NO_2^-–N SARR inhibition was never sufficient to achieve stable PN.

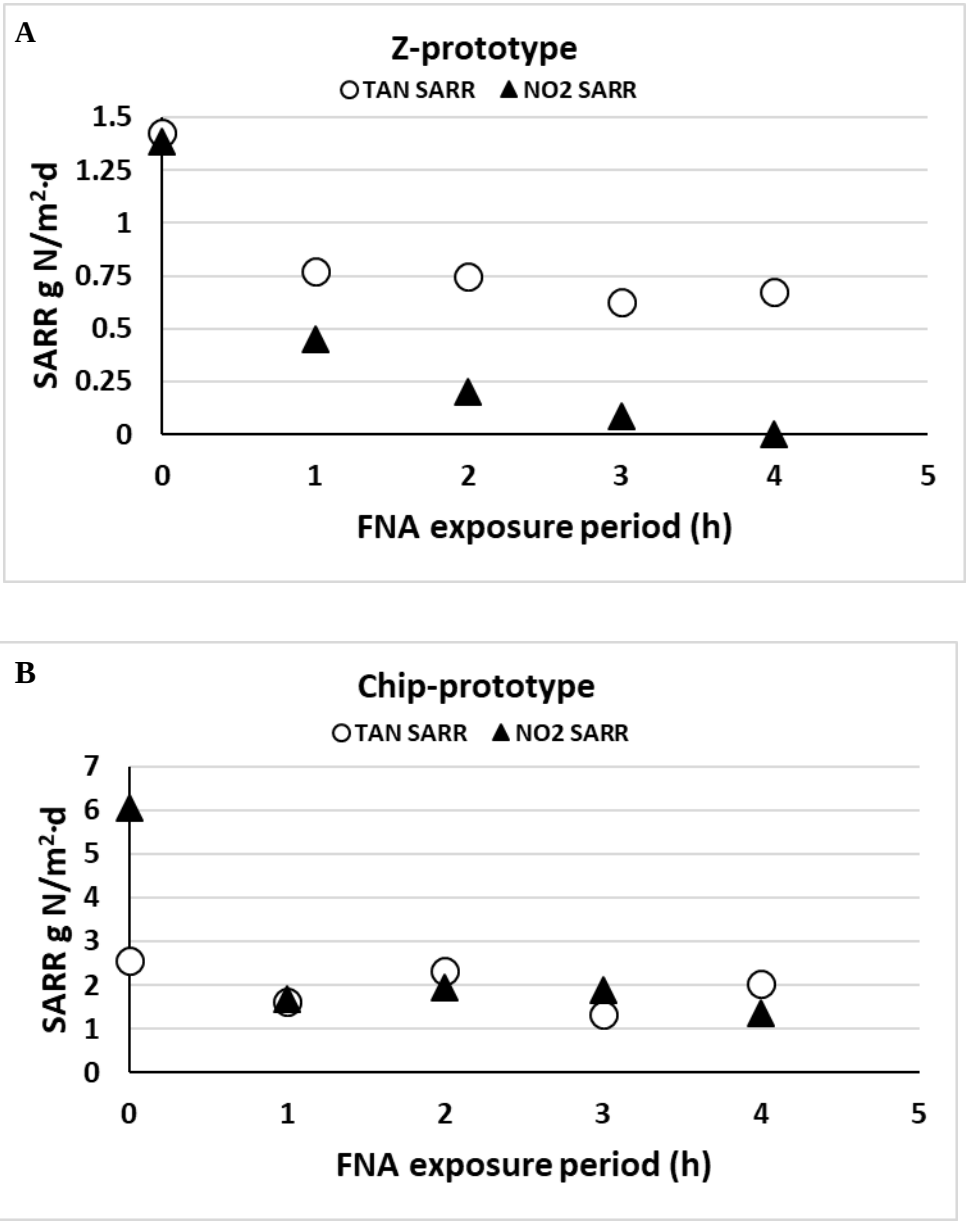

Figure 5.1 Nitritation (AOB) removal rates (○) and nitratation (NOB) removal rates (▲) for z-prototype (A) and chip-prototype (B).

Table 5.1 Nitritation (AOB) removal rates and inhibition percentage, and nitratation (NOB) removal rates and inhibition percentage for the z-prototype and the chip-prototype.

z-prototype	TAN SARR (g TAN-N/m^2·d)	TAN SARR Inhibition (%)	NO_2^--N SARR (g NO_2^--N/ m^2·d)	NO_2^--N SARR Inhibition (%)
Baseline	1.43 ± 0.05	-	1.39 ± 0.06	-
1 hour	0.78 ± 0.03	45.61 ± 1.7	0.45 ± 0.02	67.57 ± 3.1
2 hour	0.75 ± 0.03	47.47 ± 1.7	0.20 ± 0.01	85.59 ± 3.9
3 hour	0.625 ± 0.02	56.14 ± 2.1	0.09 ± 0.004	93.69 ± 4.3
4 hour	0.675 ± 0.24	52.63 ± 1.9	0.0 ± 0	100.0 ± 0
chip-prototype	TAN SARR (g TAN-N/m^2·d)	TAN SARR Inhibition (%)	NO_2^--N SARR (g NO_2^--N/ m^2·d)	NO_2^--N SARR Inhibition (%)
Baseline	2.56 ± 0.09	-	6.05 ± 0.28	-
1 hour	1.61 ± 0.06	37.23 ± 1.4	1.68 ± 0.08	72.3 ± 3.3
2 hour	2.32 ± 0.08	9.57 ± 0.4	1.94 ± 0.09	68.02 ± 3.1
3 hour	1.32 ± 0.05	26.6 ± 1.0	1.88 ± 0.09	68.15 ± 3.1
4 hour	2.04 ± 0.07	20.21 ± 0.7	1.36 ± 0.06	77.48 ± 3.6

5.5.2 Biofilm Characteristics

Biofilm characteristics measured in this study for the z-prototype and chip-prototype carriers at 20°C include the biofilm mass (Figure 5.2a), thickness (Figure 5.2b) and morphology (Figure S5.3a-b). The average biofilm mass measurements were 1.7 ± 0.23 and 17 ± 1.58 mg biofilm/carrier for the z-prototype and chip-prototype, respectively. Note the average biofilm mass measurements were obtained by measuring the biofilm mass of a batch of 20 carriers simultaneously; the error was not calculated. The biofilm thicknesses measurements were 38 ± 2.55 and 319 ± 10.87 μm for the z-prototype and chip-prototype, respectively. The chip-prototype carrier had an order of magnitude larger biofilm thickness and biofilm mass per carrier than the z-prototype carrier. The morphology of the z-prototype had a thin, irregular biofilm that was thicker near the carrier walls and thinner near the middle of the carrier cells. There was also biofilm growth on a portion of the carrier walls that were unprotected; however, the biofilm was very thin. The chip-prototype biofilm was very thick and many of the carrier pores were clogged. The z-prototype

and chip-prototype were exposed to the same shear, with an average velocity gradient G of 216 s^{-1} (eqns 9.1 and 9.2). This mixing velocity is greater than the minimum mixing velocity of 185 s^{-1} found by Garcia (2016) who operated a similar system; however, the velocity gradient used during the batch tests was on the low end of velocity gradient ranges conventionally used (Melcer, 2015; Garcia, 2016). Thus, the mixing within the reactor did not provide significant biofilm thickness loss.

The biofilm thickness and biofilm mass per carrier for the chip-prototype were an order of magnitude greater than the biofilm thickness and biofilm mass per carrier for the z-prototype. The surface areas for the z-prototype and chip-prototype were very similar and had similar biofilm thickness: mass ratios; thus, the two carrier types had similar biofilm densities. This similarity in biofilm density is in contrast to what has been seen in literature where an increase in biofilm thickness is often associated with a decrease in biofilm density (Piculell *et al.*, 2016; Schopf *et al.*, 2019). This difference in biofilm characteristics yet similar biofilm densities between the z-prototype and chip-prototype is due to the significant difference in carrier geometry while operating at conventional loading rates where the carriers are not excessively stressed as biofilm stress has been shown to increase biofilm thickness and reduce density (Flemming, 1993; White and Gadd, 2000; Bjornberg *et al*., 2009).

To compare the approximate bacterial activity of the z-prototype and the chip-prototype the normalized AOB and NOB activity rates were calculated. The normalized AOB and NOB activity rates can be approximated using baseline nitrification kinetics, biofilm thickness (Table 5.3), and biofilm mass (Table 5.4) and will be represented as SARR/µm or SARR/mg biofilm where SARR is expressed using units of g $N/m^2 \cdot d$. The z-prototype carrier had more than 5 times higher AOB activity and more than 2 times higher NOB activity per biofilm mass or per biofilm

thickness than the chip-prototype. This difference in activity could be due to the bacterial density of the biofilm and the theory that only a portion of the biofilm is used for any one process and that only the top layer of the biofilm is most active (Liu *et al.*, 1994); therefore, the most active portion of the biofilm is the entirety of the z-prototype biofilm but only a portion of the chip-prototype biofilm volume; therefore, the activity efficiency of the z-prototype would be higher (Liu *et al.*, 1994; Torresi *et al.*, 2016).

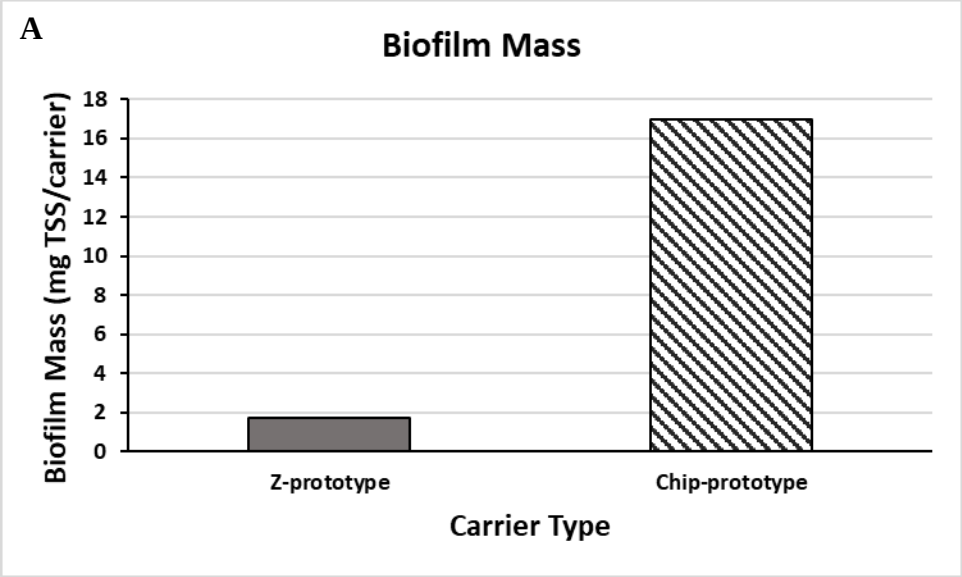

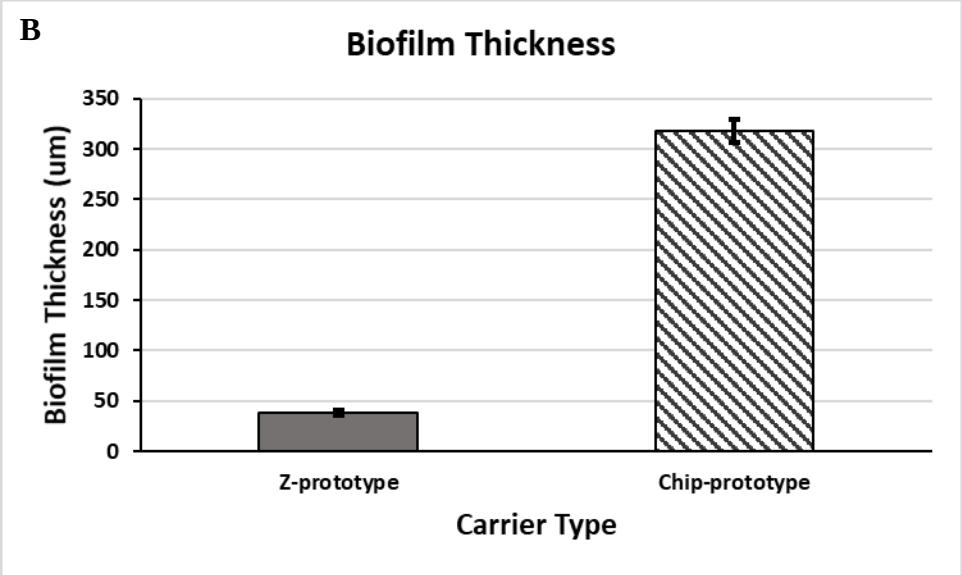

Figure 5.2 Biofilm mass (A) and biofilm thickness (A) for the z-prototype (dark grey) and chip-prototype (hatched).

Table 5.2 Biofilm mass and thickness of the z-prototype and chip-prototype

Carrier Type	Biofilm Mass (mg TSS/Carrier)	Biofilm Thickness (μm)
z-prototype	1.7 ± 0.23	38 ± 2.55
chip-prototype	17 ± 1.58	319 ± 10.87

Table 5.3 Baseline AOB and NOB activity normalized for biofilm thickness

Carrier Type	AOB Activity (SARR/ μm thickness)	NOB Activity (SARR/ μm thickness)
z-prototype	0.0375	0.0366
chip-prototype	0.0067	0.0158

Table 5.4 Baseline AOB and NOB activity normalized for biofilm mass

Carrier Type	AOB Activity (SARR/ mg biomass)	NOB Activity (SARR/ mg biomass)
z-prototype	0.838	0.818
chip-prototype	0.151	0.355

5.5.3 Microbiome

The microbiomes are analysed by quantifying the percent abundance along with the Shannon and Simpson alpha-diversity indexes. Table 5.5 presents the top 20 most abundant genera of the chip-prototype and the z-prototype of the total 465 and 403 observed OTUs, respectively. The top 20 most abundant genera account for 71.4% of the total abundance in the chip-prototype microbiome while the top 20 most abundant genera account for 80.5% of the total abundance in the z-prototype microbiome. *Nitrosomonas* was the second most abundant bacteria for both the chip-prototype and the z-prototype, at relative abundances of 10.2% and 11.2%, respectively. *Nitrospira* was the third most abundant bacteria for the chip-prototype (9.5%); however,

Nitrospira was only the 16th most abundant bacteria for the z-prototype (1.2%). The difference in *Nitrospira* abundance and biofilm mass, due to the difference in carrier geometry, could be a reason that the NO_2^--N SARR is higher in the chip-prototype than the z-prototype. The most abundant genus in the chip-prototype was *Xanthamonas* (13%), which has been theorized to be involved in TAN oxidation (Dosta *et al.*, 2015). The most abundant genus in the z-prototype was *Hyphomicrobium* (12.3%) which is a heterotroph that is most likely a result of the organic carbon present in the diluted centrate used for continuous operations.

Table 5.5 Top 20 most abundant bacteria for the chip-prototype and z-prototype

Genus	Chip-prototype Abundance (%)	Z-prototype Abundance (%)
Nitrosomonas	10.24	11.19
Xanthomonas	12.99	4.45
Hyphomicrobium	4.07	12.26
Defluviimonas	3.40	7.94
Nitrospira	9.48	1.22
f__Anaerolineaceae_OTU_12	5.55	4.73
Devosia	2.31	7.15
Rhodobacter	4.10	4.53
f__Sphingomonadaceae_OTU_36	1.48	4.07
Planctomyces	1.44	4.01
Pedomicrobium	1.76	3.27
o__DB1-14_OTU_28	3.39	0.94
MNG7	0.85	3.21
Meganema	0.92	2.87
f__Phyllobacteriaceae_OTU_15	1.53	2.03
Pirellula	1.25	2.16
f__Saprospiraceae_OTU_153	2.86	0.21
Bosea	0.10	2.82
f__Anaerolineaceae_OTU_86	1.52	1.18
f__Chitinophagaceae_OTU_69	2.19	0.27

The alpha-diversity (Figure 5.3) is a representation of the diversity within the microbiome. The Shannon index represents both the richness (number of different bacteria) as well as the

evenness (abundance of each bacteria) while the Gini - Simpson index represents dominance as it does not take into account the richness, only the evenness and total number of organisms without distinguishing between species. The Shannon index values of the chip-prototype and z-prototype are 4.05 and 3.92, respectively; therefore, the chip-prototype had a similar Shannon index diversity to the z-prototype. The Shannon index values are lower than the values seen from nitrifying MBBR operating at a municipal wastewater treatment plant pilot study (Suarez *et al*., 2019). This difference in diversity may be due to the difference in source waters as in this study the water source is diluted centrate while the pilot study used a constantly changing municipal wastewater. The chip-prototype and z-prototype had Gini - Simpson indices of 0.954 and 0.962 where 0 represents a single bacteria system and 1 represents the maximum diversity, thus demonstrating that the systems have similar diversities. These Gini –Simpson index values are similar to other nitrifying biofilm systems (Wang *et al*., 2018; Jia *et al*., 2018). The difference in results from the Shannon and the Gini - Simpson index is most likely due to how the indexes were calculated and what they represent. Although the diversity indices are very similar for the chip-prototype and the z-prototype, the chip-prototype shows 465 observed OTUs while the z-prototype shows 403 observed OTUs, demonstrating that the chip-prototype has a higher richness. Conversely, the top 10 most abundant bacteria accounts for 58.4% and 54.6% of the total abundance for the chip-prototype and z-prototype, respectively, demonstrating that the z-prototype has a higher evenness, despite similar diversities.

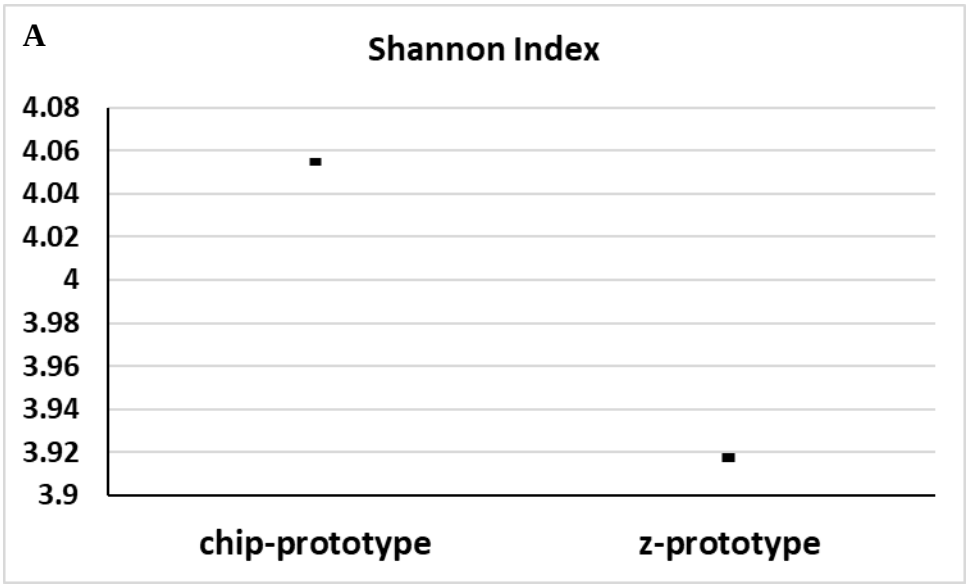

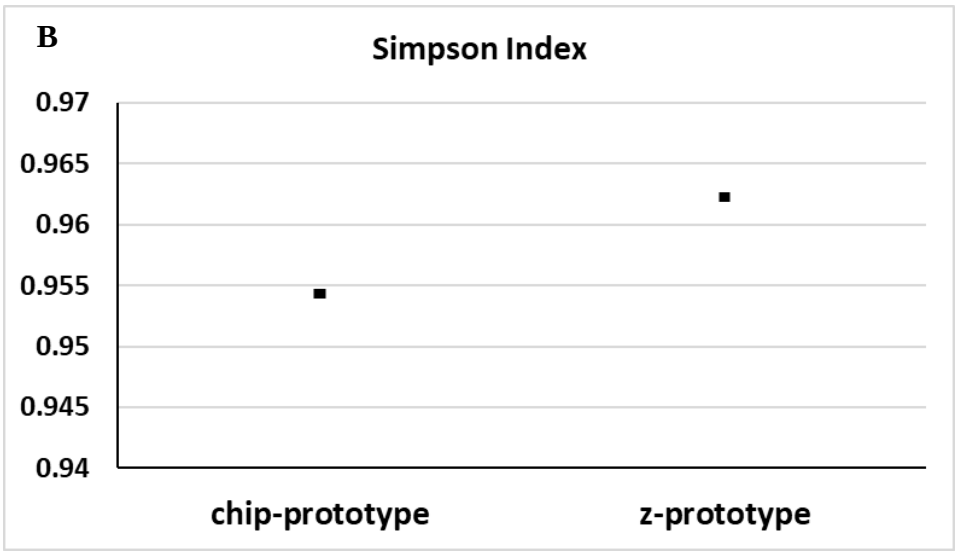

Figure 5.3 Shannon (A), and Simpson (B) alpha-diversity indexes for chip-prototype and z-prototype

The chip-prototype had higher baseline TAN SARR and NO_2^--N SARR kinetics than the z-prototype. The chip-prototype experienced a very different response to FNA than the z-prototype, as stable PN was not achieved with the chip-prototype even after 4 hours of exposure

to the synthetic centrate solution. Conversely, sufficient PN (93% NO_2^--N SARR inhibition) was achieved with the z-prototype after 3 hours of exposure, and PN (100% NO_2^--N SARR inhibition) was achieved with the z-prototype after 4 hours of exposure to the synthetic centrate. Furthermore, both the chip-prototype and the z-prototype maintained significant TAN SARR kinetics; however, the z-prototype experienced higher TAN SARR inhibition than the chip-prototype even with similar abundances of *Nitrosomonas*. Therefore, the carrier design has a significantly greater effect on inhibition response than the microbiome. This is likely due to the fact that the biofilm on the chip-prototype carrier was allowed to grow unrestricted and, therefore, became very thick, while the z-prototype carrier, by design, defined the maximal biofilm thickness and therefore had a very thin biofilm. This difference in biofilm thickness and mass is likely the defining factor for inhibition effects as well as microbiome populations. This study shows that carrier geometry controlled biofilm thickness is likely a preferential strategy for achieving consistent PN.

5.6 Conclusions

Undefined biofilm thickness (chip-prototype carrier) versus defined maximal biofilm thickness (z-prototype carrier) carrier design strategies were investigated through batch testing to determine the ideal biofilm thickness definition strategy for achieving PN using FNA exposure. Through batch testing, it was found that the ideal biofilm thickness strategy was to use a defined maximal biofilm thickness strategy because only the z-prototype was able to achieve complete NOB inhibition at the FNA exposure times tested. The z-prototype at 20°C was able to achieve PN after 3 hours of exposure to 0.88 mg FNA/L, while the chip-prototype was unable to achieve stable PN without further nitratation during the batch tests even at 4 hours of exposure. In addition, there was no clear indication that further exposure would have allowed the chip-prototype to

achieve complete NOB inhibition with maintained stable nitritation; likely due to the extent that the biofilm thickness was able to be achieved.

5.7 Supplemental Material

Figure S5.1 Z-prototype carrier top-view

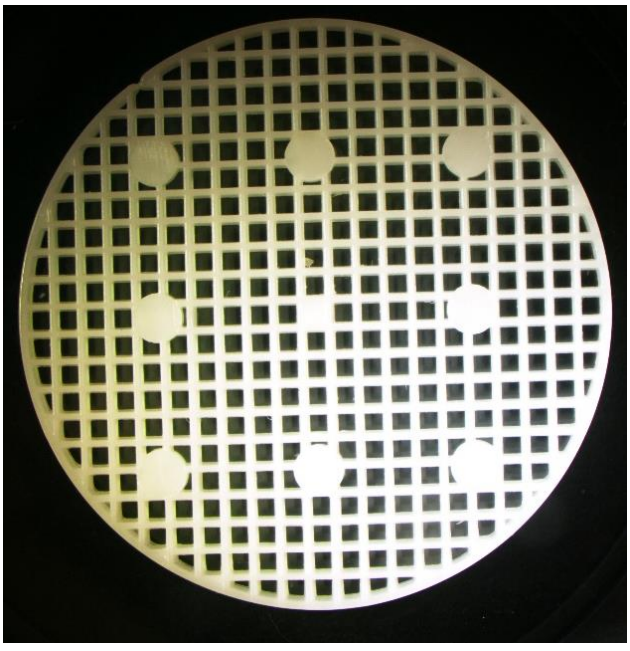

Figure S5.2 Chip-prototype carrier top-view

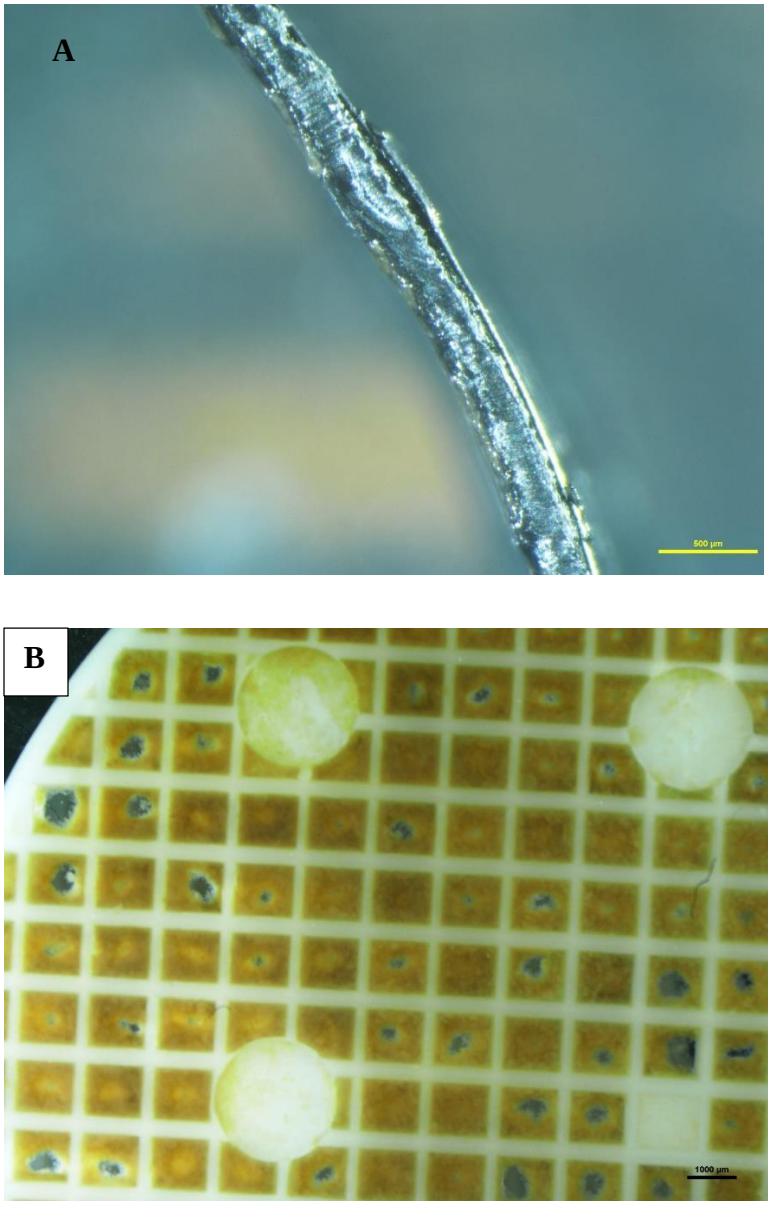

Figure S5.3 Images of cross-section of z-prototype (A) and top-down view of chip-prototype (B) demonstrating biofilm morphology. The scale bar of the z-prototype (A) is 500µm, the scale bar for the chip-prototype (B) is 1000µm

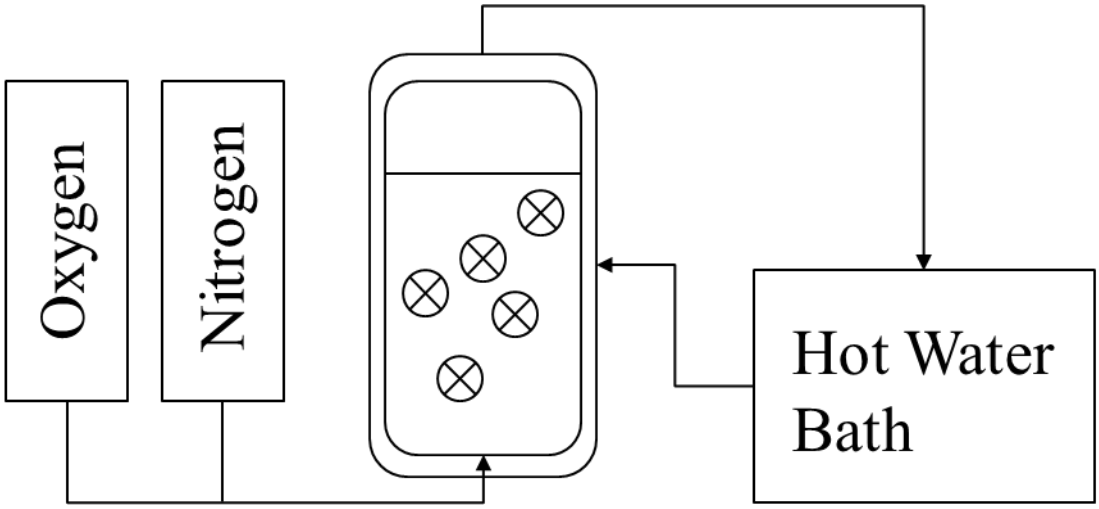

Figure S5.4 Experimental schematic

5.8 References

Albertsen, M., Karst, S.M., Ziegler, A.S., Kirkegaard, R.H., and Nielsen, P.H. (2015) Back to Basics – The Influence of DNA Extraction and Primer Choice on Phylogenetic Analysis of Activated Sludge Communities. *PLOS ONE* 10: e0132783

Anthonisen, A.C., Loehr, R.C., Prakasam, T.B.S., Srinath, 12 E.G., (1976). Inhibition of Nitrification by Ammonia and 13 Nitrous Acid. *Water Pollution and Control Federation* 48, 835–852

Bjornberg C, Lin W, Zimmerman R.A. (2009) Effect of temperature on biofilm growth dynamics and nitrification in a full-scale MBBR system. *Proceedings of the Water Environment Federation*, WEFTEC 2009: Session 61 through 70:4407-4426

Bolger, A.M., Lohse, M., and Usadel, B. (2014) Trimmomatic: A flexible trimmer for Illumina sequence data. *Bioinformatics* 30: 2114–2120

Caporaso, J.G., Kuczynski, J., Stombaugh, J., Bittinger, K., Bushman, F.D., Costello, E.K., Fierer, N., Peña, A.G., Goodrich, J.K., Gordon, J.I., Huttley, G.A., Kelley, S.T., Knights, D., Koenig, J.E., Ley, R.E., Lozupone, C.A., McDonald, D., Muegge, B.D., Pirrung, M., Reeder, J., Sevinsky, J.R., Turnbaugh, P.J., Walters, W.A., Widmann, J., Yatsuneko, T., Zaneveld, J., Knight, R. (2010) QIIME allows analysis of high-throughput community sequencing data. *Nature Methods* 7: 335–336

Caporaso, J.G., Lauber, C.L., Walters, W. a, Berg-Lyons, D., Huntley, J., Fierer, N., Owens, S.M., Betley, J., Fraser, L., Bauer, M., Gormley, N., Gilbert, J.A., Smith, G., Knight, R. (2012) Ultra-high throughput microbial community analysis on the Illumina HiSeq and MiSeq platforms. *The ISME journal* 6: 1621–4

Edgar, R.C. (2013) UPARSE: highly accurate OTU sequences from microbial amplicon reads. *Nature methods* 10: 996–8

Christensson, M, Ekström, S., Anderson Chan, A., Le Vaillant, E., Lemaire, R. (2013) Experience from start-ups of the first ANITA Mox plants. *Water Science and Technology* 67(12): 2677-2684

Dosta, J., Vila, J., Sancho, I., Basset, N., Grifoll, M., Mata-Alverez, J. (2015) Two-step partial nitritation/Anammox in granulation reactors: Start-up operation and microbial characterization. *Journal of Environmental Management* 164: 196-205

Duan, H., Ye, L., Lu, X., Yuan, Z. (2019) Overcoming nitrite oxidizing bacteria adaptation through alternating sludge treatment with free nitrous acid and free ammonia. *Environmental Science and Technology* 53(4): 1937-1946

Flemming, H.C. (1993) Biofilms and environmental protection. *Water Science and Technology* 27:1-10

Fux, C., Huang, D., Monti, A., Siegrist, H. (2004) Difficulties in maintaining long-term partial nitritation of ammonium-rich sludge digester liquids in a moving-bed biofilm reactor (MBBR). *Wat. Sci. Tech* 49: 53-60

Garcia, K. (2016) The effect of biofilm carrier length on nitrification in moving bed biofilm reactors: an examination of mixing intensity, shock loadings, and pH changes. Thesis https://digitalrepository.unm.edu/ce_etds/115. Accessed March 27, 2021

Gilbert, E.M., Agrawal, S., Schwartz, T., Horn, H., Lackner, S. (2015) Comparing different reactor configurations for Partial Nitritation/ Anammox at low temperatures. *Water Research* 81: 92-100

Hellinga, C., Schellen, A.A.J.C., Mulder, J.W., van Loosdrecht, M.C.M., Heijnen, J.J., 1998. The SHARON process: an innovative method for nitrogen removal from ammonium-rich waste water. *Water Science and Technology* 37, 135–142

Jia, W., Chen, Y., Zhang, J., Li, C., Wang, Q., Li, G., Yang, W. (2018) Response of greenhouse gas emissions and microbial community dynamics to temperature variation during partial nitrification. *Bioresource Technology* 261: 19-27

Lackner, S., Gilbert E.M., Vlaeminek, S.E., Joss, A., Horn, H., van Loosedrecht, M.C.M. (2014) Full-scale partial nitritation/anammox experiences – an application survery. *Water Research* 55: 292-303

Lemaire, R., Zhao, H., Thomson, C., Christensson, M., Piveteau, S., (2014) Mainstream Deammonification with ANITA TM Mox Process, in: *Proceedings of WEFTEC*. New Orleans, USA, September 27-October 1, 2014

Liu, Y., and Capderville, B. (1994) Kinetics behaviors of nitrifying biofilm growth in wastewater nitrification process. *Environ. Technol*. 15(11): 1001-1013

Magoč, T. and Salzberg, S.L. (2011) FLASH: fast length adjustment of short reads to improve genome assemblies. *Bioinformatics* (Oxford, England) 27: 2957–63

McIlroy, S.J., Kirkegaard, R.H., McIlroy, B., Nierychlo, M., Kristensen, J.M., Karst, S.M., Albertsen, M., Nielson, P.H. (2017) MiDAS 2.0: An ecosystem-specific taxonomy and online database for the organisms of wastewater treatment systems expanded for anaerobic digester groups. *Database*, Volume 17, bax016 DOI: https://doi.org/10.1093/database/bax016

Melcer, H. (2015) Mass transfer characteristics of floating media in MBBR and IFAS fixed-film systems. *Water Intelligence Online*, 14. doi:10.2166/9781780407050

Metcalf and Eddy, Wastewater Engineering: Treatment and Resource Recovery. McGraw-Hill, New York, USA, 5th edition., 2014

Mulder, A. (2003) The quest for sustainable nitrogen removal technologies. *Water Science and Technology* 48: 67-75

Piculell, M., Welander, P., Jönsson, K., Welander, T. (2015) Evaluating the effect of biofilm thickness on nitrification in moving bed biofilm reactors. *Environmental Technology* 6: 732-743

Piculell, M., Suarez, C., Chunyan, L., Christensson, M., Persson, F., Wagner, M., Hermansson, M., Jönsson, K., Welander, T. (2016a) The inhibitory effects of reject water on nitrifying populations grown at different biofilm thicknesses. *Water Research* 104: 292-302

Piculell, M., Christensson, M., Jönsson, K., Welander, T. (2016b) Partial nitrification in MBBRs for mainstream deammonification with thin biofilms and alternating feed supply. *Water Science and Technology* 73(6): 1253-1260

Quast, C., Pruesse, E., Yilmaz, P., Gerken, J., Schweer, T., Yarza, P., Peplies, J., Glöckner, F.O. (2013) The SILVA ribosomal RNA gene database project: Improved data processing and web-based tools. *Nucleic Acids Research* 41: D590–D596

R Core Team (2017) R: A language and environment for statistical computing

Rusten, B., Eikebrokk, B., Ulgenes, Y., Lygren, E. (2006) Design and operations of the Kaldnes moving bed biofilm reactors. *Aquacultural Engineering* 34(3): 322-331

Schopf, A., Delatolla, R., Kirkwood, K. (2019) Partial nitritation at elevated loading rates: Design curves and biofilm characteristics. *Biosystems and Bioprocess Engineering* 42: 1809-1818

Shalini, S., Joseph, K. (2012) Nitrogen management in landfill leachate: application of SHARON, Anammox, and combined SHARON-Anammox process. *Waste Management* 32(12): 2385-2400

Siegrist, H., Salzberg, D., Eugster, J., Joss, A. (2008) Anammox brings WWTP closer to energy autarky due to increased biogas production and reduced aeration energy for N-removal. *Water Science and Technology* 57(3):383-388

Strous, M., Heijnen, J.J., Kuenen, J.G., Jetten, MSM. (1998) The sequencing batch reactor as a powerful toll to study very slowly growing micro-organisms. *Applied Microbiology and Biotechnology* 50: 589-596

Suarez, C., Piculell, M., Modin, O., Langenheder, S., Persson, F., Hermansson, M. (2019) Biofilm thickness matters: Deterministic assembly of different functions and communities in nitrifying biofilms. *Scientific Reports*. doi: 10.1038/s41598-019-41542-1

Third, K., Paxman, J., Schmid, M., Strous, M., Jetten, M.S.M., Cord-Ruwisch, R. (2005) Enrichment of anammox from activated sludge and its application in the CANON process. *Microbial Ecology* 49: 236-244

Torresi, E., Fowler, S.J., Polesel, F., Bester, K., Anderson, H.R., Smets, B.F., Plosz, B.G., Christensson, M. (2016) Biofilm thickness influences biodiversity in nitrifying MBBRs – Implications on Micropollutant removal. *Environmental Science and Technology* 50: 9279-9288

Van Loosedrecht, M.C.M., Salem, S. (2006) Biological treatment of sludge digester liquids. *Water Science and Technology* 53 (12): 11-20

Wang, C., Liu, S., Xu, X., Zhang, C., Wang, D., Yang, F. (2018) Achieving mainstream nitrogen removal through simultaneous partial nitrification, anammox, and denitrification process in an integrated fixed film activated sludge reactor. *Chemosphere* 203: 457-466

Wang, Q., Garrity, G.M., Tiedje, J.M., and Cole, J.R. (2007) Naive Bayesian classifier for rapid assignment of rRNA sequences into the new bacterial taxonomy. *Applied and Environmental Microbiology* 73: 5261–7

Wang, Z., Liang, H., Qu, F., Ma, J., Chen, J., Li, G. (2013) Start-up of a gravity flow CANON-like MBR treating surface water under low temperature. *Chemical Engineering Journal* 217:466-474

Wang, Q., Ye, L., Jiang, G., Hu, S., Yuan, Z., (2014) Side-stream sludge treatment using free nitrous acid selectively eliminates nitrite oxidizing bacteria and achieves the nitrite pathway. *Water Research* 55, 245–55. doi:10.1016/j.watres.2014.02.029

Jumpstart Consortium Human Microbiome Project Data Generation Working Group (2012) Evaluation of 16s rDNA-based community profiling for human microbiome research. *PLOS ONE* 7: e39315

White C, Gadd GM (2000) Copper accumulation by sulfate reducing bacterial biofilms. *FEMS Microbiology Letter* 183:313-318

CHAPTER 6 – INVESTIGATION OF COPPER INHIBITION OF NITRIFYING MOVING BED BIOFILM REACTORS DURING LONG TERM OPERATIONS

6.1 Context

Chapter 6 presents the research article entitled *Investigation of copper inhibition of nitrifying moving bed biofilm reactors during long term operations* and has been published in *Bioprocess and Biosystems Engineering* in July 2018. This article discusses the kinetic and biofilm shifts that occur due to copper during long term operations.

6.2 Abstract

Copper, a prevalent heavy metal in industrial mining wastewaters, has been shown to inhibit nitrification in wastewater treatment systems. Biofilm treatment systems have an inherent potential to reduce inhibition. This study investigated the effects of copper concentration on nitrifying biofilms in moving bed biofilm reactor (MBBR) systems across long term operation using influent ammonia concentrations representative of gold mining wastewater. Conventional isotherm models did not adequately model the attachment of copper to the biofilm. Long term nitritation was shown to be uninhibited at influent copper concentrations between 0.13-0.61 mg Cu/L. Nitratation was inhibited with influent copper concentrations of 0.28-0.61 mg Cu/L. There was no statistically significant difference in biofilm characteristics, including biofilm thickness, mass and density, across all copper concentrations tested; however, changes in biofilm morphology were observed. The demonstrated resistance of the nitrifying biofilm to copper inhibition makes the MBBR system a promising technology for treating ammonia in mining wastewaters.

6.3 Introduction

Gold mining is a multi-billion-dollar industry with high activity in countries such as China, Russia, Australia, the United States and Canada (USGS, 2016). Mining wastewaters often contain total ammonia nitrogen (TAN) concentrations of greater than 100 mg NH_4^+-N/L due to the use of nitrogen-based explosives and cyanide in conventional mining and gold extraction processes (Environment Canada, 2009; Canada Gazette, 2012). Ammonia discharge from mining wastewaters has been shown to be toxic to receiving natural waters and hence is regulated in countries such as the United States and Canada (US EPA, 1972; Fisheries Act, 2002).

Nitrification is the two-step biological oxidation of ammonia to nitrate. Ammonia is first oxidized to nitrite (nitritation) by ammonia oxidizing bacteria (AOB), and subsequently from nitrite to nitrate (nitratation) by nitrite oxidizing bacteria (NOB). Nickel, chromium, arsenic, and copper are commonly occurring heavy metals in industrial wastewaters and mining wastewaters that inhibit nitrification at concentrations as low as 0.25 mg Ni/L, 0.25 mg Cr/L and 0.1 mg Cu/L in nitrifying bacterial cultures (Skinner and Walker, 1961). The inhibitory effects of copper on nitrifying bacteria in pure cultures and activated sludge (AS) have been studied extensively (Skinner and Walker, 1961; Cenci and Morozzi, 1979; Sato *et al*., 1988; Gerardi, 2002; Juliastuti *et al*., 2003; Çeçen *et al*., 2010; Ochoa-Herrera *et al*., 2011). Copper inhibition can cause cell lysis, the disruption of enzyme pathways, and structural changes in cellular DNA (Sterrit and Lester, 1980; Hu *et al*., 2003).

Known values for the half maximal inhibitory concentration of copper (IC50), where a response is inhibited by fifty percent, were determined in previous studies through conventional kinetic testing on AS and isolated nitrifiers using O_2 and CO_2 respiration analysis, or through triphenyl tetrazolium chloride (TTC) testing in batch tests (Cenci and Morozzi, 1979; Çeçen *et al*.,

2010). A review of the literature shows that the reported IC50 values for copper vary greatly, with values ranging between 0.08 and 40 mg Cu/L (Skinner and Walker, 1961; Cenci and Morozzi, 1979; Sato *et al*., 1988; Gerardi, 2002; Juliastuti *et al*., 2003; Çeçen *et al*., 2010; Ochoa-Herrera *et al*., 2011). The observed discrepancy in the inhibitory range can be attributed to the differing experimental conditions including: testing on bacterial isolates or environmental samples from various wastewaters; variations in pH; suspended solids concentrations; TAN concentrations; and the availability of molecules that complex with copper in each experiment (Serrit and Lester; 1980; Sato *et al*., 1988). Various researchers have emphasized the importance of the copper species, and its subsequent impact on toxicity, providing another potential reason for the large discrepancy in reported inhibitory copper concentrations. Free, ionized copper (Braam and Klapwijk, 1981; Çeçen *et al*., 2010) and specific copper complexes (Sato *et al*., 1988; Lee *et al*., 2009) have been shown to cause greater inhibition. Finally, batch testing has been extensively used to estimate copper inhibition. This testing method has been shown to overestimate the concentration required to cause inhibition in long-term operations, and may therefore be deemed an inappropriate choice to approximate chronic inhibition effects in treatment facilities (Hu *et al*., 2004; Özbelge *et al*., 2007; Şengör *et al*., 2011).

Biofilm technologies are an alternative to conventional suspended growth treatment systems. Biofilm processes have demonstrated the capacity to achieve similar treatment targets to suspended growth systems while requiring smaller carbon and ecological footprints (Ødegaard, 1999), due to increased cellular density in the reactor. The moving bed biofilm reactor (MBBR) is an attached growth water and wastewater treatment technology that maintains biofilms on carriers that are kept in motion in the treatment basin. The motion of the carriers reduces large sloughing events and eliminates the need for backwashing in these systems (Ødegaard, 1999). Therefore, the

MBBR technology has been selected for the present study as a low operational intensity and cost-effective technology with the potential for ammonia removal from mining wastewaters. The potential application of the MBBR technology to mining wastewater is contingent on the ability of the nitrifying biofilm to remain uninhibited by the naturally occurring copper concentrations inherent to mining wastewaters.

In comparison to suspended growth treatment systems, biofilm systems such as the MBBR have demonstrated the potential for greater resilience to unfavourable environmental conditions such as temperature fluctuations, low temperatures, and chemical toxicity including copper inhibition (White and Gadd, 2000; Delatolla *et al*., 2009; Hoang *et al*., 2014; Young *et al*., 2016). Biofilms provide a structural barrier in the form of extracellular polymeric substance (EPS) that restricts the access of toxins to the deeply embedded cells. The close proximity of bacterial cells to one another in biofilms also enhances communication via quorum sensing, upregulation of efflux genes, and transference of advantageous genes as response mechanisms to toxins (Flemming, 1993; Flemming *et al.,* 2007; Lee *et al*., 2009; Delatolla *et al.,* 2009; Hoang *et al*., 2014; Young *et al*., 2016a; Young *et al*., 2016b). Antibiotic resistance is an example of a genetic trait that can be transferred between cells (Burmølle *et al*., 2014). Although previous studies have identified the resilience of biofilms, the mechanism by which biofilms mitigate heavy metal toxicity has been subject to debate. Harrison *et al.* (2004) found no difference in the minimum inhibitory concentrations of heavy metals for pure cultures of bacteria grown in the planktonic state compared to those grown in a single-species biofilm, reducing the likelihood of the EPS as an explanation for resistance to inhibition. Conversely, Lee *et al.* (2009) found that nitrification was sharply inhibited at a concentration of 25 mg Cu/L in suspended growth reactors, while nitrification was unaffected in reactors that combined both sessile and suspended growth at this

concentration. Teitzel and Parsek (2003) found that bacterial biofilms in a rotating-disk biofilm reactor were up to 600 times more resilient to heavy metals compared to planktonic cells. As the majority of studies investigating the inhibition of nitrifiers by copper have been based on AS or pure cultures, copper inhibition of nitrifying biofilm treatment technologies requires further investigation to evaluate the potential of the MBBR technology for nitrification of mining wastewaters.

The fate of copper in biofilm reactors will likely affect the inhibition of nitrifying populations in the attached growth MBBR system. Copper in biofilm technologies has been shown to be distributed between the bulk liquid and biofilm-attached phases (Hu *et al*., 2003; Hu *et al*., 2004; Lee *et al*., 2009; Şengör *et al*., 2011). In the bulk liquid phase, copper exists in the form of dissolved copper, copper complexes or as solid precipitate (White and Gadd, 2000; Lee *et al*., 2009; Çeçen *et al*., 2010). In the attached phase, copper can be found either attached to the surface of the biofilm via adsorption or encapsulation, or distributed within the biofilm (Flemming, 1993; White and Gadd, 2000; Hu *et al*., 2003; Young *et al*., 2016a). The distribution of copper between bulk and attached phases has previously been modeled by isotherms such as the Freundlich isotherm, the Langmuir isotherm and the Redlich-Peterson isotherm (Freundlich, 1906; Langmiur, 1918; Redlich and Peterson, 1959; Hu *et al*., 2003; Black *et al*., 2014; Tran *et al*., 2017). Previous isotherm modelling demonstrated that attached growth biomass possesses a greater maximum adsorbate concentration capacity than suspended growth biomass and that partition coefficients, indicative of the bulk-attached phase equilibrium, were greater in continuous flow systems compared to batch tests (Hu *et al*., 2003; Hu *et al*., 2004; Black *et al*., 2014). Long term operational studies of the attachment of copper to biofilms and subsequent knowledge of the inhibitory effects on nitrification during long term operation of biofilm technologies and in particular the MBBR

technology, is currently understudied. This knowledge gap has restricted the potential for use of cost-effective biofilm ammonia removal technologies such as the MBBR to treat mining wastewaters.

This work studies the fate and effects of copper during long-term operation of the nitrifying MBBR technology, at copper concentrations representative of ammonia-containing gold mining wastewaters. The partitioning of copper between the bulk and attached phases in the MBBR was determined quantitatively and compared to traditional isotherm models, and the effects of copper concentration on nitrification kinetics (both nitritation and nitratation), biofilm characteristics (thickness, mass, and density), and biofilm morphology (microscopic observation) are reported. This is the first study to quantitatively assess the effect of copper as a chronic contaminant during long-term operation of a nitrifying MBBR system.

6.4 Methods and Materials

6.4.1 Experimental Set-up

Four identical, laboratory scale, continuous-flow MBBRs (R1, R2, R3 and R4) with an operating volume of 750 mL (h = 10 cm) each were operated in parallel using synthetic wastewater to mimic the ballasted sand treated gold mining wastewater from the Eleonore mine operating in James Bay, QC, Canada (Fig. S6.1). This effluent mining wastewater contains elevated ammonia concentrations with an average copper concentration of 0.543 ± 0.02 mg Cu/L. The four laboratory scale reactors were fed from the same synthetic influent that was spiked with a copper (II) solution to achieve target concentrations of 0.1, 0.3, 0.5 and 0.7 mg Cu/L for nitrifying MBBRs R1, R2, R3 and R4, respectively. The range of copper values selected for this study also coincide with the mining effluent guidelines of Canada and the US, which stipulate an average monthly effluent of less than 0.15 mg Cu/L to 0.30 mg Cu/L, with a one-time monthly maximum composite sample of

0.45 mg Cu/L and a one-time monthly maximum single sample of 0.60 mg Cu/L (US EPA, 1988; Fisheries Act, 2002).

The laboratory scale MBBRs were kept constantly mixed via aeration. Each reactor initially housed AnoxKaldnes^{TM} (Lund, Sweden) K5 carriers (bulk surface area of 800 m^2/m^3) with a percent fill of 46%. This percent fill is within the conventional range of 25-67% for percent fill values used for MBBR systems (Ødegaard, 1999; WEF 2009) and was selected to enable efficient movement of the carriers in the laboratory reactors. The clean carriers of the four reactors were originally housed in a single 4 L reactor and were seeded with carriers harvested from the same integrated fixed film activated sludge (IFAS), carbon removal and partial nitrogen removal municipal wastewater treatment plant in Hawkesbury, ON, Canada. After sufficient biofilm growth on the carriers occurred in the single reactor and acclimation to elevated ammonia concentrations compared to municipal systems, the carriers were distributed to the four reactors. The reactors were operated with a synthetic wastewater devoid of elevated copper concentrations for a period of one month to allow the biofilm to acclimate to the reactor conditions such as air flow rate and reactor flow dynamics prior to the addition of elevated copper concentrations. The copper concentrations during this period of acclimatization were maintained at a trace concentration of 0.026 mg Cu/L. The reactors achieved over 97% ammonia removal consistently for the final two weeks of the acclimatization period, prior to the start of the experiments.

Each of the four reactors was operated with a hydraulic retention time (HRT) of 5 h throughout the study. Aeration was provided at a rate of 4 L/min ($G = 299\ s^{-1}$, eqns 9.1 and 9.2) to each reactor providing a dissolved oxygen (DO) concentration of 8.7 ± 0.2 mg O_2/L to ensure adequate movement of the MBBR carriers. The reactors were operated at a temperature of 18.1 ± 0.7˚C and a pH of 8 ± 0.2 throughout the study. The initial surface area loading rate (SALR) of 1.6

± 0.003 g N/m^2·d. was increased to 2.45 ± 0.03 g N/m^2·d over 205d with the reactors being operated at the final loading rate for 125 days. The influent TAN concentration of 125 mg TAN/L was kept constant throughout the experiment to provide a consistent feed to the biofilm communities and keep the TAN at a concentration typical to industrial mining wastewater. Two control reactors were used for this experiment to (i) ensure that copper was not attached via sorption to the surface of clean high-density polyethylene carriers or to the side walls of the acrylic reactors, and (ii) isolate the effects of copper on nitrification kinetics and biofilm characteristics from the effects of the ammonia loading rate. To ensure copper was neither attached to the carriers nor to the reactor, a 3 L acrylic control reactor (C1) was filled with clean, unseeded carriers and was fed with a copper concentration of 0.70 mg Cu/L and 125 mg NH_4^+-N/L for the duration of the study. To isolate the effects of copper from the effects of ammonia loading rate, a 4 L control reactor (C2) with no added copper was operated at an SALR of 2.45 g N/m^2·d to match the ammonia loading rates at the end of the experimental period.

6.4.2 Synthetic Wastewater Composition

The synthetic wastewater (SWW) recipe used in this study was a combination of the recipe used by Delatolla *et al*. (2009), and an empirical mining SWW recipe that mimicked the effluent wastewater of the Eleonore mine. The ammonia concentration of the mining wastewater was 125 mg /L of TAN, which is representative of gold mining wastewaters (Archeampong, 2013). The SWW used in this study was prepared in tap water and contained 0.590 g/L $(NH_4)_2SO_4$, 1.625 g/L $NaHCO_3$, 0.071 g/L $MgSO_4{\cdot}7H_2O$, 0.029 g/L $CaCl_2{\cdot}2H_2O$, 0.079 g/L KH_2PO_4, and 0.005 g/L $FeSO_4{\cdot}7H_2O$. Carbon sources were added to mimic the Eleonore mine wastewater as 4.86 mg/L of peptone (18.07 mg COD/L), 2.592 mg/L of sodium acetate (1.75 mg COD/L) and 4.86 mg/L of dextrose (5.18 mg COD/L) to provide a total soluble chemical oxygen demand (sCOD)

concentration of 25 mg/L and an sCOD: N ratio of 1:5. Trace elements necessary for cellular reproduction were added to the synthetic wastewater at concentrations of 0.1 mg/L $MnCl_2 \cdot 4H_2O$, 0.025 mg/L $Na_2MoO_4 \cdot 2H_2O$, 0.1025 mg/L $CuSO_4 \cdot 5H_2O$. Additional copper was added at concentrations of 0.393, 1.18, 1.96 and 2.75 mg/L $CuSO_4 \cdot 5H_2O$ to reactors R1, R2, R3 and R4, respectively, to provide the target total copper concentrations. Final influent copper concentrations were measured to be 0.13 ± 0.01, 0.28 ± 0.02, 0.44 ± 0.04 and 0.61 ± 0.04 mg Cu/L for R1, R2, R3 and R4, respectively. These influent copper concentrations will be used to distinguish the reactors for the remainder of this article to reflect the operational conditions used in the experiment. To isolate the effects of copper on the nitrifying biofilm, other inhibitory compounds found in the mining wastewater such as arsenic and cyanide were not added to the synthetic wastewater.

6.4.3 Analytical Methods

To monitor the performance of the reactors, the following parameters were measured in triplicate using standard methods (APHA, 1989): ammonia (Nessler method, 4500C-NH_3); nitrite (4500B-NO_2^-); nitrate (4500A-NO_3^-); sCOD (HACH 8000, HACH company, 2014); total suspended solids (TSS); and volatile suspended solids (VSS) (2540D). pH was measured using a SympHony VWR pH probe (Radnor, PA, USA) while DO and temperature were measured using a HACH Flexi HQ30d DO probe (Loveland, CO, USA). Copper concentrations, nitrogen kinetics and biofilm mass measurements were obtained through periodic sampling over a period of 130 d following identification of steady state, with steady state operation defined as effluent ammonia and effluent copper concentrations remaining in a range of ±10% of the average values.

Bulk phase copper was analysed using a modified version of standard method 3030B (APHA, 1989). Forty-millilitre samples were collected from the influent feed and from the bulk liquid of the reactors. The samples were prepared by centrifugation at 8150 × g for 30 min to

separate the solids from the bulk liquid, after which 2 mL of supernatant was extracted and diluted to 10 mL using a 1.25% nitric acid solution, providing a final concentration of 1% nitric acid. The samples were diluted further with distilled water (5× dilution) to mitigate sodium interference with copper measurements. The samples were measured using the Agilent 8800 Triple Quadrupole Inductive Coupled Plasma Mass Spectrometry (ICP-MS) (Santa Clara, CA) with a detection limit of 4 ppb (µg/L).

The concentration of copper attached to biofilm on carriers was also measured using the Agilent 8800 ICP-MS. Samples were prepared according to a modified version of standard method 3030-E (APHA, 1989). Over the length of the experiment 35 carriers from each test reactor (R1, R2, R3, R4 and C1) were harvested and were dried at 105˚C for a minimum of 8 h. After drying, the carriers were cooled in a desiccator for 1 h and then weighed. Biofilm was detached from the carriers and digested in 50% nitric acid by heating the submersed biofilm and nitric acid solution to 100°C for 15 min. The cleaned carriers were dried in an oven at 105˚C for a minimum of 8 h after which they were cooled in a desiccator for 1 h and weighed to determine the biofilm mass attached to the carriers. The digested biofilm in acid solution was diluted to have a final concentration of 1-2% nitric acid using distilled water to prepare the sample for ICP-MS analysis. Preliminary protocol testing ensured that the mass of the polyethylene carriers was unaffected by the biofilm digestion process. A clean carrier was also processed with each test run as a blank to confirm that carrier mass was unaffected during the entire process. The attached concentration of copper was determined by dividing the total mass of copper by the mass of biofilm on the carrier. This method does not distinguish between adsorbed or absorbed copper; hence, the copper measured in this study via this method is referred to as copper attached to the biofilm.

The concentration of copper attached to suspended solids was quantified using the Agilent 8800 ICP-MS as above. Samples were prepared according to the modified version of standard method 3030-E as previously described apart from the following changes (APHA, 1989). Suspended solids were collected from the effluent ports of each of the reactors. The effluent samples were centrifuged at 8150 × *g* for 30 min after which the supernatant was removed and the remaining solids placed in crucibles and dried in an oven at 105˚C for a minimum of 8 h. The solids were placed in a desiccator to cool for 1 h and weighed. 50% nitric acid was added to each crucible and heated to 100°C for 120 min on a hot plate. The digested acid was then diluted to attain a 1-2% nitric acid concentration as required for ICP-MS analysis. The crucibles were rinsed and dried for a minimum of 8 h at 105˚C, cooled in a desiccator for 1 h and weighed. The difference in mass before and after digestion was used to quantify the mass of the suspended solids. The concentration of copper attached to the suspended solids was determined by dividing the total mass of copper found by the mass of suspended solids used. Again, this method does not distinguish between adsorbed or absorbed copper and hence the copper measured in this study via this method is referred to as copper attached to the suspended solids.

6.4.4 Biofilm Thickness and Morphology

Biofilm thickness and morphology were measured and observed using Variable Pressure Scanning Electron Microscopy (VPSEM). Twenty-eight images were acquired using the Tescan USA Inc, Vega II-XMU SEM (Cranberry, PA, USA), at ~40 Pa, for each of the influent copper conditions at steady state. Twenty images per condition were acquired at 60× magnification, for the purpose of quantifying biofilm thickness and analysing morphology. Four images were acquired at 600× magnification to analyze biofilm morphology. Lastly, four images per condition

was acquired at 6× magnification to provide an overall image of the carrier, and additionally to quantify potential biofilm anomalies.

Biofilm thickness measurements were acquired using MedCalc Digimizer Image Analysis Software V.4.6.1 (Ostend, Belgium). A minimum of 1000 profile measurements were acquired per influent copper condition to ensure accuracy. Biofilm anomalies such as clogged or empty pores were eliminated from the thickness measurement data set as the biofilm thickness of clogged or empty pores cannot be measured; therefore, the number of clogged and empty pores were enumerated for the purpose of comparison. Biofilm morphology heterogeneity and roughness were qualitatively compared between the different conditions using images at 60× and 600× magnification.

6.4.5 Biofilm Mass Measurements

Biofilm mass was quantified according to a modified version of the procedure described in Forrest *et al.* (2008). Carriers were dried in an oven at 105˚C and the dry mass was measured. Biofilm removal from the carriers was achieved using acid digestion as described in the methods section above and the biofilm dry mass was calculated as the difference between the mass of the carrier with biofilm and the mass of the carrier with the biofilm removed.

6.4.6 Isotherms

The Freundlich (eqns 6.1 and 6.2), Langmuir (eqns 6.3 and 6.4), and Redlich-Peterson (eqn 6.5) isotherms were used to describe the bulk and attached phase copper interactions (Freundlich, 1906; Langmuir, 1918; Redlich and Peterson, 1959, Tran *et al*., 2017). The equations are described below

The standard equation (eqn 6.1) and linearized forms (eqn 6.2) of the Freundlich isotherm are as follows:

$$q_e = K_F C_e^n \qquad \text{(Eqn. 6.1)}$$

$$log q_e = n log C_e + log K_F \qquad \text{(Eqn. 6.2)}$$

Where q_e is the amount of adsorbate uptake at equilibrium (mg/g), C_e is the adsorbate concentration at equilibrium (mg/L), K_F is the Freundlich constant (mg/g)/(mg/L)^n, and n is the Freundlich intensity parameter (dimensionless).

The standard equation (eqn 6.3) and Scatchard linearization (eqn 6.4) for the Langmuir isotherm are as follows:

$$q_e = \frac{Q^0_{max} + K_L C_e}{1 + K_L C_e} \qquad \text{(Eqn. 6.3)}$$

$$\frac{q_e}{C_e} = -K_L q_e + Q^0_{max} K_L \qquad \text{(Eqn. 6.4)}$$

Where q_e is the amount of adsorbate uptake at equilibrium (mg/g), C_e is the adsorbate concentration at equilibrium (mg/L), Q^0_{max} is the maximum saturated monolayer adsorption capacity of the adsorbant (mg/g), and K_L is a constant related to the affinity between an adsorbent and adsorbate.

The standard form of the Redlich-Peterson isotherm (eqn 6.5) is as follows:

$$q_e = \frac{K_{RP} C_e}{1 + a_{RP} C_e^g} \qquad \text{(Eqn 6.5)}$$

Where q_e is the amount of adsorbate uptake at equilibrium (mg/g), C_e is the adsorbate concentration at equilibrium (mg/L), g is the exponent whose value must be between 0 and 1 (dimensionless), K_{RP} (L/g) and a_{RP} (mg/L)$^{-g}$ are Redlich-Peterson constants.

6.4.7 Statistical Methods

Statistical significance was determined using student t-tests with a *p*-value <0.05. All measured parameters are presented with a 95% confidence interval. Statistical correlations were determined using Pearson's correlation method (Laerd Statistics, 2020). P-values from t-tests are presented in supplemental materials (Tables S-2 and S-3).

6.5 Results and Discussion

6.5.1 Copper Phase Partitioning

The fate of the influent copper in the systems is critical to understanding the inhibition of copper on nitrifying biofilms during long term operation in MBBR systems. To determine the fate of copper, the distribution of copper in the bulk liquid phase, attached to the biofilm and attached to the suspended solids was quantified (Table S6.1). The bulk influent and effluent copper concentrations were statistically significantly different for all influent copper concentrations; however, after long term operations the influent and effluent copper concentrations were steady. There was a statistically significant difference in the effluent bulk phase copper concentration relative to the influent copper concentration (Fig. 6.1), with the control reactor that was operated with clean, non-seeded carriers (C1) showing no statistically significant loss of copper in the system from the influent to the effluent. Further, no copper was detected when subjecting the carriers from the non-seeded control reactor (C1) to the attached copper measurement protocol, indicating that copper did not attach to the clean carrier itself and all attachment of copper in reactors tested was to biofilm. Hence, the difference in bulk phase copper from influent to effluent is due to the attachment of copper to the biofilm and to the biofilm solids in suspension (Fig. 6.2), with the suspended solids being detached biofilm from the carriers as the influent was void of solids. The concentration of copper attached to biofilm on the carriers was statistically significantly

different at all influent copper concentrations (Fig. 6.2). The concentration of copper attached to biofilm in suspension was found to be statistically significantly different between the different conditions tested except for the systems with an influent copper concentration of 0.28 and 0.44 mg Cu/L. The concentration of copper on the biofilm on the carriers was not statistically significantly different from the corresponding copper concentration on the suspended solids except for the system with 0.13 mg Cu/L. A copper mass balance was observed with mass balances of 104.1, 112.3, 104.7, and 100 % for influent copper concentrations of 0.1, 0.3, 0.45, and 0.6 mg Cu/L, respectively.

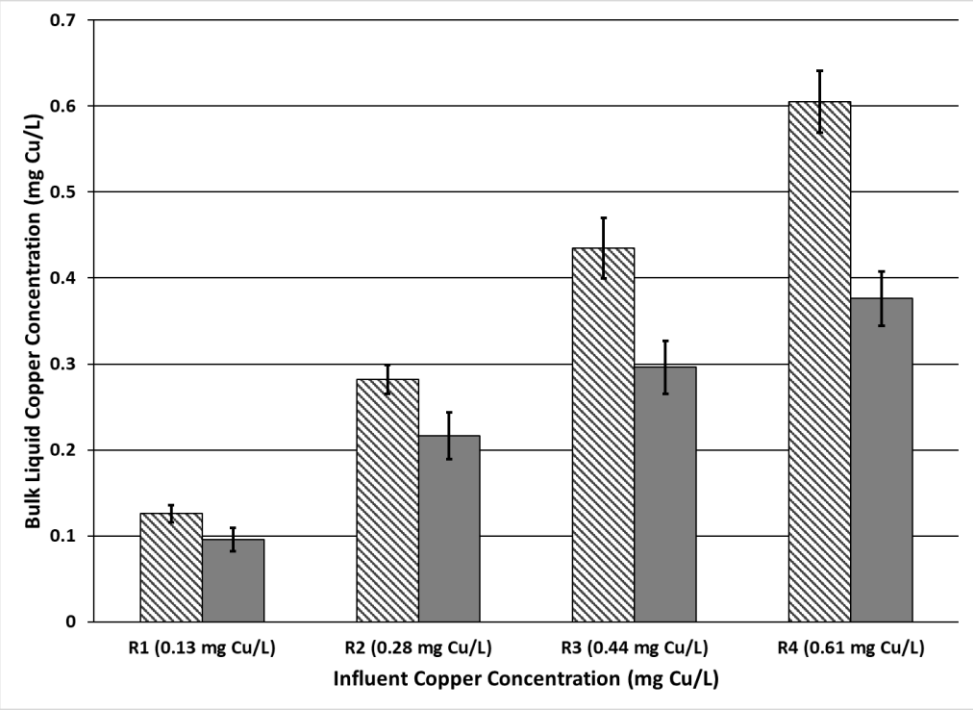

Figure 6.1 Bulk liquid influent (pattern) and effluent (solid) copper concentrations (average ± 95% CI)

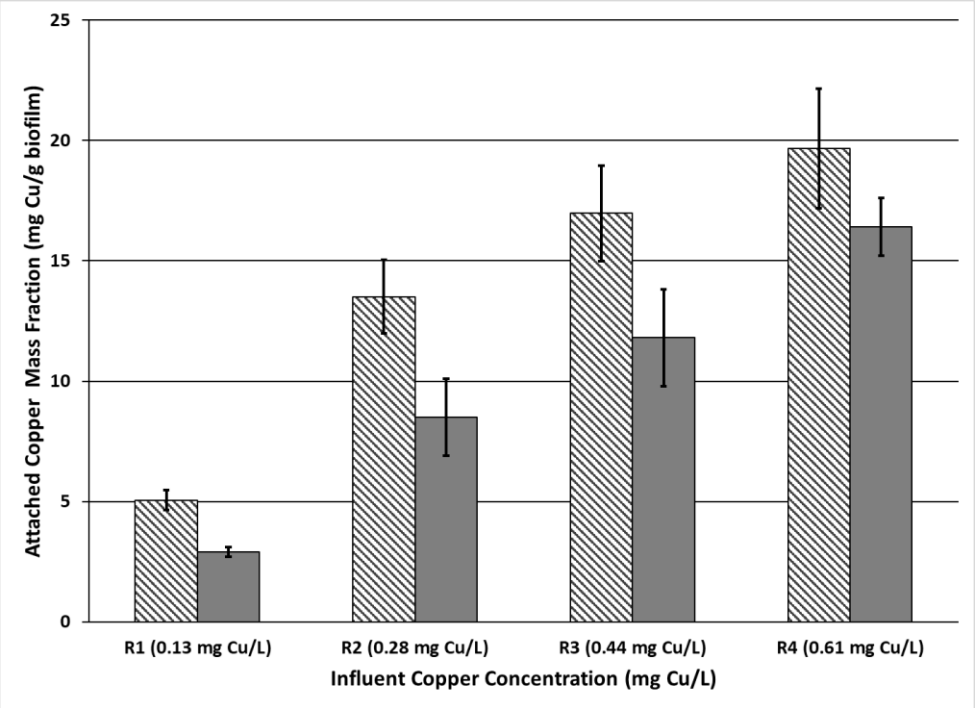

Figure 6.2 Attached copper to biofilm (pattern) and suspended solids (solid) (average ± 95% CI)

During the experiments, the bulk phase copper concentrations reached steady state 40 d after the initial addition of copper across the four test reactors at varying copper concentrations. However, the copper attached onto the biofilm across the four test reactors achieved steady state 80 d after the initial addition of copper (40 d after the bulk phase reached steady state). Steady state was defined as operation with effluent TAN, nitrite, and nitrate concentrations within ± 10% of their average values. The difference in the influent and effluent copper concentrations of the four test reactors increased across the 40 d of operation until the maximum difference was achieved and copper attachment to the biofilm stabilized. This period of increasing attachment of copper to the biofilm thus prevented the biofilm copper concentration from reaching an equilibrium. Once the influent and effluent copper concentrations steadied the copper attachment to the biofilm in the reactors required an additional 40 d of operation to stabilize with significant fluctuations of the

copper mass fraction of the biofilm to reach steady state. These fluctuations in the copper mass fraction measurements were likely due to the dynamic growth characteristics of biofilm systems, which generate new biofilm surface areas for bulk phase copper attachment through the process of erosion, abrasion or grazing from predation (Bryers, 1987; Flemming, 2007). Previous research using batch testing has demonstrated complete copper sorption onto suspended and attached growth over a period of 1 h to 4 h (Hu *et al*., 2003; Hu *et al*., 2004; Lee *et al*., 2008; Çeçen *et al*., 2010). As batch tests, the systems in these studies were dosed with a finite concentration of copper so the sorption was limited to initial dose as opposed to a continuous system which consistently loads the reactor with copper. During the present study, between 25 - 38% of the influent copper was removed from the bulk phase due to the dynamic biofilm equilibrium, compared to greater than 90% removal shown in batch test studies (Hu *et al*., 2003; Black *et al.,* 2014).

In this study, a positive relationship can be seen between the attached copper concentrations and, the influent and effluent copper concentrations (Figs. 6.1 and 6.2). To model the relationship to effluent concentration, the Freundlich (Fig. 9.1), Langmuir (Fig. 9.2), and Redlich-Peterson isotherm equations (eqns 6.1 – 6.5) were applied to the four test reactors after an extended period of operation (after 200 d of operation including over 130 d of steady state operation) and; therefore, to four dynamic biofilm systems. The isotherm models were determined using linear regression and optimisation methods (Langmuir, 1918) (Table 6.1). The degree of correlation (R^2) values were 0.560, 0.576 and 0.585 for the Freundlich, Langmuir and Redlich-Peterson isotherms, respectively. The correlations between the data and the isotherm models are weak; therefore, the models do not adequately represent biofilm copper attachment. In the Redlich-Peterson isotherm the 'g' and 'a_{RP}' constants are system specific descriptors that can indicate the sorption mechanism. If the 'g' value is 1 and 'a_{RP}' value is close to 1 then the sorption mechanism is that of the Langmuir

isotherm while if the 'g' value is 1 and the 'a_{RP}' value is significantly greater than 1 then the sorption mechanism is that of the Freundlich isotherm. If the 'g' value is greater than 1 then the isotherm models cannot adequately describe the sorption mechanism. The 'g' value and 'a_{RP}' values were found to be 2.12 and 3.32, respectively, which supports the conclusion of inadequate description by the conventional isotherm models (Redlich and Peterson, 1959; Vasanth and Sivanesan, 2006; Tran *et al*., 2017).

Table 6.1 Calculated isotherm parameters over all influent copper concentrations (0.13-0.61 mg Cu/L)

Freundlich Isotherm			
K_f $(mg/g)/(mg/L)^n$	n ( )		R^2 ( )
35.73	0.677		0.560
Langmuir Isotherm			
K_L (L/mg)	Q^0_{Max} (mg/g)		R^2 ( )
2.14	41.29		0.576
Redlich-Peterson Isotherm			
K_{RP} (L/g)	a_{RP} (mg/L)	g ( )	R^2 ( )
69.87	3.32	2.12	0.585

The inadequacy of the modeling can be attributed to the dynamic nature of the biofilm and the length of the experiment. As the biofilm grows, entrapment of particles can occur (White and Gadd, 2000). Since sorption generally refers to the bonding of the adsorbate to adsorption sites due to surface energy, particle entrapment is not a consideration in the derivation of these isotherms (Do, 1998). Most isotherm modelling occurs based on batch test derived data with a contact time ranging from a few hours to a few days with samples of sludge or biofilm that are removed from operation. In this study, the testing occurred over an extended period of 330 d; as such, the biofilms

were exposed to a constant concentration of copper, and constant shear ($G = 299\ s^{-1}$). The constant concentration of copper and shear forces resulted in the constant shedding and growth of biofilm, which resulted in the constant attachment and detachment of copper; thus, creating a dynamic equilibrium between biofilm and copper that is not represented by adsorption isotherms.

6.5.2 Nitrification Kinetics

Nitrification kinetics based on TAN, nitrite and nitrate concentrations were quantified over an extended period of operation lasting over 130 d after achieving steady state, as indicated by the ammonia removal rate being stabilized within ±7.5% (Table 6.2). The TAN surface area loading rate (SALR), surface area removal rate (SARR) and removal efficiencies were shown to not be statistically significantly different across all influent copper concentrations including the control reactor (C2), which was operated with biofilm-attached-carriers and no additional copper. The SARRs across all copper concentrations were comparable to the expected values of 2.0-2.5 g NH_4^+-N/ m^2·d for the DO concentration of 8.7±0.2 mg O_2/L (Ødegaard, 1999). Hence, nitritation inhibition was not observed for the tested copper concentrations, indicating that the AOB population was uninhibited up to copper concentrations of 0.61 mg Cu/L.

A comparison of the percent of nitrite as NO_x and the effluent nitrite concentration showed that there is no statistically significant difference between performance of the control (C2) reactor and the reactors receiving the and lowest copper concentration of 0.13 mg Cu/L, nor between the concentrations of 0.28 mg Cu/L and 0.44 mg Cu/L. The percentage of nitrite as NO_x was statistically significantly higher at the influent copper concentration of 0.61 mg Cu/L compared to the other copper loaded systems. Nitrite is a transitory species in the two-step process of nitrification and the accumulation of nitrite in the highest copper loaded system indicates incomplete oxidation of ammonia to nitrate, nitrification. The trend of increasing nitrite

accumulation following an increase in copper concentrations, as indicated by the positive Pearson's correlation value of 0.785, has also been previously observed in batch treatment systems (Scullion *et al*., 2007). The highest percent of NO_x as nitrite of 42.7±3.03% at a loading rate of 0.61 mg Cu/L in the present study strongly indicates nitratation inhibition and that the NOB were inhibited by copper. This inhibition was present, to a lesser extent, in the reactors with copper concentrations of 0.28 and 0.44 mg Cu/L, while the lowest influent copper concentration of 0.13 mg Cu/L and the control (C2) experienced no nitratation inhibition. The fact that nitritation, unlike nitratation, was not inhibited demonstrates that copper had a greater inhibitory effect on the NOB population rather than the AOB population and, by extension, that NOB are more susceptible to inhibition by copper. Previous studies have confirmed that NOB have greater sensitivity to unionized ammonia and free nitrous acid than AOB (Anthonisen *et al*., 1976) and thus are more easily inhibited by these compounds despite the faster growth rate of NOB (Keenan *et al*., 1979). Hu *et al*. (2003) suggested that the steps of nitrification are affected by copper concentrations via membrane disintegration, and the inhibition of cell reproduction, cell activity and enzyme activity (Sterrit and Lester, 1980; Hu *et al*., 2003).

Table 6.2 Effluent nitrogen concentrations and speciation (average ± 95% confidence interval)

	Influent Copper Concentration (mg Cu/L)	SALR (g $N/m^2 \cdot d$)	SARR (g $N/m^2 \cdot d$)	Percentage of Ammonia Oxidized (%)	Nitrite Concentration (mg NO_2^--N/L)	Nitrite as NO_x (%)	Nitrogen Mass Balance (%)
R1	0.13 ± 0.01	2.41 ± 0.05	2.31 ± 0.05	95.3 ± 1.6	6.14 ± 1.5	5.0 ± 1.2	101.4
R2	0.28 ± 0.016	2.45 ± 0.05	2.26 ± 0.06	92.5 ± 0.8	18.1 ± 3.7	15.8 ± 3.6	100.4
R3	0.44 ± 0.035	2.45 ± 0.06	2.21 ± 0.06	90.3 ± 0.7	15.4 ± 1.2	13.6 ± 1.0	98.3
R4	0.61 ± 0.035	2.47 ± 0.06	2.24 ± 0.05	90.8 ± 0.8	45.7 ± 15.8	42.7 ± 3.0	99.8
C2	0.00	2.5 ± 0.06	2.3 ± 0.06	92.0 ± 1.2	6.05 ± 1.1	5.0 ± 0.9	102.3

6.5.3 Biofilm Characteristics

The structure and characteristics of the biofilm, and as such the EPS that houses the cells, including the biofilm thickness, mass, density, and morphology (Table 6.3), can be indicative of the health of the biofilm. There were statistically significant differences in biofilm thicknesses found between the 0.13 mg Cu/L and 0.28 mg Cu/L conditions ($p=0.04$), and the 0.13 mg Cu/L and 0.44 mg Cu/L ($p=0.035$); however, the p-values were close to the threshold of $p=0.05$; therefore, the difference may not be meaningful considering the large error of the biofilm thicknesses. The velocity gradient was high ($G = 299\ s^{-1}$) (Melcer, 2015) which could have contributed to the similar biofilm thicknesses across the different copper loading conditions. There were no statistically significant differences between the un-clogged biofilm thickness for any of the other condition configurations (Fig. 6.3). There were no statistically significant differences among the four different copper conditions tested relating the mass of the biofilm, nor the density of the biofilm (Fig. 6.4). The seeded control reactor (C2) was shown to have statistically significantly lower biofilm thickness and biofilm mass from the copper added systems; however, the biofilm densities were not statistically significantly different between C2 and the copper added systems. The unseeded reactor (C1) was analysed for attached growth and it was found that no biofilm had attached to the unseeded carriers throughout the length of the experiment. Studies have demonstrated that an increase in biofilm thickness can be observed following enhanced stress on the bacterial community from sources such as substrate loading rate, the presence of inhibitors, external shear forces, and temperature (Bryers, 1987; White and Gadd, 2000; Bjornberg *et al*., 2009). While the presence of copper did have an effect on biofilm thickness, as demonstrated by the statistically significant difference between the copper added systems and C2, there was no correlation, as determined by the low Pearson's correlations values, between influent copper

concentration and biofilm thickness (r = 0.12) and biofilm mass (r = –0.27), respectively (Leard Statistics, 2020).

Table 6.3 Biofilm characteristics (average ± 95% confidence interval)

	Influent Copper Concentration (mg Cu/L)	Biofilm Thickness (µm)	Clogged Carrier-Pores (no./carrier)	Empty Carrier-Pores (no./carrier)	Biofilm Mass (mg/carrier)	Biofilm Density (kg/m^3)	Total Suspended Solids (mg /L)	SRT (d)
R1	0.13 ± 0.01	352.3 ± 69.1	0	0	27.5 ± 1.7	32.3 ± 10.3	13.9 ± 3.3	49.5 ± 11.8
R2	0.28 ± 0.016	304.7 ± 60.7	0	1	25.9 ± 1.9	35.1 ± 11.9	12.3 ± 4.4	52.6 ± 15.5
R3	0.44 ± 0.035	304.4 ± 55.7	0	1	24.9 ± 2.3	33.9 ± 11.5	13.6 ± 4.4	45.7 ± 14.4
R4	0.61 ± 0.035	323.1 ± 92.8	11	6	25.2 ± 1.7	32.3 ± 16.2	14.2 ± 5.9	43.2 ± 14.1
C2	0.00	238.3 ± 55.0	0	0	22.3 ± 1.7	38.7 ± 15.4		

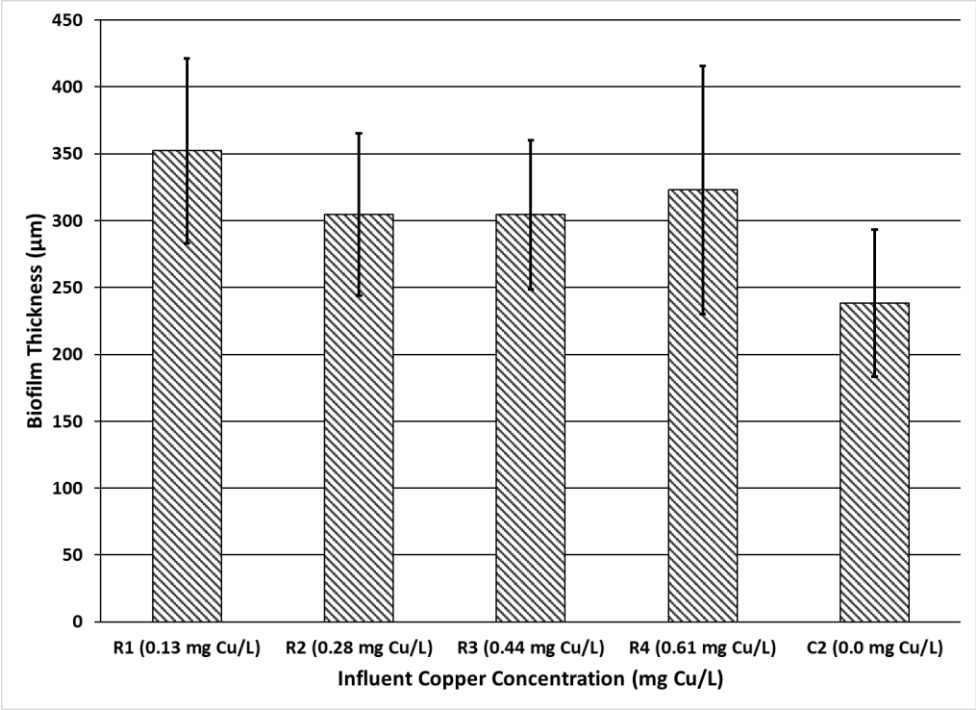

Figure 6.3 Mean biofilm thicknesses by influent copper concentration (average ± 95% CI)

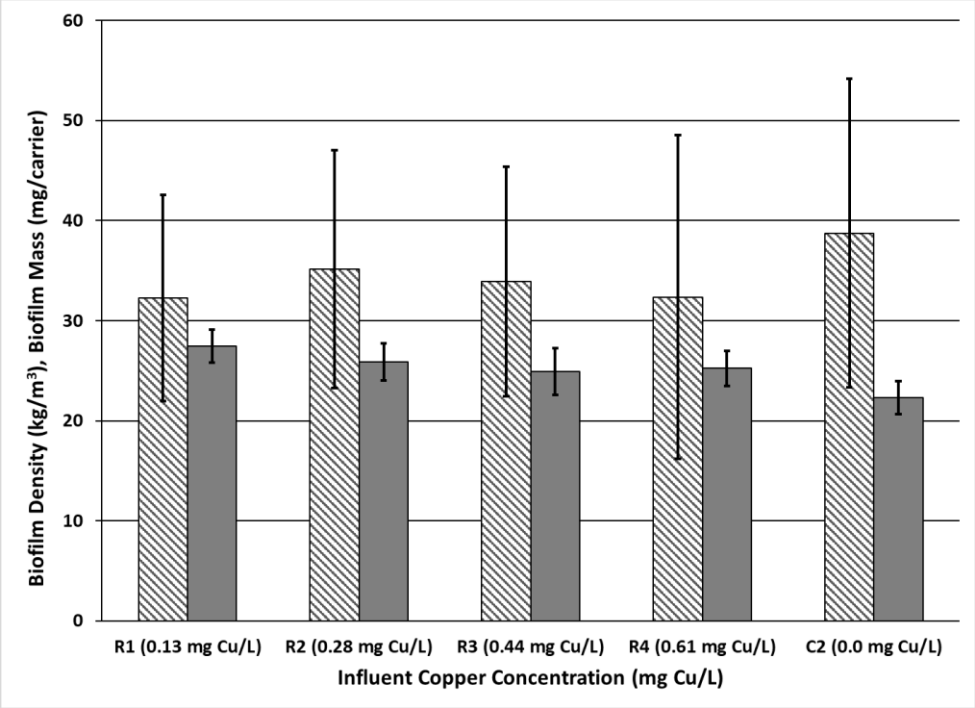

Figure 6.4 Density of biofilm (pattern) and mass of biofilm (solid) on MBBR carriers (average ± 95% CI)

The biofilm morphology was analysed qualitatively, to determine changes in the morphology of the biofilm. The biofilm, at 60× magnification, was observed to be smooth and uniform along the inner surfaces of the biofilm carriers at an influent copper concentration of 0.13 mg Cu/L (Fig. 6.5a). However, the biofilm appeared to become increasingly heterogeneous and the roughness increased along the biofilm carrier as influent copper concentrations increased (Fig. 6.5b-d). Changes in biofilm morphology and cohesiveness were also observed at 600× magnification following an increase in influent copper concentrations (Fig. S6.2a-d).

Biofilm morphology, in the form of clogged or bare carrier-pores (pores in the carriers on which biofilm grows), can be quantified at the macro-scale (Table 6.4). There was no statistically significant difference in the number of clogged carrier-pores for influent copper concentrations of 0.13, 0.28 and 0.44 mg Cu/L, and there was no statistically significant difference in the number of

bare carrier-pores between the influent copper concentrations of 0.28 and 0.44 mg Cu/L. At copper concentrations of 0.13 mg Cu/L there were no bare or clogged carrier-pores in any of the 64 pore spaces of each carrier observed using VPSEM imaging. At influent copper concentrations of 0.28 and 0.44 mg Cu/L there were 0 clogged carrier-pores and an average of 1 pore without any biofilm growth per carrier, respectively. At the influent copper concentration of 0.61 mg Cu/L there was an average of 11 clogged carrier-pores and 6 bare carrier-pores across 20 carriers examined. Although the mass of biofilm per carrier was statistically significantly similar at each influent copper concentration the morphology of the biofilm differed which could cause differences in nitrification. The clogged biofilm surfaces, as in the case of exposure to 0.61 mg Cu/L, provided a reduced biofilm surface area along the inside of the biofilm carrier which was expected to reduce the overall mass transfer of substrates and DO (Beer *et al*., 1994). It is believed that the reduction in mass transfer could have had an impact on nitrite accumulation as seen in the system with influent copper concentrations of 0.61 mg Cu/L.

The entrapment and accumulation of copper on the biofilm's surface (White and Gadd, 2000) can contribute to the reduction in mass transfer and oxygen penetration through the reduction of biofilm pores that act as channels for contact with the bulk liquid and allows the transfer of substrates to the biofilm (Beer *et al*., 1994). Studies have shown that AOB may be found in close proximity to the liquid interface of nitrifying biofilms and metabolize ammonia to nitrite for uptake by NOB found deeper in the biofilm (Beer *et al*., 1994; Schramm *et al*., 1996). Therefore, AOB have access to the limited oxygen supply prior to the NOB, that suggests that there would be insufficient oxygen available to the NOB to achieve complete nitratation.

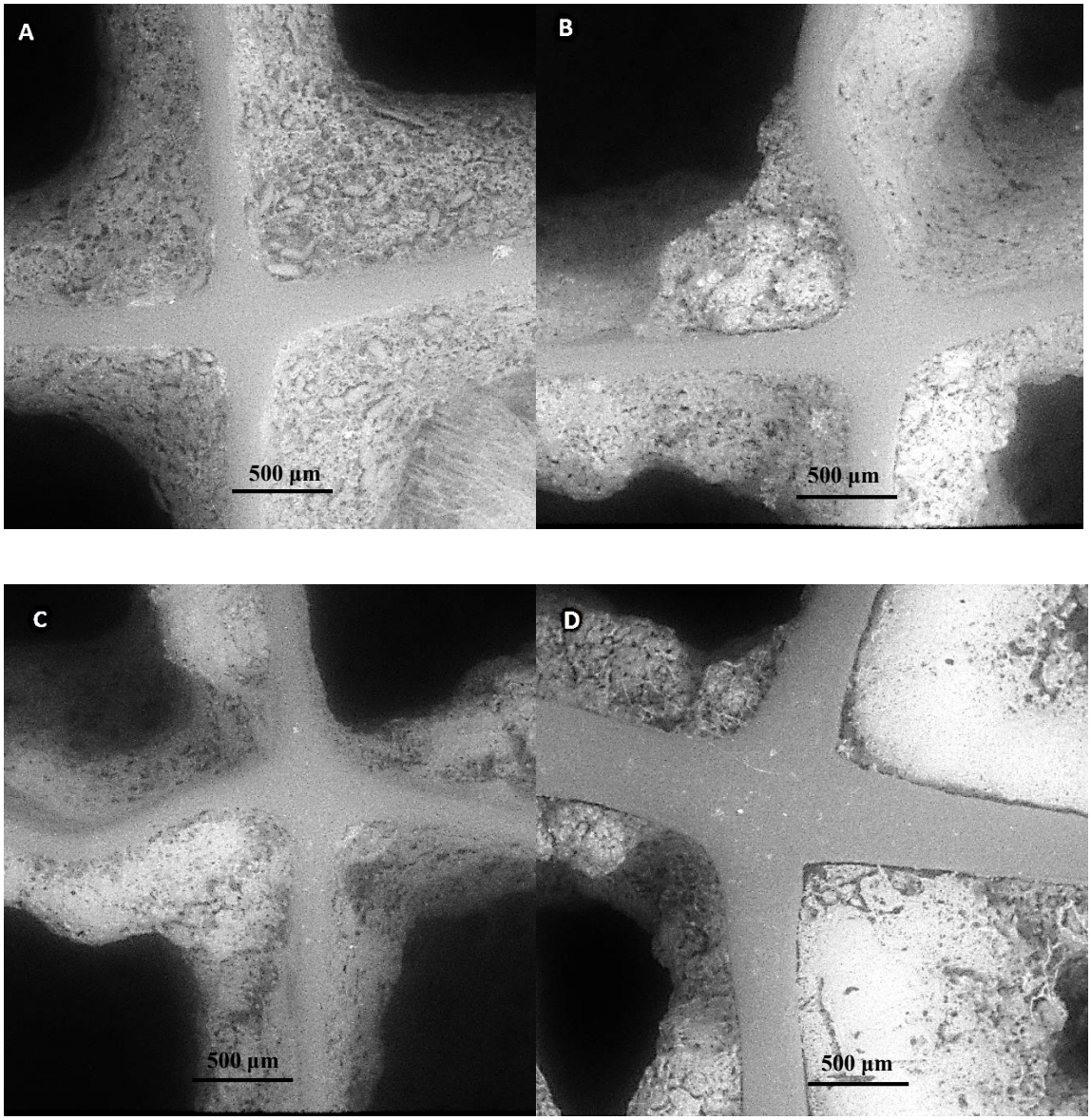

Figure 6.5 VPSEM images of biofilm on carriers, 60× magnification: a) 0.13 mg Cu/L addition, b) 0.28 mg Cu/L addition, c) 0.44 mg Cu/L addition, d) 0.61 mg Cu/L addition

While the encapsulation of copper can reduce apparent toxicity of free copper through immobilisation (Sterrit and Lester, 1980), some free copper can diffuse through the biofilm which can directly inhibit nitrification (Braam and Klapwijk, 1981; Çeçen *et al*., 2010). NOB have been shown to be more sensitive than AOB to inhibitors (Scullion *et al*., 2007); therefore, NOB may be more susceptible to inhibitors such as free copper than AOB, as demonstrated by the nitrite

accumulation at influent copper concentration of 0.61 mg Cu/L. Therefore, two mechanisms for the observed reduction in nitratation are proposed: NOB may be directly inhibited by free copper that diffused through the biofilm leading to cellular damage; or the NOB may be indirectly inhibited through the reduction of surface area and thus available oxygen via the reduction of biofilm porosity due to the accumulation of copper precipitate, and the clogging of carrier-pores due to increased biofilm thickness (Blackburne *et al*., 2007).

6.6 Conclusion

This article reports the effects of copper on nitrifying biofilm performance and characteristics during long-term operation of MBBR systems, including: the attachment of copper to the biofilm; the effect of copper concentration on nitritation and nitratation kinetics; and the effects of copper concentration on nitrifying MBBR biofilm characteristics and morphology. Copper was distributed between the bulk phase and the attached phase, where copper was attached to the sessile biofilm and suspended solids. Due to the attachment of copper to the biofilm, the effluent bulk phase copper concentrations were significantly lower than the influent bulk phase concentrations. The study demonstrates that the relation between the attached and bulk phase copper cannot be adequately modeled by conventional isotherms, likely due to copper accumulation in the biofilm. The TAN SARR were not statistically significantly different across all copper concentrations, with a TAN percent removal greater than 90% being observed for all copper concentrations tested. This suggests that nitritation was not impacted by the copper concentrations tested in this study. Nitrite accumulation was observed at copper concentrations of 0.28 mg Cu/L or greater, reaching a maximum nitrite accumulation of 42.7% of total NO_x at 0.61 mg Cu/L, indicating that at higher copper concentrations there were was inhibition of the NOB. Biofilm mass, thickness and density were not found to statistically significantly differ across the

influent copper concentrations except when compared to the control reactor (C2); however, biofilm morphology became increasingly rough and heterogeneous with increasing copper concentrations. Therefore, while there were statistically significant differences in biofilm thickness, mass and density between the copper-loaded reactors and the control reactor (C2), there was no direct correlation between copper concentration and biofilm characteristics or nitritation. The results suggest that there are multiple possible mechanisms for the inhibition of nitratation, ranging from direct inhibition from copper-cell interactions to indirect inhibition including reduction of oxygen mass transfer. This work demonstrates that at copper concentrations typical to North American gold mining effluents, the MBBR technology can provide sufficient nitrification even at high ammonia loading rates.

6.7 Supplemental Material

Table S6.1 Bulk and attached phase copper concentration (average ± 95% confidence interval, p = 0.05)

Reactor	Influent Copper Concentration (mg Cu/L)	Effluent Dissolved Copper Concentration (mg Cu/L)	Attached Copper on Biofilm (mg Cu/g biofilm)	Attached Copper on Suspended Solids (mg Cu/g solids)	Copper Mass Balance (%)
R1	0.13 ± 0.01	0.095 ± 0.01	5.0 ± 0.4	2.9 ± 0.2	104.1
R2	0.28 ± 0.02	0.21 ± 0.03	13.5 ± 1.5	8.5 ± 1.6	112.3
R3	0.44 ± 0.04	0.30 ± 0.03	17.0 ± 2.0	11.8 ± 2.0	104.7
R4	0.61 ± 0.04	0.38 ± 0.03	19.7 ± 2.5	16.4 ± 1.2	100
C1	0.61 ± 0.04	0.56 ± 0.03	-	-	-

Table S6.2 P-values of paired t-tests between influent and effluent bulk phase copper

	R1	R2	R3	R4
R1	6.36×10^{-7}	-	-	-
R2	-	2.00×10^{-7}	-	-
R3	-	-	2.33×10^{-10}	-
R4	-	-	-	6.65×10^{-15}

Table S6.3 P-values of paired t-tests

SALR	R1	R2	R3
R2	0.691	-	-
R3	0.802	0.887	-
R4	0.632	0.927	0.818
SARR	R1	R2	R3
R2	0.369	-	-
R3	0.016	0.122	-
R4	0.138	0.576	0.293
Influent Bulk Copper Concentration	R1	R2	R3
R2	1.64×10^{-24}	-	-
R3	1.45×10^{-20}	5.44×10^{-12}	-
R4	7.0×10^{-25}	5.90×10^{-21}	9.26×10^{-11}
Effluent Bulk Copper Concentration	R1	R2	R3
R2	5.93×10^{-8}	-	-
R3	1.82×10^{-11}	0.0011	-
R4	2.66×10^{-14}	3.95×10^{-8}	0.0042
Attached Copper Concentration	R1	R2	R3
R2	1.16×10^{-8}	-	-
R3	2.59×10^{-10}	0.014	-
R4	1.17×10^{-11}	4.81×10^{-5}	0.0581
Ammonia Oxidized	R1	R2	R3
R2	2.16×10^{-5}	-	-
R3	2.39×10^{-11}	0.0029	-
R4	1.57×10^{-13}	1.40×10^{-5}	0.098
Effluent Nitrite	R1	R2	R3
R2	5.29×10^{-6}	-	-
R3	4.26×10^{-11}	0.176	-
R4	1.25×10^{-9}	2.95×10^{-7}	1.02×10^{-7}
Biofilm Thickness	R1	R2	R3
R2	0.040	-	-
R3	0.035	0.934	-
R4	0.077	0.893	0.943
Biofilm Mass	R1	R2	R3
R2	0.555	-	-
R3	0.297	0.583	-
R4	0.218	0.478	0.926

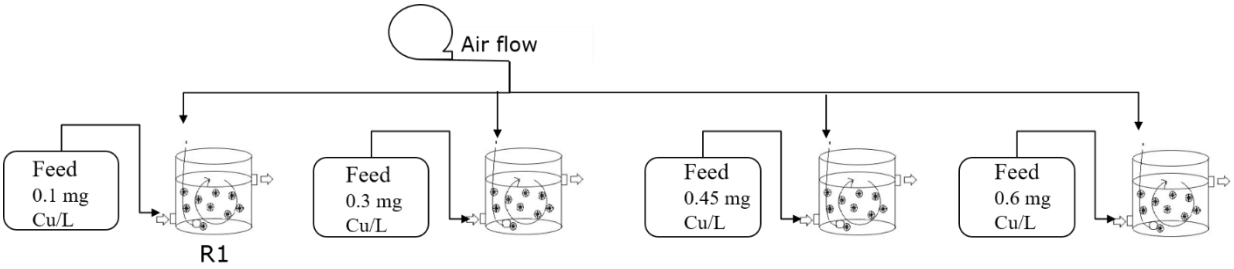

Figure S6.1 Schematic of experimental setup

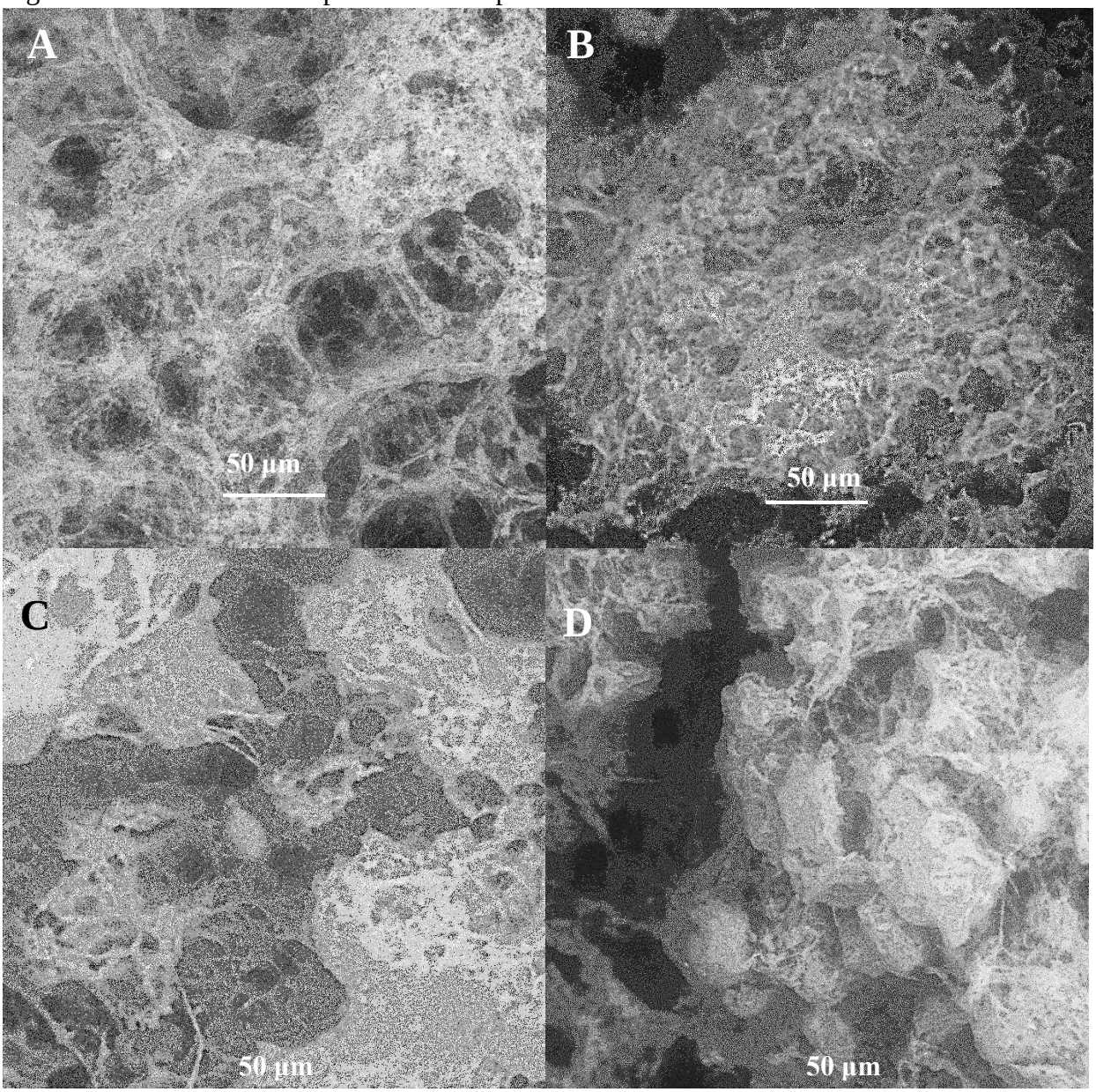

Figure S6.2 VPSEM ımages of biofilm on carriers, 600× magnification: a) 0.13 mg Cu/L addition, b) 0.28 mg Cu/L addition, c) 0.44 mg Cu/L addition, d) 0.61 mg Cu/L addition

6.8 References

Acheampong, MA., Paksirajan, K., Lens, PNL. (2013) Assessment of the effluent quality from a gold mining industry in Ghana. *Environmental Science and Pollution Research* 20:3799-3811

Anthonisen, AC., Loehr, RC., Prakasam, TBS., Srinath, EG. (1976) Inhibition of nitrification by ammonia and nitrous acid. *Water Pollution Control Federation* 48:835-852

APHA, AWWA, WEF (1989) Standard methods for examination of water and wastewater, 17th edition. Washington, D.C.

Beer, Dd., Stoodley, P., Roe, F., Lewandowski, Z. (1994) Effects of biofilm structures on oxygen distribution and mass transport. *Biotechnology and Bioengineering* 43: 1131-1138

Bjornberg, C., Lin, W., Zimmerman, RA. (2009) Effect of temperature on biofilm growth dynamics and nitrification in a full-scale MBBR system. *Proceedings of the Water Environment Federation*, WEFTEC 2009: Session 61 through 70:4407-4426

Black, R., Sartaj, M., Mohammadian, A., Qiblawey, HAM. (2014) Biosorption of Pb and Cu using fixed and suspended bacteria. *Journal of Environmental Chemical Engineering* 2:1663-1671

Blackburne, R., Vadivelu, VM., Yuan, Z., Keller, J. (2007) Kinetic characterisation of an enriched *Nitrospira* culture with comparison to *Nitrobacter*. *Water Research* 41: 3033-3042

Braam, F., Klapwijk, A. (1981) Effect of copper on nitrification in activated sludge. *Water Research* 15:1093-1098

Bryers, JD. (1987) Biologically active surfaces: processes governing the formation and persistence of biofilms. *Biotechnology Progress* 3: 57-68

Burmølle, M., Ren, D., Bjarnsholt, T., Sørensen, SJ. (2014) Interactions in multispecies biofilms: do they actually matter? *Trends in Microbiology* 22:84-91

Canadian Fisheries Act: Metal Mining Effluent Regulations (2002) Retrieved from the Justice Laws website: http://laws-lois.justice.gc.ca/eng/regulations/SOR-2002-222/page-1.html. Accessed 20 April 2017

Çeçen, F., Semerci, N., Geyik, AG. (2010) Inhibitory effects of Cu, Zn, Ni, and Co on nitrification and relevance of speciation. *Journal of Chemical Technology and Biotechnology* 85:520-528

Cenci, G., and Morozzi, G. (1979) The validity of the TTC-test for dehydrogenase activity of activated sludge in the presence of chemical inhibitors. *Zentralblatt fur Bakteriologie, Parasitenkunde, Infektionskrankheiten und Hygiene* 169:320-330

Delatolla, R., Tufenkji, N., Comeau, Y., Gadbois, A., Lamarre, D., Berk, D. (2009) Kinetic analysis of attached growth nitrification in cold climates. *Water Science and Technology* 60:1173-1184

Do, DD. (1998) Adsorption analysis: Equilibrium and Kinetics. Imperial College Press, London

Environmental code for practice of metal mines (2009) Environment Canada, Ottawa. https://www.ec.gc.ca/lcpe-cepa/documents/codes/mm/mm-eng.pdf. Accessed 20 April 2017

Flemming, HC. (1993) Biofilms and environmental protection. *Water Science and Technology* 27:1-10

Flemming, HC., Neu, TR., Wozniak, DJ. (2007) The EPS Matrix: The "House of Biofilm Cells". *Journal of Bacteriology* 189:7945-7947

Forrest, D., Delatolla, R., Kennedy, K. (2008) Carrier effects on tertiary nitrifying moving bed biofilm reactor: An examination of performance, biofilm and biologically produced solids. *Environmental Technology* 37: 662-671

Freundlich, H. (1906) Über die Adsorption in Losungen. *Z Phys Chem* 57:385-471

Gerardi, MH. (2002) Nitrification and denitrification in the activated sludge process. *Environmental Protection Magazine Series*. John Wiley and Sons, Inc. New York.

Harrison, JJ., Cerl, H., Stremick, CA., Turner, RJ. (2004) Biofilm susceptibility to metal toxicity. *Environmental Microbiology* 6:1220-1227

Hoang, V., Delatolla, R., Laflamme, E., Gadbois, A. (2014) An investigation of moving bed biofilm reactor nitrification during long-term exposure to cold temperatures. *Water Environment Research* 86:36-42

Hu, Z., Chandran, K., Grasso, D., Smets, BF. (2003) Impact of metal sorption and internalization on nitrification inhibition. *Environmental Science and Technology* 37:728-734

Hu, Z., Chandran, K., Grasso, D., Smets, BF. (2004) Comparison of nitrification inhibition by metals in batch and continuous flow reactors. *Water Research* 38:3949-3959

Juliastuti, SR., Baeyens, J., Creemers, C., Bixio, D., Lodewyckx, E. (2003) The inhibitory effects of heavy metals and organic compounds on the net maximum specific growth rate of the autotrophic biomass in activated sludge. *Journal of Hazardous Materials* B100:271–283

Keenan, JD., Steiner, RL., Fangarol, AA. (1979) Substrate inhibition of Nitrification. *Journal of Environmental Science Health* A14:377-397

Langmuir, I. (1918) The adsorption of gases on plane surfaces of glass, mica and platinum. *Journal of the American Chemical Society* 40:1361-1403

Leard Statistics (2020) Pearson's product moment correlation. *Statistical Tutorials and Software Guides*. Received March 27, 2021 from https://statistics.laerd.com/statistical-guides/pearson-correlation-coefficient-statistical-guide.php

Lee, LY., Ong, SL., Ng, HY., Hu, JY., Koh, YN. (2008) Simultaneous ammonia-nitrogen and copper removal and copper recovery using nitrifying biofilm from the ultra-compact biofilm reactor. *Bioresource Technology* 99: 6614-6620

Lee, YW., Tian, Q., Ong, SK., Sato, C., Chung, J. (2009) Inhibitory effects of copper on nitrifying bacteria in suspended and attached growth reactors. *Water, Air and Soil Pollution* 203:17-27

Melcer, H. (2015) Mass transfer characteristics of floating media in MBBR and IFAS fixed-film systems. *Water Intelligence Online*, 14. doi:10.2166/9781780407050

Mineral commodity summaries (2016) U.S. Geological Survey, Virginia. http://dx.doi.org/10.3133/70140094. Accessed 10 June 2017

Ochoa-Herrera, V., Leon, G., Baniban, Q., Afield, J., Sierra-Alvares, R. (2011) Toxicity of copper (II) ions to microorganisms in biological wastewater treatment systems. *Science of Total Environment* 412-413: 380-385

Ødegaard, H. (1999) The moving bed biofilm reactor. *Water Environmental Engineering and Reuse of Water*, Hokkaido Press:250-305

Özbelge, TA., Özbelge, HO., Altinten, P. (2007) Effect of acclimatization of microorganisms to heavy metals on the performance of activated sludge process. *Journal of Hazardous Materials* 142:332-339

Redlich, O., Peterson, DL. (1959) A useful adsorption isother. *Journal of Physical Chemistry* 63:1024

Sato, C., Leung, SW., Schnoor, JL. (1988) 'Toxic response of *Nitrosomonas europaea* to copper in inorganic medium and wastewater. *Water Research* 22:1117-1127

Schramm, A., Larsen, LH., Revsbech, NP., Ramsing, NB., Amann, R., Schleifer, KH. (1996) Structure and function of a nitrifying biofilm as determined by in situ hybridization and the use of microelectrodes. *Applied and Environmental Microbiology* 62:4641-4647

Scullion, J., Winson, M., Matthews, R. (2007) Inhibition and recovery in a fixed microbial film leachate treatment system subject to shock loadings of copper and zinc. *Water Research* 41:4129-4138

Şengör, SS., Gikas, P., Moberly, JG., Peyton, BM., Ginn, TR. (2011) Comparison of single and joint effects of Zn and Cu in continuous flow and batch reactors. *Journal of Chemical Technology and Biotechnology* 87:374-380

Skinner, FA., Walker, N. (1961) Growth of *Nitrosomonas europaea* in batch and continuous culture. *Archiv für Mikrobiologie* 38:339-349

Sterrit, RM., Lester, JN. (1980) Interactions of heavy metals with bacteria. *The Science of the Total Environment* 14:5-17

Teitzel, GM., Parsek, MR. (2003). Heavy metal resistance of biofilm and planktonic Pseudomonas aeruginosa. *Applied and Environmental Microbiology* 69:2313-2320

Tran, HN., Hosseini-Bandegharaei, A., Chao, H-P. (2017) Mistakes and inconsistencies regarding adsorption of contaminants from aqueous solutions: a critical review. *Water Research* 120:88-116

U.S. Clean Water Act, 33 U.S.C. § 1251 et seq. (1972) U.S Environmental Protections Agency, Washington. https://www.epa.gov/laws-regulations/summary-clean-water-act. Accessed February 2017

U.S. Ore mining and dressing effluent regulations, 40 C.F.R § 440 (1988) U.S Environmental Protections Agency, Washington. https://www.epa.gov/eg/ore-mining-and-dressing-effluent-guidelines. Accessed April 20 2017

Vasanth, K., Sivanesan, S. (2006) Equilibrium data, isotherm parameters and process design for partial and complete isotherm of methylene blue onto activated carbon. *Journal of Hazardous Materials* 134:237-244

Water Environment Federation, American Society of Civil Engineers (2009) Design of municipal wastewater treatment plants, MoP8, 5th edition. WEF Press, McGraw Hill, New York

Wastewater systems effluent regulations (2012) Canada Gazette, July 18 2012, Part II, vol. 146, No. 15. http://www.gazette.gc.ca/rp-pr/p2/2012/index-eng.html. Accessed February 2017

White, C., Gadd, GM. (2000) Copper accumulation by sulfate reducing bacterial biofilms. *FEMS Microbiology Letter* 183:313-318

Young, B., Delatolla, R., Ren, B., Kennedy, K., Laflamme, E., Stintzi, A. (2016a) Pilot-scale tertiary MBBR nitrification at 1°C: characterization of ammonia removal rate, solids settleability and biofilm characteristics. *Environmental Technology* 37: 2124-2132

Young, B., Banihashemi, B., Forrest, D., Kennedy, K., Stinzi, A., Delatolla, R. (2016b) Meso and micro-scale response of post carbon removal nitrifying MBBR biofilm across carrier type and loading. *Water Research* 91:235-243

CHAPTER 7- DISCUSSION, CONCLUSIONS, AND SYNTHESIS

This dissertation advances the current knowledge of biological nitrogen removal for municipal and industrial wastewater treatment by advancing design strategy, system configurations, and investigating interactions between biofilms and inhibitors. Specifically, this dissertation aims to address critical challenges facing municipal nitrogen removal and mining wastewater treatment by using attached growth technologies. This dissertation develops new knowledge by developing a novel, passive, and low operationally intensive design strategy for achieving partial nitritation (PN) using the moving bed biofilm reactor (MBBR) technology for industrial wastewaters. This dissertation contributes new knowledge on carrier design strategies of defined biofilm thickness and undefined biofilm thickness and the impact of this design choice on the effects of free nitrous acid (FNA) to achieve PN for municipal wastewaters. Furthermore, this research contributes new knowledge on the effects of copper on nitrifying MBBR systems during long term operations.

7.1 Partial Nitritation with Elevated Loading Rates

Chapters 3 and 4 provide the findings on achieving MBBR PN by operating at elevated TAN SALR values for main-stream and side-stream low carbon, tertiary TAN removal for more than three years. This work isolates the effects of TAN SALR values of 3, 4, 5, and 6.5 g TAN/m^2·d on the macro-, meso-, micro-, and molecular-scale MBBR technology and housed biofilm by evaluating nitritation and nitratation kinetics, biofilm characteristics, cell viability, and the microbiome at each of the TAN SALR values investigated.

At the macro-scale, operation at TAN SALR values of 3, 4, 5, and 6.5 g TAN/m^2·d resulted in TAN SARR values of 2.0, 3.2, 3.7, 3.5 g TAN/m^2·d and nitrite accumulation percentages of 8.4,

44.1, 59.1, and 99.8%, respectively. The changes in TAN SARR and nitrite accumulation due to the increase in TAN SALR values from 3 to 4 g TAN/m^2·d indicates a shift in biofilm activity towards PN from full nitrification. Furthermore, there was a significant increase in TAN SARR values from 2 to 3.5 g TAN/m^2·d observed at TAN SALR values of 4, 5, and 6.5 g TAN/m^2·d which suggests a new, zero-order, TAN SARR limit. The nitrite accumulation reached 99.8% at a TAN SALR value of 6.5 g TAN/m^2·d, indicating that nitrite oxidizing bacteria (NOB) activity is suppressed and PN is achieved. Furthermore, the relation between TAN SALR and nitrite accumulation is strongly linear (R^2 = 0.97) and has the potential to be used for the design and implementation of PN MBBR systems.

At the meso-scale, biofilm characteristics including thickness, mass, density, and morphology, were quantified to understand the impact of elevated TAN SALRs on the biofilm. There is a statistically significant increase in biofilm thickness with increasing TAN SALRs; however, there was only a statistically significant increase in biofilm mass when the TAN SALR value increased from 4 to 5 g TAN/m^2·d, meaning that there was a statistically significant decrease in biofilm density as the TAN SALR values increased from 3 to 4 g TAN/m^2·d and 5 to 6.5 g TAN/m^2·d; however, there was no statistically significant change in biofilm density as the TAN SALR increased from 4 to 5 g TAN/m^2·d. There was a trend of increasing biofilm morphological roughness with an increase in TAN SALR values. Therefore, the elevated TAN SALR values have a significant impact on the biofilm characteristics. The increased biofilm thickness may contribute to the decrease in NOB nitratation activity due to a decrease in oxygen penetration into the biofilm, which would therefore contribute to the suffocation of the NOB.

At the micro-scale and molecular-scale, the area of biofilm covered by cells and cell viability are not shown to be statistically significantly different at the TAN SALR values tested except at a

TAN SALR of 5 g TAN/m^2·d where the area of biofilm covered by cells and cell viability are lower than at the other TAN SALR values. At the molecular-scale, there are notable shifts in beta-diversity and the microbiome abundance as the TAN SALR values increase from 3 to 6.5 g TAN/m^2·d, most notably the statistically significant increase in ammonia oxidizing bacteria (AOB) abundance from 2.26% to 17.34%, and the statistically significant decrease in NOB abundance from 5.85% to 2.0%. The abundance of NOB is still significant when operating at a TAN SALR value of 6.5 g TAN/m^2·d; however, the nitrate production is negligible, thus demonstrating that the NOB are being suppressed by operating at elevated loading rates and PN is achieved. As this study was performed for more than three years, and PN was achieved for more than ten months, elevated TAN SALR values has been demonstrated to be a robust, low operational intensity design strategy for achieving PN.

7.1.1 Novel Contributions and Practical Implications

This study is the first study to use elevated TAN SALRs as a design strategy for attached growth technologies to achieve PN without limiting DO or using inhibitors. This study provides new knowledge on the macro-, meso-, micro, and molecular-scale effects of operating at elevated TAN SALR values and develops new fundamental knowledge needed to design a MBBR system using elevated TAN SALR values to achieve PN. This study demonstrates a novel, low operational intensity, and potentially robust design strategy to achieve PN using the MBBR technology as a pre-treatment for anammox treatment for low carbon, tertiary wastewater treatment. The findings of this study provide proof of concept for achieving PN using elevated TAN SALR values and set the groundwork for further research at municipal TAN concentrations. Futhermore, patenting the work for specific applications is being pursued.

7.2 Impact of Defined Biofilm Thickness on Partial Nitritation by Free Nitrous Acid Exposure

Chapter 5 provides new knowledge on the effects of maximal defined biofilm thickness on FNA inhibition with the intention to achieve PN for municipal, low-carbon, tertiary TAN removal. This study compares two types of carriers, one designed for a maximal defined biofilm thickness (z-prototype), and one that is not designed for a maximal defined biofilm thickness (chip-prototype) and how these biofilm thickness definition strategies impacted the effects of FNA inhibition on AOB nitritation kinetics and NOB nitratation kinetics. Maximal defined biofilm thickness means that the carriers are designed such that a specific section of the biofilm is protected and anything that grows outside of the section will be removed through abrasion, erosion, or shear forces, thus maintaining a specific maximum biofilm thickness throughout a variety of conditions, whereas carriers that do not have a maximal defined biofilm thickness will have a greater variance in biofilm thicknesses throughout a variety of conditions.

The effects of maximal defined biofilm thickness versus undefined biofilm thickness are compared by performing nitritation and nitrataton kinetics batch tests after exposure to FNA for 1, 2, 3, and 4 hours and the macro-, meso-, and molecular scale were investigated. On a macro-scale, it was found that PN was achieved with the z-prototype carrier after 3 and 4 hours of exposure to FNA while PN was not achieved with the chip-prototype even after 4 hours of exposure to FNA. At the meso-scale, the chip-prototype had ten times the biofilm thickness and biofilm mass as the z-prototype, and statistically significantly similar biofilm densities. The difference in biofilm thickness and biofilm mass is due to the carrier designed defined biofilm thickness of the z-carrier and the undefined biofilm thickness of the chip-prototype and these difference in biofilm thickness and mass significantly contributed to the difference in biofilm responses to FNA exposure. At the molecular-scale, there was a significant difference in alpha-

diversity and in microbiome as the chip-prototype had a significantly higher abundance of NOB than the z-prototype which may have contributed to the inhibition effects of FNA on the NOB. As only the z-prototype achieved PN, the maximal defined biofilm thickness proved to be the preferred carrier design choice for achieving PN.

7.2.1 Novel Contributions and Practical Applications

This study is the first study to compare a defined maximal biofilm thickness to undefined maximal biofilm thickness as a carrier design choice for achieving PN using FNA exposure. This study provides new knowledge on how the carrier design choice of maximal defined biofilm thickness can be used to achieve PN with FNA exposure. This research is currently being used by the industrial partner, AnoxKaldnes, to develop a process to achieve PN for municipal, tertiary, low carbon wastewater treatment.

7.3 Copper Inhibition of Nitrifying MBBR for Long Term Operations

Chapter 6 provides the findings of the effects of copper exposure on nitrifying MBBR systems over long term operations. In this study, four identical, parallel nitrifying MBBR systems were exposed to different copper concentrations of 0.1, 0.3, 0.45, and 0.6 mg Cu/L for over 11 months to simulate the long term operations that would be seen in gold mining wastewater treatment for TAN removal. The copper concentrations were chosen to represent regulation limits set by the Canadian government for mining effluent discharge. The results showed that there was no statistically significant difference in TAN SARR values at each copper concentration, and there was no statistically significant difference in TAN SARR between the reactors exposed to copper and the control reactor thus demonstrating that there was no statistically significant inhibition of AOB activity.

There was a statistically significant difference in NOB activity, presented as nitrite accumulation, at influent copper concentrations of 0.1, 0.3, 0.45, and 0.6 mg Cu/L. There was no statistically significant difference in nitrite accumulation between the control and 0.1 mg Cu/L indicating that there was no NOB inhibition; however, the nitrifying MBBR systems exposed to influent copper concentrations of 0.3, 0.45 and 0.6 mg Cu/L were statistically significantly different from the control reactor indicating NOB inhibition. At influent copper concentrations of 0.3 and 0.45 mg Cu/L there was no statistically significantly different nitrite accumulation, and 0.6 mg Cu/L had statistically significantly higher nitrite accumulation than any other copper exposure; therefore, there is a trend of increasing nitrite accumulation, and therefore NOB inhibition, with an increase in copper exposure. Furthermore, while there is no statistically higher difference in biofilm characteristics at each influent copper concentration; there is a positive trend of increasing biofilm thickness and roughness with increasing influent copper concentration. At an influent copper concentration of 0.6 mg Cu/L, the biofilm had either become so thick that it clogged the carrier-pores or was completely absent, leaving empty carrier-pores. The results demonstrate that no AOB nitritation inhibition was observed at influent copper concentrations of 0.1, 0.3, 0.45, and 0.6 mg Cu/L thus demonstrating the capacity of the nitrifying MBBR to remove TAN from wastewater containing copper.

7.3.1 Novel Contribution and Practical Application

This study is the first study to investigate the effects of copper exposure on nitrifying biofilm during long term operations. Previous studies on the effect of copper exposure on nitrifying biofilms were either batch tests that overestimate the resiliency of the biofilm, or short term studies that do not accurately reflect long term operations. The findings of this study were used by the industrial partner as evidence of the long term resiliency of the nitrifying biofilm for use in treating

gold mining wastewater, and for the design and implementation of nitrifying MBBR systems in gold mining impacted wastewater treatment at the Eleanor gold mine in Quebec, Canada.

7.4 Synthesis

This dissertation consists of three studies relating to nitrifying MBBR systems. Study 1 (Chs 3 and 4) and 2 (Ch 5) operate with the intention of suppressing NOB activity while maintaining sufficient AOB activity to achieve PN while study 3 (Ch 6) operates with the intention of maintaining both AOB and NOB activity with the presence of an inhibitor. While study 3 takes advantage of the protective properties of the biofilm to allow the AOB and NOB to adapt to copper inhibition, studies 1 and 2 aim to completely suppress NOB activity despite the biofilm resiliency. The resiliency of biofilms to toxicity and inhibitory conditions, as demonstrated by study 3, demonstrates a significant, well documented, challenge for achieving PN which relies on the suppression of NOB activity or NOB population. Study 1 bypasses the biofilm resiliency challenge by operating at elevated TAN loading rate which results in NOB activity suppression by depriving the NOB of oxygen. The proposed mechanism for depriving the NOB of oxygen is by preferential uptake of oxygen by AOB in the presence of TAN, meaning that as long as sufficient TAN is available, the AOB will consume all available oxygen. Study 2 uses FNA to suppress the NOB; however, this strategy has been proven to be difficult to achieve during long term operations. Study 2 looks to defining a maximum biofilm thickness via carrier design to facilitate PN with long term FNA exposure and, by defining a thin maximum biofilm thickness, the carrier design aims to reduce the resiliency of biofilms. Therefore, although studies 1 and 2 have different objectives than study 3 relative to the protective properties of biofilms and how these properties effect bacterial adaptation, the importance of biofilm properties is a common theme throughout this dissertation.

Operation at elevated TAN loading rates, exposure to FNA, and exposure to copper were all shown to have a suppression effect on NOB activity. FNA and copper exposure cause NOB suppression through toxicity, whereas elevated TAN loading rates suppress NOB through oxygen deprivation. Nitrite accumulation is observed during each study, which means that FNA is present during each study; however, as the FNA concentration is pH dependent, temperature dependent, and nitrite dependent, the conditions of each study heavily influence the FNA presence. Study 1 (Chs 3 and 4) and study 3 (Ch 6) operated at a pH of 7.5-8, a temperature of 20°C, and nitrite concentrations ranging from 6-68 mg NO_2^--N/L resulting in FNA concentrations of 8.48E−5 to 2.1E−3 mg HNO_2-N/L; whereas study 2 (Ch 5) used an exposure solution with a pH of 6, a temperature of 30°C, and a nitrite concentration of 500 mg NO_2^--N/L resulting in a FNA concentration of 0.88 mg HNO_2^--N/L. Therefore, the FNA exposure from study 2 is more than 100-fold higher than those of studies 1 and 3. Furthermore, the FNA concentrations present in study 1 and 3 are significantly lower than the inhibitory concentration of 0.02 HNO_2^--N/L and thus, do not contribute to NOB suppression demonstrated in the studies.

The achievement of PN is an objective of both study 1 (Chs 3 and 4) and study 2 (Ch 5); however, both studies use different strategies to achieve PN. Study 1 uses the passive, low operationally intensive design strategy to achieve PN while study 2 uses a simulation of periodic exposure to a high strength centrate to achieve PN. Study 1 uses a design strategy that requires no monitoring or adjustment to suppress NOB activity; whereas study 2 uses toxicity to suppress NOB activity, which demonstrates an advantage of study 1 as adaptation to toxicity has been a challenge for attached growth systems. Therefore, achieving PN using elevated loading rate has operational benefits over using FNA exposure. Conversely, using elevated TAN loading rate to achieve PN can be susceptible to fluctuating mainstream influent TAN concentrations making it

difficult to maintain steady elevated loading rates whereas toxicity due to FNA exposure is independent of the mainstream influent composition and may have more consistent PN. Further research for study 1 could consist of pilot studies to test the passive strategy with real wastewater, especially fluctuating influents and TAN concentrations typical to municipal treatment. Study 2 would benefit from continuous operations, rather than batch tests, with periodic exposure to FNA to determine NOB adaptation and the ideal exposure times.

CHAPTER 8 - FUTURE WORK

This section presents suggestions for future work related to the research of this dissertation.

8.1 Future Work for Achieving Partial Nitritation using Elevated TAN Loading Rates

To enhance the understanding of achieving partial nitritation (PN) using elevated TAN loading rates, a number of additional studies can be suggested. Primarily, the studies of achieving PN using an elevated TAN loading rate design strategy were operated at TAN concentrations much higher than conventional municipal concentrations. While operating at elevated TAN concentrations was useful to allow for greater flexibility in fill fraction, it may have effects on the direct applicability of the design curve on designs for municipal operations; therefore, the first suggestion is to operate at elevated loading rates using TAN concentrations more typical to municipal treatment (15- 50 mg TAN/L). Furthermore, research should be performed using real post-carbon removal wastewater as the wastewater used for the studies discussed in this dissertation was synthetic. Using other carrier geometries to optimise the design strategy may be useful to optimise the biofilm thickness.

To gain increased knowledge of the effects elevated TAN loading rates on the nitrifying kinetics, a number of additional tests can be performed. An oxygen uptake rate test can be used to directly quantify the activity of the biofilm. Furthermore, a model can be created to obtain a deeper understanding of what occurs within the biofilm in regards to biofilm substrate penetration and activity. While modelling can approximate what is occurring within the biofilm with the given data, direct measurement of oxygen penetration into the biofilm can be measured using oxygen sensors. Understanding the depth of oxygen penetration and activity within the

biofilm would provide additional support for the theorised mechanism of NOB activity suppression observed.

8.2 Future Work for the Impact of Defined Maximum Biofilm Thickness on Partial Nitritation using Free Nitrous Acid Exposure

This study focused on the impact of using a defined maximum biofilm thickness carrier design strategy to achieve PN using free nitrous acid (FNA). Future work for the study is to perform continuous operation tests at different influent concentrations to quantify adaptation and determine optimal FNA exposure times and eventually develop a treatment strategy around FNA exposure to achieve PN for mainstream PN/A. Furthermore, optimisation of the maximum biofilm thickness should be performed for continuous operations.

8.3 Future Work for Copper Inhibition of Nitrifying MBBR during Long Term Operations

This study focused on the effects of copper inhibition on nitrifying MBBR during long term operations. Future work for this study includes performing long-term operations at higher concentrations to quantify the effects of elevated copper concentrations on nitrifying biofilms. Furthermore, direct measurement of precipitated copper and quantification of porosity would increase understanding of the effects of copper on the biofilm.

CHAPTER 9 - APPENDIX

9.1 Determining G-Value

The G-value is the average velocity gradient, representing mixing within the reactor. The Power dissipation equation (eqn 9.1) and G-value equation (eqn 9.2) are described below (Camp and Stein, 1943; Bewtra and Nicholas, 1964; Droste and Gehr, 2018)

$$P = p_a Q_a ln\left(\frac{10.3+h}{10.3}\right) \quad \text{(eqn 9.1)}$$

Where P is the power of the mixing due to aeration (J/s), p_a is the atmospheric pressure (kN/m^2), Q_a is the air flow rate (m ^{3}/s), h is the height of the reactor (m).

$$G = \sqrt{\frac{P}{\mu V}} \quad \text{(eqn 9.2)}$$

Where G is the amount of mixing (s^{-1}), μ is the viscosity of the fluid (N·s/m^2), V is the volume of the working volume of the reactor (m^3).

9.2 Chapter 5 - Batch Testing Data

The following are the results pertaining to the research presented in Chapter 5 and were obtained from the free nitrous acid (FNA) exposure batch tests where tables 9.1-9.4 are the total ammonia nitrogen (TAN) and NO_2^--N concentrations for the z-prototype and the chip-prototype, respectively, for the ammonia oxidizing bacteria (AOB) and nitrite oxidizing bacteria (NOB) activity tests, respectively. Tables 9.5-9.8 are the total nitrogen mass balances for the z-prototype and chip-prototype, respectively, for the AOB and NOB activity tests, respectively.

Table 9.1 Z-prototype AOB activity test results by exposure time

Time (min)	Baseline (mg TAN/L)	1 hour (mg TAN/L)	2 hours (mg TAN/L)	3 hours (mg TAN/L)	4 hours (mg TAN/L)
0	44	45.1	45.4	44.4	46.1
20	43.2	46.9	43.9	44.1	
40	42.8	44.4	43.6	42.6	
60	41.8	44.4	43.4	42.4	
80	39.8	43.6	42.2	43.3	
100	39	42.9	42	41.3	
120	38.3	42	42.4	41.9	43.4

Table 9.2 Z-prototype NOB activity test results by exposure time

Time (min)	Baseline (mg NO_2^-–N/L)	1 hour (mg NO_2^-–N/L)	2 hours (mg NO_2^-–N/L)	3 hours (mg NO_2^-–N/L)	4 hours (mg NO_2^-–N/L)
0	30.7	31	30.4	31.2	29.9
20	28.7	29.9	29.9	30.5	30.2
40	28.2	30.5	30.0	30.9	29.9
60	27.1	30.1	30	30.7	30.2
80	27.1	29.7	29.9	30.9	29.8
100	26.5	29.7	29.3	31.5	30.2
120	25.1	29.2	29.6	30.9	30.3

Table 9.3 Chip-prototype AOB activity test results by exposure time

Time (min)	Baseline (mg TAN/L)	1 hour (mg TAN/L)	2 hours (mg TAN/L)	3 hours (mg TAN/L)	4 hours (mg TAN/L)
0	44	45.4	45.9	43.6	46.1
20	42.4	43.5	43	42	
40	41.0	42.9	41.7	40.7	
60	39.4	42.1	40.7	39.9	
80	37.5	40.7	39.7	39	
100	36.4	39.7	37.7	37.6	
120	34.6	39.5	37.4	36.7	38.6

Table 9.4 Chip-prototype NOB activity test results by exposure time

Time (min)	Baseline (mg NO_2^-–N/L)	1 hour (mg NO_2^-–N/L)	2 hours (mg NO_2^-–N/L)	3 hours (mg NO_2^-–N/L)	4 hours (mg NO_2^-–N/L)
0	30.5	30.8	30.3	31.4	30.6
20	25.7	29.5	28.9	30.4	30.1
40	23	28.9	28.1	29.8	29.5
60	18.9	28.2	27.2	29.2	28.6
80	15.1	27.2	25.6	28.2	27.6
100	12.2	25.5	24.7	28.3	27.2
120	8.3	24.6	23.2	26.5	25.6

Table 9.5 Z-prototype AOB total nitrogen concentrations and nitrogen balance

	Baseline	1 hour	2 hours	3 hours	4 hours
Initial TN (mg/L)	44.2	45.4	45.5	44.8	46.1
Final TN (mg/L)	43.0	45.5	45.7	44.8	45.9
N Balance (%)	97.3	100.2	100.4	100	99.3

Table 9.6 Z-prototype NOB total nitrogen concentrations and nitrogen balance

	Baseline	1 hour	2 hours	3 hours	4 hours
Initial N (mg/L)	30.7	31.4	30.8	31.2	29.9
Final N (mg/L)	30.6	30.7	30.4	30.9	30.3
N Balance (%)	99.9	99.1	98.7	98.9	101.5

Table 9.7 Chip-prototype AOB total nitrogen concentrations and nitrogen balance

	Baseline	1 hour	2 hours	3 hours	4 hours
Initial N (mg/L)	44.4	45.8	46.0	44.1	46.2
Final N (mg/L)	42.6	46.4	44.5	40.2	45.2
N Balance (%)	96.0	101.3	96.8	91.1	97.8

Table 9.8 Chip-prototype NOB total nitrogen concentrations and nitrogen balance

	Baseline	1 hour	2 hours	3 hours	4 hours
Initial N (mg/L)	30.8	31.3	30.5	31.5	29.8
Final N (mg/L)	29.9	28.7	31.5	32.2	30.2
N Balance (%)	97.0	91.6	103.1	102.5	101.7

9.3 Chapter 6 - Isotherm Plots

The following plots are Freundlich and Langmuir isotherms pertaining to Chapter 6.

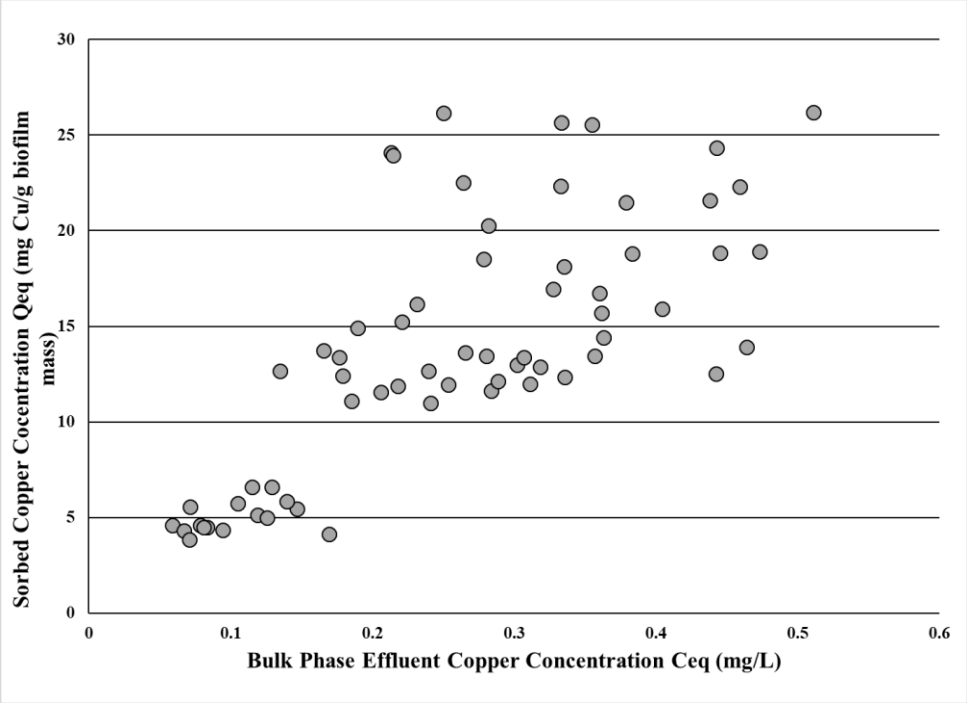

Figure 9.1 Freundlich Isotherm

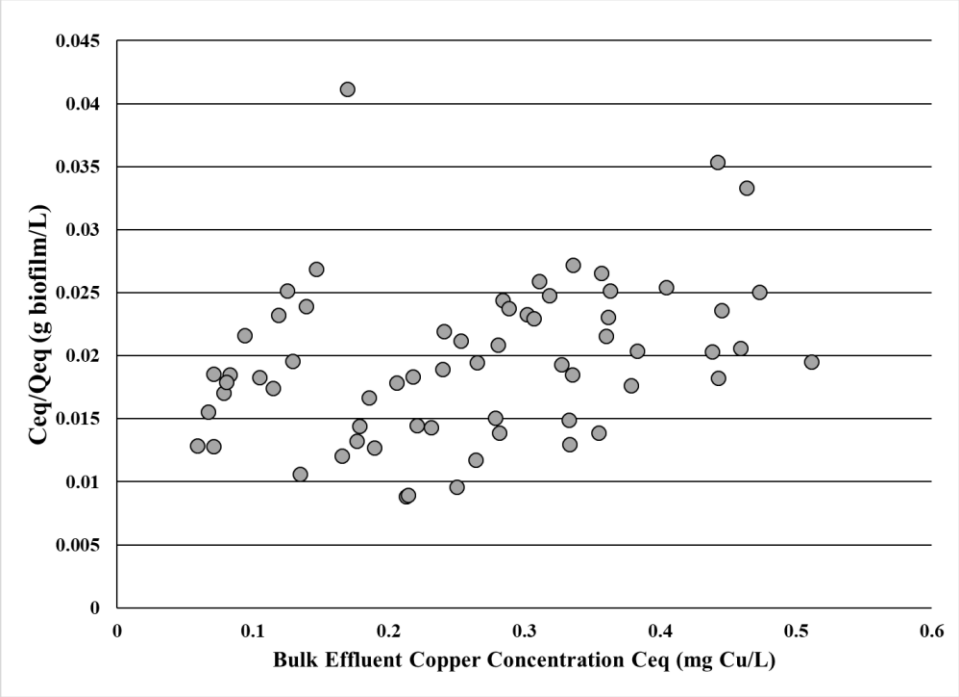

Figure 9.2 Langmuir Isotherm

9.4 References

Bewtra, J.K. and Nicholas, W.R (1964) Oxygenation from diffused air in aeration tanks. *Journal Water Pollution Control Federation.* 3r6 (10): 1195-1224. http://www.jstor.org/stable/25035151

Camp, T.R. and Stein, P.C. (1943) Velocity gradients and internal work in fluid motion. *Journal of Boston Society of Civil Engineers*. 30(4): 219-227

Droste, R. and Gehr, R. (2018) *Theory and Practice of Water and Wastewater Treatment*, John Wiley & Sons, Incorporated. *ProQuest Ebook Central*, https://ebookcentral.proquest.com/lib/ottawa/detail.action?docID=5478976.